# NETWORK OPTIMIZATION MODELS FOR INTERDEPENDENT INFRASTRUCTURE RESTORATION

by

Suzan Iloglu

A dissertation submitted in partial fulfillment of
the requirements for the degree of

Doctor of Philosophy

(Industrial and Systems Engineering)

at the

UNIVERSITY OF WISCONSIN–MADISON

2019

Date of final oral examination: 6/20/2019

The dissertation is approved by the following members of the Final Oral Committee:
Laura A. Albert, Professor, Industrial and Systems Engineering
Jim Luedtke, Professor, Industrial and Systems Engineering
Carla Michini, Assistant Professor, Industrial and Systems Engineering
Xin Wang, Assistant Professor, Industrial and Systems Engineering
Qunying Huang, Assistant Professor, Geography

© Copyright by Suzan Iloglu 2019
All Rights Reserved

*To my parents Fatma & Ramazan Iloglu and my brother Ali Serdar Iloglu.*

# Acknowledgments

First and foremost, I acknowledge my academic advisor Laura A. Albert for being an amazing role model not only professionally, but also personally. I am deeply indebted to her time, patience and dedication over the years. She has been not only a great thesis advisor, but also an unparalleled role model for me in every aspect. I extend my acknowledgment to my dissertation committee members: James Luedtke, Xin Wang, Qunying Huang, and especially Carla Michini, who provided very useful feedback and spent long hours with me to improve the last chapter of this thesis. The valuable feedback my committee members provided was essential to substantially improving this manuscript.

I am grateful to fellow and visiting students in the Industrial and Systems Engineering Department at UW-Madison. In addition to Jose Nunes Arez and Tom Van Acker, I especially appreciate my academic "cousins" for enduring the entire ups and downs of graduate student life we have been through together: Eli Towle; for being an amazing supportive buddy during my PhD and Amanda Smith, for being a great listener over a coffee. I would like to thank my academic "siblings" Soovin Yoon (a great conference roommate), for her calm and positive energy, Kay Zheng, for her support and lead and Eric DuBois (the mean one) for consistently teasing and joking around with me. I also would like to thank Michal Kwarta (MK) for helping me with Matlab plots. I would like to thank Kemal Afacan, for his support during the first two years of my PhD. I also thank Sam Plapinger, for being a very supportive friend after we met during our RAND Summer Associate journey. Another special thank you is for my forever best friend Pinar Kemanli, for being next to me during all of my hard moments and for her endless support. Also

thank you to another best friend of mine, Ayse Ozdogan Dolcek, for always being there for me even though she moved far away. Last but not least, I thank Arturo Ramirez (Petete) for his support and wisdom during the last year of my PhD.

I especially thank my parents Fatma-Ramazan Iloglu and my amazing brother Ali Serdar Iloglu for being endless sources of wisdom, support and motivation. I would like to thank my beautiful little niece, Lina Iloglu. Due to the busy last months of my PhD, I did not have a chance to see her until her very first birthday. Another special thank to my grandfather Sukru Esersoy, who I could not have a chance to see one last time when he passed away three years ago. I always feel his support and motivation behind me.

There have been both very good and bad moments during my PhD. I appreciate my close family members and friends for the sacrifices they have made and the patience they have shown. I know that we cannot have it all once in this life and at times we need to sacrifice some parts. I apologize for the moments I happened to sacrifice during my PhD and could not be next to the people who are very important to me. At the end, my ultimate goal is to create a "butterfly effect" and to start a small impact in this world.

This dissertation would not have been possible without the help, support and courage of the many amazing people who are in my life or have passed through my life. Any errors which remain are my sole responsibility.

# Contents

# List of Tables

# List of Figures

# Abstract

Effective restoration of infrastructure systems play a crucial role in recovery after disasters. Understanding the functions and services of infrastructure systems, especially during the response to natural and man-made disasters, requires accounting for the interdependencies and decentralized nature of these systems. This issue is particularly critical when delivering time-sensitive services and commodities. We model the recovery of infrastructure systems by including interdependencies between them as network models, and we present three integer programming models.

First, we present an integrated restoration and location (IRLP) problem, which is a P-median problem variation, with the objective to minimize the cumulative weighted distance between the emergency responders and the calls for service over the time horizon by coordinating the activities of two types of service providers. We locate emergency responders (facilities) on a network over a finite time horizon while network recovery crews install arcs. The installation part of the problem is modeled as a scheduling problem with identical parallel servers (the repair crews), where an arc can be used by the emergency responders when installation is completed. We propose Lagrangian relaxation formulations of the problem, which we solve using subgradient algorithm. A feasible solution is obtained using the Lagrangian relaxation, which provides an upper bound to the original problem. We test our problem with both real-world data and data sets from Beasley's OR Library to demonstrate the effectiveness of the algorithm in solving large-scale problem. The results shed light on critical components of a network whose restoration can aid emergency response efforts.

Second, we present a maximal multiple coverage and network recovery problem for the recovery and restoration of infrastructure systems after disasters. In the model, recovery crews make damaged arcs available by repairing components over a time horizon in a disrupted network. The model relocates emergency responders using the available arcs in the network to maximize multiple coverage of emergency service demand over the time horizon. We present two heuristics for the model. The first uses the Lagrangian and the linear programming relaxation solutions of the problem, and the second uses an integer rounding procedure applied to the linear programming relaxation solution. We test the model using a real-world example representing the road infrastructure and emergency services of the Bronx Borough in New York, NY during Hurricane Sandy. Our computational study suggests that our model can aid emergency managers in achieving their goals by scheduling effective restoration activities for real-time disaster recovery and long-term recovery planning. The results show that the heuristics and algorithms are effective for solving large–scale problem instances.

Third, we model the recovery of interdependent infrastructure systems after disasters as a non-cooperative game in a two-layer network, each belongs to a player. The goal of the model is to plan short term recovery of infrastructure systems after disaster in which each player wants to minimize the cost to satisfy their own demand. For comparison, we present a centralized model, where a central decision maker controls the restoration decisions of both players. The central decision maker plays a role as an authority/third player in the game and splits the recovery budget to each player according to the social welfare solution, which is the optimal solution of the centralized model. In addition, the central decision maker provides incentives to players to motivate them for collaboration in the non-cooperative game. A mechanism is proposed to decide incentives using an inverse optimization method and the inverse optimization mechanism is compared with another mechanism based on an $\alpha$-approximation algorithm to decide the fees for using inter-edges. The goal of the mechanisms is to set incentives so that a pure Nash equilibrium aligns

with the social welfare solution. We compare the Nash equilibria in which players use fees obtained from the mechanisms. We prove that with the inverse optimization method fees, the centralized optimal solution value becomes a pure Nash equilibrium, and with the $\alpha$-approximation algorithm fees, the centralized model optimal solution value becomes an $\alpha$-approximate pure Nash equilibrium in the facility location and restoration games. We use the potential function method to analyze the efficiency of the game using the Price of Stability (PoS). We present a case study in which we consider the recovery efforts of telecommunication infrastructure companies and provide results for the facility location and restoration games.

# Chapter 1

# Introduction

## 1.1 Overview

Critical infrastructure is physical systems such that emergency services, telecommunication, power and transportation services that play an essential role in the functioning of security, safety and economy of the society. Disasters can damage critical infrastructure systems and interfere these basic services. For example, in 2012, Hurricane Sandy caused an estimated $\$65$ billion in damage to the East Coast of the United States including damaging road and transportation infrastructure. The Tappan Zee Bridge, the Bayonne Bridge, the Hugh L. Carey Tunnel, and the Queens-Midtown Tunnel were all seriously damaged (Force (2013)). The damage resulted in severe consequences. For example, a fire that occurred during the hurricane in Breezy Point, a neighborhood in the New York City borough of Queens, destroyed 126 houses. Serious damage to the roads made it difficult for responders to reach the houses in a timely manner, allowing the fire to spread and ultimately destroy more houses (Jennings (2013)). Also, Hurricane Sandy created 15 million cubic yards of debris due to the strong winds and heavy rains. The debris blocked roads, tunnels and transportation corridors in the effected areas and made the trips longer. Further, during Hurricane Katrina, around 2,000 cell towers were damaged. Destruction of the communications companies' facilities and so the communication services, which disaster victims rely on creates vulnerabilities to response disaster casualties (Miller (2006)). The

main goal of recovery efforts is reducing the impacts of disasters on communities to protect public safety. Results of these studies suggest that considering interdependencies between infrastructure systems may contribute to the effective recovery process after disasters for the public safety. In the proposal, we present three research models that apply integer programming formulations to model the recovery of infrastructure systems by including interdependencies.

In Chapter 2, we study how to coordinate the recovery efforts of road repair crews and emergency responders after disaster to effective response to disasters. We do so by introducing and analyzing integrated network design and scheduling models that determine how two types of service responders should work together to guide the restoration and recovery of infrastructure such as roads so that emergency services can be better delivered during the recovery period. The models locate emergency responders (facilities) on a network over a finite time horizon while network recovery crews install damaged arcs. The installation part of the models is modeled as a scheduling problem with identical parallel servers (the repair crews), where an arc can be used by the emergency responders when installation is completed. We propose Lagrangian relaxation formulations of the models, which we solve using subgradient algorithm. A feasible solution is obtained using the Lagrangian relaxation, which provides an upper bound to the original models. We test our models with both real-world data and data sets from Beasley's OR Library to demonstrate the effectiveness of the algorithm in solving large-scale models.

In Chapter 3, we present a maximal multiple coverage and network recovery problem that considers the interdependency between disaster recovery performance of the network recovery crews and emergency service responders. This model studies how to effectively cover emergency demands with backup coverage by locating and relocating emergency responders on a network, subject to relocation restrictions, while recovering a network over a finite time horizon. After restoration is completed, the disrupted components become available in the network. Emergency responders deliver emergency relief and services

more effectively by changing locations as more components in the network are restored during the recovery process. The restoration of the network represents repairing physical components of the road infrastructure. The proposed model coordinates both scheduling and assignments of network repair crews and activities of emergency response crews. The model combines three different parts in one model. The network recovery part models arc installations by identical repair crews over a finite time horizon. The relocation part models location changes of emergency responders using arcs that are initially available or become available following restoration. The coverage part considers covering demands with backup if there are available arcs in the network to do so. We introduce two heuristics, each of which provides a feasible solution for the problem as well as a lower bound to the optimal objective function value. The first heuristic is based on the Lagrangian relaxation solution procedure and the second heuristic is based on an integer rounding procedure for the linear programming relaxation. We present a detailed case study using real world data from Bronx Borough during Hurricane Sandy. We include computational studies to demonstrate the effectiveness of the heuristics. The solution sheds light on the prioritization of the network restoration and relocation activities of emergency responders after disasters to achieve better emergency demand coverage.

In Chapter 4, we propose a game theoretical approach to model the interdependencies between critical infrastructure systems. We study facility location and restoration games with two players as a two–layer network in which each network layer belongs to a player. Each layer consists of facility location and demand nodes as well as the edges between them. Players locate facilities at potential facility location nodes within their layers. Each demand node needs to be connected to at least one facility in the two–layer network using the available edges. There are two types of edges in the network: intra– and inter–edges. *Intra–edges* (within each player's layer) connect a player's demand nodes to the player's facility location nodes. *Inter–edges* (between layers) connect a player's demand nodes to the other player's facility location nodes. In addition to the initially available edges in the

network, each player can install intra–edges within their layer or install inter–edges between layers. Each player can only install intra– and inter–edges that are connected to their own facilities. We capture the interdependencies between the layers by allowing each player to install inter–edges for the other player and to share facilities with each other. The goal of each player is to minimize the cost to satisfy demand in their own network using facilities in both layers that are connected to their own demand by available edges. Players pay a cost for each of their facility that they open and for each intra– and inter–edge that they use to satisfy their demand. We assume that an edge between a facility node and a demand node belongs to the player who owns the facility. If a player uses an inter–edge to satisfy their own demand, the player pays a fee to the other player who installs the edge and owns the facility, in addition to the cost of using the inter–edge. Each player has a budget to install intra– or inter– edges in the two-layer network. The main goal of this chapter is to provide mechanisms using an inverse optimization method and $\alpha$ approximation algorithm to decide the fees for using inter–edges. The goal of the mechanisms is to set fees so that the pure Nash equilibrium of the game aligns with the centralized model optimal solution. In the centralized model, a central decision maker decides the location of facilities, assigns facilities to demand using available edges, and installs new edges in the two–layer network. The objective of the centralized model is to minimize the total cost of satisfying the demand of all players. Due to the multi–agent ownership of the interdependent infrastructure systems, we cannot guarantee that players will obey the central decision maker, which leads us to a non–cooperative setting. We prove that when players use the fees, the optimal solution of the centralized model becomes a pure Nash equilibrium and when players use the $\alpha$–approximation algorithm fees, the optimal solution of the centralized model becomes an $\alpha$–approximation pure Nash equilibrium. We present a case study in which we use telecommunication infrastructure companies and provide results for the facility location and restoration games. Computational results show the effectiveness of the mechanism designs to achieve a Nash equilibrium, which aligns with the optimal solution of the

centralized model.

## 1.2 Integer Programming

We provide a brief introduction to integer programming, which involves making decisions under given data with decision variables restricted to be integer.

### 1.2.1 Integer Programming Modeling

Let $A$ is a $n \times n$ matrix of coefficients. Let $c \in \mathbb{R}^n$ and $b \in \mathbb{R}^n$ are vectors of coefficients. An integer programming model can be expressed in a canonical form as:

$$\begin{aligned} Z_{IP} := \min\ & c^T x \\ \text{subject to } & Ax \geq b \\ & x \in \mathbb{Z}^n \end{aligned} \tag{IP}$$

Binary integer programming or 0-1 integer programming is the special case of the integer programming when integer variables can only be 0 or 1 (i.e., $x \in \{0,1\}^n$).

Since the integer programming models restrict variables to be only integers, the problems generally hard to solve. Hence, various number of techniques and methodologies are used to obtain a feasible solution. General first step for these methodologies is to relax the integer variables (i.e., $x \in [0,1]^n$), then we obtain a linear relaxation of the integer programming model. Rounding the linear relaxation solution to construct a feasible solution for the integer programing is a technique commonly applied, but it is possible to obtain an infeasible solution by simple rounding. Another well used method is relaxing a constraint, which possible makes the integer programming hard to solve and putting the relaxed

constraint to objective function with weight (the Lagrangian multiplier), called Lagrangian relaxation. We describe the Lagrangian relaxation technique next.

### 1.2.2 Lagrangian Relaxation

Let us introduce the Lagrangian relaxation [1] of the IP problem. Let $u$ is a dual variable for every constraint of $Ax \geq b$. The $u > 0$ is a vector of Lagrangian multiplier in $\mathbb{R}^n$. Then the Lagrangian relaxation problem is

$$Z(u) := \min\ c^T x + u^T(b - Ax) \tag{1.2.1}$$

$$x \in \mathbb{Z}^n \tag{1.2.2}$$

which provides a lower bound on $Z_{IP}$ and the tightest of all bounds is

$$Z_D := \max Z(u).$$

**Theorem 1.1.** *$Z(u)$ provides a lower bound for $Z_{IP}$.*

*Proof.* Let $x^\star$ be the optimal solution to the IP problem.

$$Z(u) \leq c^T x^\star + u^T(b - Ax^\star) \leq Z_{IP}$$

Since $x^\star$ is the optimal solution, the inequality follows from the equality $Z_{IP} = c^T x^\star$ and inequality $Ax^\star \geq b$, where $u \geq 0$. □

Lagrangian relaxation has been applied to many combinatorial optimization problems. The solution of the algorithm is useful for several ways. The lower bound obtained using the Lagrangian relaxation provides a lower bound in a branch and bound algorithm for the original problem. Then the lower bound can guide us to choose branching variable

[1] Notation and information in this section are adapted from Fisher (2004).

in the next branch. In addition a good quality feasible solution can be constructed using the Lagrangian relaxation solution. We apply the Lagrangian relaxation to the models we present in Chapter 2 and 3.

### 1.2.3 Facility Location Problems

In this section, we briefly describe facility location problems that have been widely used in many different application areas by government agencies and private companies. [2] One of the most important areas that facility location problems have been used is to locate emergency service facilities to optimize the response time for emergencies. We present two well-studied location problems, namely the P-median problem and the maximal coverage location problem. The models presented in Chapter 2 and 3 are drawn upon facility location literature.

#### P - Median Problem

The goal of the P - median problem is to identify the location of P facilities on a network so that the total weighted distance between facility locations and demand points is minimized. Let us introduce parameters and decision variables to formulate the integer programming formulation of the problem.

*Parameters:*

- $I$ = the set of demand nodes
- $J$ = the set of facility location nodes
- $d_i$ = demand at node $i \in I$
- $P$ = the number of facilities to locate
- $c_{ij} =$ distance between demand node $i \in I$ and facility location node $j \in J$

[2] Notation and information in this section are adapted from Daskin (2011).

*Decision variables:*

- $z_{ij}$ = 1 if demand node $i \in I$ is served by a facility at node $j \in J$, otherwise 0.
- $y_j$ = 1 if a facility is located at node $j \in J$, otherwise 0.

With this notation, the P-median problem may be formulated as follows:

$$\min \sum_{i \in I} d_i c_{ij} z_{ij} \tag{1.2.3}$$

$$\text{s.t} \sum_{j \in J} z_{ij} = 1 \qquad \text{for } i \in I \tag{1.2.4}$$

$$z_{ij} \leq y_j \qquad \text{for } i \in I,\ j \in J \tag{1.2.5}$$

$$\sum_{j \in J} y_j \leq P \tag{1.2.6}$$

$$y_j \in \{0, 1\} \qquad \text{for } j \in J \tag{1.2.7}$$

$$z_{ij} \in \{0, 1\} \qquad \text{for } i \in I, j \in J \tag{1.2.8}$$

The objective function (1.2.3) minimizes the total demand weighted distance between each demand node and the facility location node. Constraint (1.2.4) ensures each demand node is served by only one facility. Constraint set (1.2.5) ensures that demand node $i \in I$ is served by location $j \in J$ if a facility is located at node $j \in J$ (e.g. $y_j = 1$). Constraint 1.2.11 requires to locate at most $P$ facilities at location nodes in the $J$. Constraint (1.2.7) and (1.2.8) are the integrality constraints on the decision variables.

Next, we present another well-studied location problem, namely maximal coverage problem.

**Maximal Coverage Location Problem**

The goal of the maximal coverage location problem is to maximize the number of demand that can be reached within the required service standard using a given number of locations. The additional list of parameters, variables and the integer programming formulation of the problem are as follows.

*Parameter:*

- $N_i$ = { j | if facility $j \in J$ can cover demand node $i$ }

*Decision variables:*

- $x_i$ = 1 if demand node $i \in I$ is covered, otherwise 0.

With this notations, the maximal coverage problem may be formulated as follows:

$$\max \sum_{i \in I} d_i x_i \tag{1.2.9}$$

$$\text{s.t } x_i \leq \sum_{j \in N_i} y_j \qquad \text{for } i \in I \tag{1.2.10}$$

$$\sum_{j \in J} y_j \leq P \tag{1.2.11}$$

$$y_j \in \{0, 1\} \qquad \text{for } j \in J \tag{1.2.12}$$

$$x_i \in \{0, 1\} \qquad \text{for } i \in I \tag{1.2.13}$$

The objective function (1.2.9) maximizes the number of demand covered. Constraint set (1.2.10) requires at least one facility located in any locations in the set $N_i$ to consider demand at the node $i \in I$ to be covered. Constraint (1.2.11) requires to locate at most $P$ facilities at location nodes in the set $J$. Constraint (1.2.12) and (1.2.13) are the integrality constraints on the decision variables.

There are many variations of the maximal coverage problem and P-median problem in the literature as well as different methodologies including the Lagrangian relaxation algorithm to solve them. In Chapter 2 and 3, we present combinatorial optimization problems from the facility location problem literature. In Chapter 4, we present a game theoretical approach applied to a combinatorial optimization problem.

## 1.3 Game Theory

Game theory is a way to model interactions between agencies [3]. Game theory can contribute important insight in the combinatorial optimization when decision makers are involved with combinatorial optimization problems and classic optimization theory does not suffice. A game includes a set of players $N = \{1, \ldots, n\}$, and for each player a set of strategies and payoffs that describe the outcome of the game (wins or loses). Strategy set includes information about what a player do in every possible situation. Let's assume there are two players. Player I chooses a strategy from the set of possible strategies for Player 1 and then Player II chooses a strategy from the set of possible strategies for Player 2, then they play the game and compute the payoff for each player. *Zero sum game* is one of the most known game in the game theory in addition to the *Prisoner's dilemma*. In a *zero sum game*, the amount one player wins, the other loses.

There are mainly two themes of games, namely *cooperative games* and *non-cooperative games*. In the *cooperative games*, the players are collaborating to achieve better payoff and the joint revenue reasonably distributed between players who join the collaboration. In the *noncooperative games*, each player acts independently to maximize its own payoff given its belief on how other players behave.

Next, we present brief information about *non–cooperative games* and *cooperative games*. We refer the reader to Barron (2013) and Curiel (2013) for more detailed information about

[3] Notation and information in this section are adapted from Barron (2013).

game theory and its applications.

### 1.3.1 Non–cooperative Games

The non–cooperative games consider a game in which players are competing with each other. The main concept in the non–cooperative games is Nash equilibrium.

Let's $S_n$ be the strategy set for player $n \in N$ and $z_n$ be a strategy profile of player $n$. When each player $n \in N = \{1, 2\}$ chooses strategy $z_n$ then Player 1 obtains payoff $u_1(z_1, z_2)$ and Player 2 obtains payoff $u_2(z_1, z_2)$. Thus $u(z_1, z_2) = (u_1(z_1, z_2), u_2(z_1, z_2))$ is the payoff function evaluated at $(z_1, z_2) \in S_1 \times S_2$. Note that the payoff depends on the strategy profile chosen by Player 1 as well as the strategies chosen by Player 2. As a result, $(S_1 \times S_2, u)$ is a non-cooperative game with 2 players.

**Definition 1.** *A strategy profile $z^* \in S_1 \times S_2$ is a Nash equilibrium if no unilateral deviation in strategy by any single player is profitable for that player, i.e.,*

$$z_1 \in S_1 : u_1(z_1^*, z_2^*) \leq u_1(z_1, z_2^*)$$

$$z_2 \in S_2 : u_2(z_1^*, z_2^*) \leq u_2(z_1^*, z_2)$$

**Definition 2.** *An $\alpha$–approximate equilibrium is a pair of strategies $(z_1^\star, z_2^\star)$ with payoffs $u_1(z_1^\star, z_2^\star)$ and $u_2(z_1^\star, z_2^\star)$ such that if the best response to $z_2^\star$ has payoff $u_1(\bar{z}_1, z_2^\star)$ and the best response to $z_1^\star$ has payoff $u_2(z_1^\star, \bar{z}_2)$ then $u_1(z_1^\star, z_2^\star) \geq \alpha u_1(\bar{z}_1, z_2^\star)$ and $u_2(z_1^\star, z_2^\star) \geq \alpha u_2(z_1^\star, \bar{z}_2)$ (Feder et al. (2007)).*

**Definition 3.** *A game is an exact potential game if and only if a potential function $\phi$ exist such that*

$$\phi(\hat{z}_1, \bar{z}_2) - \phi(\bar{z}_1, \bar{z}_2) = u_1(\hat{z}_1, \bar{z}_2) - u_1(\bar{z}_1, \bar{z}_2)$$

$$\phi(\bar{z}_1, \hat{z}_2) - \phi(\bar{z}_1, \bar{z}_2) = u_2(\bar{z}_1, \hat{z}_2) - u_2(\bar{z}_1, \bar{z}_2)$$

*for $\hat{z}_1, \bar{z}_1 \in S_1$, $\hat{z}_2, \bar{z}_2 \in S_2$.*

**Definition 4.** *The price of stability (PoS) of a game is the ratio between the best objective function value of one of its equilibrium and that of an optimal social outcome. The PoS is relevant for games in which there is some objective authority that can influence the players a bit, and maybe help them converge to a good Nash equilibrium.*

**Theorem 1.2.** *Suppose there is a potential function $\phi$ for a potential game, and assume further that for any outcome S, we have*

$$\frac{cost(S)}{A} \leq \phi(S) \leq B \cdot cost(S) \tag{1.3.1}$$

*for some constants $A, B \geq 0$, where $cost(S)$ is the social cost function which is the sum of the players' costs under one decision maker. Then the price of stability is at most $A \cdot B$ (Tardos and Wexler (2007), Theorem 19.13).*

In Chapter 4, we present a non–cooperative game applied to a combinatorial optimization problem. We show that the game is a potential game and we find a bound for the price of stability. Further, we provide two mechanism design algorithms based on an inverse optimization and an $\alpha$–approximation algorithm to provide players incentives to motivate players for collaborating in the non–cooperative setting.

**Inverse Optimization**

Inverse optimization problems are defined as follows: Let $F$ denote the set of feasible solutions of an optimization problem $P = \min\{cx : x \in F\}$ in which $c$ is a specified cost vector. Let $x^\star$ be a given feasible solution. The solution $x^\star$ may or may not be an optimal solution of $P$ with respect to the cost vector $c$. The inverse optimization problem is to perturb the cost vector $c$ to $d$ so that $x^\star$ is an optimal solution of $P(d) = \min\{dx : x \in F\}$ with respect to $d$ and $||d - c||$ is minimum, where $||d - c||_p$ is some selected $L_p$ norm (Ahuja and Orlin (1998)).

**Primal–dual method**

Let us consider the linear program

$$\min c^T x$$
$$\text{subject to:} Ax \geq b$$
$$x \geq 0$$

and its dual

$$\max b^T y$$
$$\text{subject to:} A^T y \leq c$$
$$y \geq 0$$

where $A \in Q^{m \times n}$, $c, x \in Q^n$, and $b, y \in Q^m$. Let's assume that $c \geq 0$. In the primal-dual method of Dantzig, Ford, and Fulkerson, they assume that we have a feasible solution $y$ to the dual. Initially we can set $y = 0$. In the primal-dual method, either we will be able to find a primal solution $x$ that obeys the complementary slackness conditions with respect to $y$, thus proving that both $x$ and $y$ are optimal, or we will be able to find a new feasible dual solution with a greater objective function value (Goemans and Williamson (1997)).

## 1.4 Contributions

We propose three research models that apply integer programming formulations to model the network design and formation problems with the application to interdependent infrastructure systems.

In Chapter 2, we introduce an integrated restoration and location problem (IRLP) and model the interdependencies between road infrastructure system and emergency

service providers. We study a P-median model variation with the goal of minimizing the cumulative weighted distance between emergency responders and demand nodes over a time horizon. We also introduce the c-IRLP, an extension to this model to approximately model components of disrupted arcs between demand and facility locations. The models can be used to model the delivery of a variety of time-sensitive critical services after a disaster event occurs. The models provide insight into how the activities of the two types of service providers should be coordinated and which network components should be restored sooner during recovery.

In the Chapter 3, we introduce a maximal multiple coverage and network restoration problem (MMCaNR) for recovery and restoration of infrastructure systems after disasters. The MMCaNR problem is a maximal expected coverage problem variation with the goal of maximizing cumulative multiple coverage of emergency service demand over the time horizon. The MMCaNR problem solution provides insights into how to prioritize disrupted component installations into the network and relocate emergency responders to cover demand more effectively using available arcs following the installations.

In the Chapter 4, we establish a game–theoretic framework to provide a fundamental understanding for a class of facility location and restoration problems in a non–cooperative setting. We present two different versions of non–cooperative facility location and restoration games. The first version is *the strict control facility location and restoration* (SC–FLR) game and the second version is *the limited control facility location and restoration* (LC-FLR) game. We show that both versions of the game are potential games and we prove the existence of a pure Nash equilibrium for each version by constructing a potential function for the games. We compare the optimal solution value of the centralized model with the total payoffs of both players in the pure Nash equilibria of the games and provide a bound for price of stability using the potential function method. We propose mechanisms using an inverse optimization method and $\alpha$ approximation algorithm to decide the fees for using inter–edges. We prove that when players use the inverse optimization fees, the optimal solution

of the centralized model aligns with the total cost of the pure Nash equilibrium and when players use $\alpha$–approximation algorithm fees, the optimal solution of the centralized model becomes $\alpha$–approximation pure Nash equilibrium. We provide computational results for two telecommunication companies in Chicago to show the effectiveness of the mechanism designs by comparing the Nash equilibria payoffs with the optimal solution value of the centralized model. In the computational results, we observe that the total payoffs of the players in the Nash equilibrium obtained by minimizing the potential function is the closest one to the optimal solution value of the centralized model compare to others.

# Chapter 2

# An Integrated Network Design and Scheduling Problem for Network Recovery and Emergency Response

## 2.1 Introduction

Emergency services play an integral role in responding to emergencies during and immediately after a disaster strikes to reduce both human suffering and property loss. At these times, delivering time-sensitive services and commodities is critically important for minimizing the risk to human life and health. For example, in 2012, Hurricane Sandy caused an estimated $65 billion in damage to the East Coast of the United States including damaging road and transportation infrastructure. The Tappan Zee Bridge, the Bayonne Bridge, the Hugh L. Carey Tunnel, and the Queens-Midtown Tunnel were all seriously damaged by Hurricane Sandy (Force (2013)). As a result of damage to these bridges and other transportation infrastructure, the affected regions experienced increased congestion and commute times that lasted for days after Hurricane Sandy (Kaufman et al. (2012)). The damage resulted in severe consequences. For example, a fire that occurred during

the hurricane in Breezy Point, a neighborhood in the New York City borough of Queens, destroyed 126 houses. Serious damage to the roads made it difficult for responders to reach the houses in a timely manner, allowing the fire to spread and ultimately destroy more houses (Jennings (2013)). Also, Hurricane Sandy created 15 million cubic yards of debris due to the strong winds and heavy rains. The debris blocked roads, tunnels and transportation corridors in the effected areas and made the trips longer (FEMA (2013b)).

Damage to critical infrastructure can make the delivery of emergency services more difficult and increase response time during the recovery period. For example, in many disasters, damaged roads may have reduced capacity or may be impassable due to debris. Early stages of disaster recovery necessitate repairing this damage to critical infrastructure at the same time as critical services are delivered, thus aiding emergency response efforts. This chapter studies how to coordinate these recovery efforts. We do so by introducing and analyzing integrated network design and scheduling models that determine how two types of service responders should work together to guide the restoration and recovery of infrastructure such as roads so that emergency services can be better delivered during the recovery period.

Few papers in the literature focus on interdependent infrastructure and network recovery to quantify the performance of the dependent infrastructures over a time horizon or planning period. However, there are some notable exceptions. Several papers formulate and solve network restoration problems in which infrastructure systems with critical system services are modeled as network flows (Lee et al. (2007)). Nurre et al. (2012) introduce a new integrated network design and scheduling problem (INDS) that allows recovery crews to install nodes and arcs in the network to maximize the cumulative weighted flow through the network over a time horizon. This model can be used for short-term restoration and disaster preparedness activities. The installation components of our models have similar constraints to the model proposed by Nurre et al. (2012).

Cavdaroglu et al. (2013) propose an extension to INDS that also includes interdependencies between infrastructure systems. Instead of studying the performance of the system, the researchers focus on how quickly services are restored over the time horizon. Sharkey et al. (2015a) extend the interdependent layered network model of Lee et al. (2007, 2009) to measure the performance of a system over the restoration period. They build upon the work of Cavdaroglu et al. (2013) to consider damage scenarios that require restoration decisions for all infrastructure. Nurre and Sharkey (2014) analyze 12 different INDS problems and show that all INDS problems are at least NP-hard. A related paper by Gutfraind et al. (2012) introduces the neighbor-aided network installation problem as a discrete optimization problem to minimize the total cost of recovering a network. The authors propose a simple rule for recovering basic infrastructure networks by choosing the most accessible damaged network nodes in every iteration. Baxter et al. (2014) introduce an incremental network design problem with shortest paths that focuses on network maintenance instead of network expansion in order to minimize the total cost over the planning grid. Likewise, Engel et al. (2013) propose a theoretical framework to the incremental network design problem with minimum spanning trees. Maya Duque et al. (2016) introduce the Network Repair Crew Scheduling and Routing Problem (NRCSRP). They optimize the accessibility of demands by scheduling and routing a single recovery crew to repair roads starting from a single depot. Averbakh and Pereira (2012) introduce the Flowtime Network Construction Problem (FNCP) and the weighted version of this problem (FNCP-W). They schedule the repairing of all unavailable vertices by a single recovery crew with the objective to minimize the total recovery time of the vertices.

We study network recovery in P-median model variations. Several other studies address related issues of recovery, reliability, and vulnerability in P-median models. Wang et al. (2003) consider simultaneously opening new facilities and closing existing facilities with the objective of minimizing the total weighted travel distance for customers. They develop greedy interchange, Tabu search, and Lagrangian relaxation heuristics for the model.

Reliability is a related issue in P-median models, where network damage is modeled as facilities that are sometimes unavailable for service. Snyder and Daskin (2005) present location models that minimize cost, including the expected transportation cost of facility failure, with the goal of choosing facility locations that are concurrently reliable and inexpensive under traditional objective functions. They present reliability models for the P-median and uncapacitated fixed charge location problems, and they propose a Lagrangian relaxation algorithm to solve the models. Cui et al. (2010) propose a reliability facility location design model that extends the work of Snyder and Daskin (2005) to consider site-dependent failure probabilities as opposed to identical failure probabilities for all locations. O'Hanley et al. (2013) study the unreliable $P$-median problem by considering site-dependent failure probabilities. They introduce a technique to linearize site-dependent failure probabilities of the facilities. A limitation of these papers is that they consider independent facility failures rather than cascading failures, which limits their applicability and do not address network restoration.

Another stream of papers relevant to disasters and large-scale emergencies studies vulnerability and protection strategies in location models (Scaparra and Church (2008); Church and Scaparra (2007)). Church et al. (2004) introduce the $r$-interdiction median (RIM) problem and the $r$-interdiction covering (RIC) problem to identify the most critical facilities in the systems. These papers address the problem of identifying network protection strategies. The RIM model eliminates $r$ facilities to maximize the cumulative weighted distance, and the RIC model maximizes the amount of demand no longer covered after $r$ facilities are removed. Losada et al. (2012) propose a bilevel mixed integer linear program to optimize resilience of the system against worst-case losses. They account for recovery time of facilities and multiple disruption probabilities over time in the model. Çelik et al. (2015) consider the Stochastic Debris Clearance Problem (SDCP), which finds a sequence of roads to clear with the objective of maximizing satisfied relief demand. They model SDCP using partially observable Markov decision processes (POMDPs) that consider stochasticity

in the debris (demand).

In this study, we make the following contributions:

1. We propose a new P-median problem variation that studies the interdependency between two types of service providers: network recovery crews who install arcs in the network and emergency response crews who are located at available facility locations where they deliver essential services. We schedule the installation of arcs over a finite time horizon by network recovery crews. Emergency responders can use these arcs once installation is complete to serve demand in demand points. The goal is to minimize the weighted cumulative distance between the emergency responders and the demand points over the time horizon. An extension to this model approximately models path-based arc installations between demand and facility locations. The proposed models are novel in that they coordinate the activities of two types of service providers, whose restoration activities are interdependent.

2. We introduce Lagrangian relaxation techniques to efficiently solve the models. We formulate and solve the Lagrangian relaxation dual problems using subgradient optimization, which yields a lower bound to the optimal objective function value. We propose heuristics to obtain a feasible solution to the models and an upper bound to the optimal objective function value using the Lagrangian relaxation.

3. We conduct extensive computational studies to demonstrate how these algorithms improve the time to solve the original models, and we discuss key insights gained from solving the models. The model solutions shed light on critical components of a network whose restoration can aid emergency response efforts.

The remainder of the chapter is organized as follows. Section 2.2 provides the mathematical formulation of our models, applies the Lagrangian relaxation method to our models, and shows how to solve the relaxed models using subgradient optimization. It

also provides a heuristic for finding feasible solutions to our models using the Lagrangian relaxation solution. Section 2.3 reports computational results and discusses the practical insights obtained from the results. The models and analysis shed light on the network components that should be prioritized during network recovery. Section 2.4 provides concluding remarks.

## 2.2 Model Formulation

In this section, we introduce integrated network design and restoration models for recovering a network while providing emergency response services, and we formulate the models as integer programming models. The goal of the models is to coordinate the activities of two types of crews: emergency responders and repair crews. This is done by locating emergency responders and scheduling repair crews over a finite time horizon. At each time period, the models locate P emergency responders at open facilities in the network. The models also assign demand to open stations using available arcs in the network. This is accomplished using a multi-period P-median model, where locations are selected over time while allowing disrupted network components to be installed by network recovery crews over a time horizon. Some arcs are initially available and can be used to assign demand to open stations at any time period, and other arcs must be installed by the repair crews over a finite time horizon and can be used upon installation. To guide the decisions made over the time horizon, the objective is to minimize the cumulative weighted distance between the emergency responders and the demands over the time horizon. We first introduce the base model, and then we introduce an extension to this model.

### 2.2.1 Integrated Restoration and Location Problem (IRLP)

We start with a connected network $G = (I, A)$ where $I$ is the set of demand nodes and $A$ is the set of initially operational arcs in the network. Let $J \subset I$ be the set of potential facility

locations and $A'$ consist of all disrupted arcs that are not initially available in the network. Each arc $(i, j) \in A'$ has an associated integral installation time $p_{ij}$ and can be installed by one of the $K$ identical recovery crews over a finite horizon of $T$ time periods, which we model as a parallel machine scheduling sub-problem (Pinedo and Hadavi (1992)). Once installation is completed, an arc can be used by the emergency responders to serve demand beginning in that time period. Each demand node $i \in I$ has demand $w_{it}$ in time period $t = 1, \ldots, T$, and every arc $(i, j) \in A \cup A'$ has distance $d_{ij}$. In each time period, we locate emergency responders at $P$ of the $|J|$ potential facilities, thus making the facility open, and we assign one of these open facilities to each demand point $i \in I$. The emergency responders can be relocated in each time period. The objective is to minimize the cumulative demand-weighted distance between the demand points and facility locations over the time horizon $T$.

The model has two parts: (1) the design part locates the emergency responders at the available facilities and (2) the recovery part schedules the installation of some of the arcs. There are two types of decision variables that correspond to these two model parts. All decision variables are binary variables.

The *design decision variables* are

- $x_{ijt} = 1$ if arc $(i, j) \in A \cup A'$ is used to assign an emergency responder at facility $j$ to demand node $i$ at time $t$ and $0$ otherwise, for $t = 1, \ldots, T$, and
- $y_{jt} = 1$ if an emergency responder is located at $j \in J$ at time $t$ and $0$ otherwise, for $t = 1, \ldots, T$.

The *recovery decision variables* are

- $\beta_{ijt} = 1$ if arc $(i, j) \in A'$ is operational at time $t$ and $0$ otherwise, for $t = 1, \ldots, T$, and

- $\alpha_{kijt} = 1$ if network recovery crew $k$ completes the installation of arc $(i,j) \in A'$ at time $t$ and 0 otherwise, for $t = 1, \ldots, T$.

We formulate our model as an integer programming model as follows.

$$Z = \min \sum_{t=1}^{T} \sum_{(i,j)\in A\cup A'} w_{it} d_{ij} x_{ijt} \tag{2.2.1}$$

$$\text{s. t.} \sum_{j:(i,j)\in A\cup A'} x_{ijt} = 1 \qquad \text{for} \quad i \in I,\ t = 1, \ldots, T \tag{2.2.2}$$

$$\sum_{j\in J} y_{jt} \leq P \qquad \text{for} \quad t = 1, \ldots, T \tag{2.2.3}$$

$$x_{ijt} - y_{jt} \leq 0 \qquad \text{for} \quad (i,j) \in A \cup A',\ t = 1, \ldots, T \tag{2.2.4}$$

$$x_{ijt} \in \{0,1\} \qquad \text{for} \quad (i,j) \in A \cup A',\ t = 1, \ldots, T \tag{2.2.5}$$

$$y_{jt} \in \{0,1\} \qquad \text{for} \quad j \in J,\ t = 1, \ldots, T \tag{2.2.6}$$

$$x_{ijt} \leq \beta_{ijt} \qquad \text{for} \quad (i,j) \in A',\ t = 1, \ldots, T \tag{2.2.7}$$

$$\sum_{(i,j)\in A'} \sum_{s=t}^{\min\{T, t+p_{ij}-1\}} \alpha_{kijs} \leq 1 \qquad \text{for} \quad k = 1, \ldots, K,\ t = 1, \ldots, T \tag{2.2.8}$$

$$\beta_{ijt} - \sum_{s=1}^{t} \sum_{k=1}^{K} \alpha_{kijs} \leq 0 \qquad \text{for} \quad (i,j) \in A',\ t = 1, \ldots, T \tag{2.2.9}$$

$$\sum_{t=1}^{p_{ij}-1} \beta_{ijt} = 0 \qquad \text{for} \quad (i,j) \in A' \tag{2.2.10}$$

$$\sum_{k=1}^{K} \sum_{t=1}^{p_{ij}-1} \alpha_{kijt} = 0 \qquad \text{for} \quad (i,j) \in A' \tag{2.2.11}$$

$$\alpha_{kijt} \in \{0,1\},\ \beta_{ijt} \in \{0,1\} \qquad \text{for} \quad (i,j) \in A',\ k = 1, \ldots, K,\ t = 1, \ldots, T \tag{2.2.12}$$

The objective (2.2.1) is to minimize the cumulative weighted distance between the demands and the closest open facilities over the time horizon. Constraint set (2.2.2) requires

each demand node to be served by one emergency responder at each time period using the initial or installed arcs. Constraint set (2.2.3) locates at most $P$ emergency responders at available facilities in the network in each time period. Constraint set (2.2.4) ensures that only open facilities serve each demand node. Constraint sets (2.2.5) and (2.2.6) require the design decision variables to be binary. Constraint set (2.2.7) ensures that the installable arcs in $A'$ can only be used to assign demand nodes to facilities if the arcs have been installed prior to the time they are used. This set of constraints links the design unit with the recovery unit. Constraint sets (2.2.8) - (2.2.12) represent the network recovery unit of the model. Constraint set (2.2.8) enforces the condition that at most one arc is installed by each recovery crew in each time period, where $\alpha_{kijt} = 1$ means recovery crew $k$ begins installation of arc $(i, j) \in A'$ at time $t - p_{ij} + 1$ and completes installation at time $t$. This arc can then be used by the emergency responders starting from time $t$. Constraint set (2.2.9) requires arc $(i, j)$ to be operational since $\beta_{ijt} = 1$ can only be set to one after installation is complete. Constraint sets (2.2.10) and (2.2.11) ensure that $\beta_{ijt}$ and $\alpha_{kijt}$ cannot be set to one before the processing time for arc $(i, j)$. Constraint set (2.2.12) requires the recovery decision variables to be binary.

We assume that all emergency responders locations $j \in J$ are connected to each other so that emergency responders can change their current positions at any time period with no cost by essentially moving in the network using available arcs. As discussed in Averbakh and Pereira (2012), traveling speed in initially available components is faster than installation speed so it is reasonable enough to have no cost associated with changing locations. Gendreau et al. (2006) consider no cost associated with relocation in their maximal expected coverage relocation problem (MECRP) formulation for emergency vehicles, however, the model contains an upper bound on the number of waiting site changes to limit relocation. This assumption is practical for our models in two ways; first, emergency responders can change locations easily and make other stations operational if they are responding to a call for service on the network, and then move to another station upon completion. Second, as

we discuss later, emergency responders do not change locations often even there is no cost for doing so, and hence, this assumption is not overly restrictive. Emergency responders could be fire fighters, paramedics, and first responders, and emergency locations could be fire and rescue stations as well as temporary facilities such as schools, libraries, and other public buildings, which can be used as community health service facilities after disasters. Hence, relocating emergency responders depending on the demand and recovery process could help to reach out more people. In the case when it is not practical for emergency responders to change locations, we can simply reformulate our model as a static emergency responder location problem by restricting the location variables $y_{jt}$ to be identical for all time periods by using $y_j$ for all $j \in J$ in (2.2.3), (2.2.4), and (2.2.6). In addition, we can consider capacitated facilities to capture the availability of the emergency responders by adding a capacity constraint for each potential facility location $j \in J$ at each time period as follows:

$$\sum_{i \in I} w_{it} x_{ijt} \leq Q_j y_{jt} \text{ for } j \in J,\ t = 1, 2, ..., T,$$

where $Q_j$ represents the capacity of the facility location $j \in J$.

IRLP has two parts. The design part consists of constraint sets (2.2.2) - (2.2.6) and the recovery part consists of constraint sets (2.2.8) - (2.2.12). These two parts are linked by constraint set (2.2.7). Hence, Lagrangian relaxation allows us to split the model into two parts. In the next section, we discuss how to apply Lagrangian relaxation to this set of constraints.

**Lagrangian Relaxation**

Lagrangian relaxation is one of the most commonly used methods for hard problems in combinatorial optimization. By dualizing the constraints that make the problem "hard," the Lagrangian problem becomes an easier problem (Fisher (2004)). In IRLP, constraint (2.2.7) links the design decision variables with the restoration decision variables. Applying

Lagrangian relaxation to this set of constraints is advantageous in several ways. First, doing so decomposes it into two parts (the design part and the recovery part), which are included in the objective with a penalty term. Therefore, the relaxation is easier to solve than the original model. Second, the Lagrangian relaxation problem solution offers a lower bound on the optimal solution to the original problem. Third, a feasible solution to the original model can be constructed from the Lagrangian relaxation problem solution, which provides an upper bound to the original problem. We use this upper bound as a cut in the branch and bound tree when solving the original model, thereby reducing the computation time needed to find an optimal solution.

Now, we present the Lagrangian relaxation problem formulation on constraint set (2.2.7). Let $u_{ijt}$ be Lagrangian multiplier for $(i,j) \in A',\ t = 1, \ldots, T$, then we define Lagrangian relaxation problem as following:

$$L(u) = \min \sum_{t=1}^{T} \sum_{(i,j)\in A\cup A'} w_{it} d_{ij} x_{ijt} + \sum_{t=1}^{T} \sum_{(i,j)\in A'} u_{ijt}[x_{ijt} - \beta_{ijt}]$$

or we can rewrite $L(u)$ as

$$L(u) = \min \sum_{t=1}^{T} \sum_{(i,j)\in A\cup A'} (w_{it} d_{ij} + u_{ijt}) x_{ijt} - \sum_{t=1}^{T} \sum_{(i,j)\in A'} u_{ijt}\beta_{ijt}$$

$$\text{s. t. } (2.2.2) - (2.2.6) \text{ and } (2.2.8) - (2.2.12)$$

The Lagrangian relaxation dual is

$$\max_{u\geq 0}\ L(u)$$

The Lagrangian relaxation dual remains NP-hard since the P-median problem is em-

bedded in it. However, in practice we can quickly solve the Lagrangian relaxation dual problem using subgradient algorithm. We discuss this next.

**Subgradient Algorithm**

Subgradient optimization is used to solve the Lagrangian relaxation problem and identify a lower bound to the original model by iteratively adjusting the Lagrangian multipliers $u^n$ in iteration $n$. Starting with the given inputs, initial Lagrangian multiplier $u^0$, initial upper bound $L^*$, and initial decreasing adaption parameter $\theta^0$, each iteration of the subgradient algorithm updates the previous Lagrangian multiplier with the step size in the positive subgradient direction. The algorithm checks if the new bound is better than the previous one. We start with $\theta^0 = 2$, as suggested in Held and Karp (1971). If there is no improvement in the bound after more than $N^\star$ iterations, we reduce $\theta$ by a factor of $1/2$. If the change in the Lagrangian multiplier is not smaller than $\epsilon$ after $N$ iterations, the algorithm terminates and returns $L_{best}$, which is the best lower bound found by the subgradient algorithm. We note that the choices for $N$ and $N^\star$ values are problem specific. We use $N = 100$ and $N^\star = 2$, and our solution procedure is not sensitive to these values. We first solve the linear programming relaxation of IRLP, and we use the "shadow prices" for the dual variables associated with constraint set (2.2.7) as the initial value for Lagrangian multiplier $u^0_{ijt}$. Using this initial value of $u^0$, we optimize the Lagrangian relaxation dual problem using the subgradient algorithm as in Martin (2012).

**Lagrangian Heuristic**

We now present a heuristic that constructs a feasible solution for IRLP using the Lagrangian relaxation problem solution. Let $\bar{\beta}, \bar{y}$ and $\bar{\alpha}$ denote a feasible solution for the Lagrangian relaxation problem. Our aim is to find $\bar{\bar{x}}$ values that are feasible for constraint set (2.2.7). Let $S_1$ denote the triplet $(i, j, t)$, where the arc $(i, j) \in A'$ is operational at time $t$ and the location $j$ is open at time $t$, defined as $S_1 = \{(i, j, t) \mid \bar{\beta}_{ijt} = 1 \text{ and } \bar{y}_{jt} = 1,\ (i, j) \in A'\}$ . Let

**Algorithm 1** Subgradient Optimization Algorithm for IRLP

**Initialize:**
An initial value $u^0 \geq 0$ (assign as the shadow price associated with the Lagrangian relaxation constraint in the linear programming relaxation)
$\theta^0 := 2$
$L_{best} = -\infty$
$L^* = \sum_{t=1}^{T} \sum_{(i,j)\in A} w_{it} d_{ij}$
**Subgradient iterations**
**for** $n := 0, \ldots, N$ **do**
  Solve for $L(u^n)$ which yields $x$ and $\beta$
  $\gamma_{ijt}^n := x_{ijt}^n - \beta_{ijt}^n$
  $t^n := \theta^n (L^* - L(u^n))/||\gamma^n||^2$  step size
  $u^{n+1} := \max\{0, u^n + t^n \gamma^n\}$
  **if** $||u^{n+1} - u^n|| < \epsilon$ **then**
    Stop
  **end if**
  $L_{best} = \max(L_{best}, L(u^n))$
  **if** $L_{best}$ does not improve after $N^\star$ iterations **then**
    $\theta^{n+1} := \theta^n / 2$
  **else**
    $\theta^{n+1} := \theta^n$
  **end if**
  $n := n + 1$
**end for**
**return** $L_{best}$

$S_2$ denote the triplet $(i, j, t)$, where the facility $j$ is open for arc $(i, j) \in A$, which are initially in the network as $S_2 = \{(i, j, t) \mid \bar{y}_{jt} = 1,\ (i, j) \in\ A\}$.

To construct feasible solutions for each $t = 1, \ldots, T$ and for each $i \in I$, we set $\bar{\bar{x}}_{ij^\star t} = 1$ for $j^\star$ that solves

$$j^\star \in \arg\min_{j\in J}\{\min_{j:(i,j,t)\in S_1} w_{it} d_{ij}\ ,\ \min_{j:(i,j,t)\in S_2} w_{it} d_{ij}\}$$

and set $\bar{\bar{x}}_{ijt} = 0$ for all other $(i, j) \in A \cup A'$ and $t = 1, \ldots, T$. This assigns the demand node at $i$ to the closest open facility $j$. The solution $\bar{\beta}, \bar{\bar{x}}, \bar{y}$ and $\bar{\alpha}$ is feasible since the $\bar{\beta}$, $\bar{y}$ and $\bar{\alpha}$ values obtained from the Lagrangian relaxation solution satisfy all constraints except the Lagrangian relaxation constraint set (2.2.7). With this assignment of $\bar{\bar{x}}$, constraint set (2.2.7)

is satisfied. Finding this feasible solution from the Lagrangian relaxation for IRLP gives us an upper bound for the IRLP. This upper bound is used as a cut value in the branch and bound tree of the original problem to reduce the tree size and improve computational time.

IRLP allows us to shorten direct arcs between demand points and emergency responder locations by installing arcs without considering other possible disrupted paths between same demand points and emergency responder locations. To capture this, we include multiple parallel versions of each disrupted arc in the network to allow installation of an arc to be completed in multiple ways. In the next section, we introduce a component based integrated restoration and location problem that allows us to include new installation structures in the model to approximately include these additional features in the model.

### 2.2.2 Component based IRLP (c-IRLP)

In this section, we present the component based IRLP (c-IRLP), an extension of IRLP that considers multiple parallel versions of any installable arc to capture the component-wise benefits of installed arcs. Instead of a single arc connecting $i$ to $j$ in $A'$ as in IRLP, we introduce several *components* between $i$ to $j$, each of which corresponds to a different road on a path that can be repaired. In the c-IRLP, if we use location $j$ to serve demand at $i$ in a network, then we could possibly do a quick repair of a component to decrease its distance and then repair another component later to decrease its distance even more by repairing another component in the path. Therefore, we allow for multiple parallel versions of the arc $(i, j)$ for each of its disrupted components, each with a different cost and processing time. In addition, the c-IRLP allows a single repair of a component in the network to benefit multiple arcs in $A'$ if multiple arcs share a common component such as a road.

The c-IRLP starts with the same connected network $G = (I, A)$ as in IRLP. Different from IRLP, we define a new set $C'$ as an installable component set and we install components instead of arcs. Each component is associated with one or more arcs that all share the

component. To capture all arcs that benefit from installation of a component, we define set $AC(c)$ for each $c \in C'$ that consists of arcs $(i, j) \in A'$ whose distances are decreased after installing component $c \in C'$. Note that $A' = \cup_{c \in C'} AC(c)$ is the set of arcs installed through components.

Each component $c \in C'$ has an associated integral installation time $p_c$ and can be installed by one of the $K$ identical recovery crews over a finite horizon of $T$ time periods. Once installation of a component $c$ is complete, arcs in $AC(c)$ associated with component $c$ can be used by emergency responders to serve demand at demand points.

As in IRLP, each demand node $i \in I$ has demand $w_{it}$ in time period $t = 1, \ldots, T$ and in each time period, we locate emergency responders at $P$ of the $|J|$ potential facilities. In this model we have multiple parallel versions of the arc each with different cost, therefore, we consider the distance between demand $i$ and emergency responder location $j$ using component $c$ as $d_{cij}$. We also define $d_{0ij}$ as the initial distance between $i$ and $j$ before any installation for arcs $(i, j) \in A$. Similar to IRLP, the emergency responders can be relocated in each time period. The objective is to minimize cumulative demand-weighted distance between the demand points and facility locations over the time horizon $T$.

The model has two parts as in IRLP, and all decision variables are binary variables. In this model, we redefine the decision variables $x$, $\beta$, and $\alpha$. The variable $y$ is the same as in IRPL.

The *design decision variables* are

- $\tilde{x}_{cijt} = 1$ if arc $(i, j) \in A \cup A'$ is used to assign an emergency responder at facility $j$ to demand node $i$ at time $t$ by using installed component $c$ and $0$ otherwise, for $t = 1, \ldots, T$,
- $\tilde{x}_{0ijt} = 1$ if arc $(i, j) \in A$ is used to assign an emergency responder at facility $j$ at time $t$ by using initially available arc $(i, j) \in A$ and $0$ otherwise, for $t = 1, \ldots, T$ and

- $y_{jt} = 1$ if an emergency responder is located at $j \in J$ at time $t$ and 0 otherwise, for $t = 1, \ldots, T$.

The *recovery decision variables* are

- $\tilde{\beta}_{ct} = 1$ if component $c \in C'$ is operational at time $t$ and 0 otherwise, for $t = 1, \ldots, T$, and
- $\tilde{\alpha}_{kct} = 1$ if network recovery crew $k$ completes the installation of component $c \in C'$ at time $t$ and 0 otherwise, for $t = 1, \ldots, T$.

We formulate our model as an integer programming model as follows.

$$Z = \min \sum_{t=1}^{T} \sum_{c \in C'} \sum_{(i,j) \in AC(c)} w_{it} d_{cij} \tilde{x}_{cijt} + \sum_{t=1}^{T} \sum_{(i,j) \in A} w_{it} d_{0ij} \tilde{x}_{0ijt} \tag{2.2.13}$$

$$\text{s. t.} \sum_{c \in C'} \sum_{j:(i,j) \in AC(c)} \tilde{x}_{cijt} + \sum_{j:(i,j) \in A} \tilde{x}_{0ijt} = 1 \quad \text{for} \quad i \in I,\ t = 1, \ldots, T \tag{2.2.14}$$

$$\sum_{j \in J} y_{jt} \leq P \quad \text{for} \quad t = 1, \ldots, T \tag{2.2.15}$$

$$\tilde{x}_{cijt} - y_{jt} \leq 0 \quad \text{for} \quad c \in C',\ (i,j) \in AC(c),\ t = 1, \ldots, T \tag{2.2.16}$$

$$\tilde{x}_{0ijt} - y_{jt} \leq 0 \quad \text{for} \quad (i,j) \in A,\ t = 1, \ldots, T \tag{2.2.17}$$

$$\tilde{x}_{cijt} \in \{0, 1\} \quad \text{for} \quad c \in C',\ (i,j) \in AC(c),\ t = 1, \ldots, T \tag{2.2.18}$$

$$\tilde{x}_{0ijt} \in \{0, 1\} \quad \text{for} \quad (i,j) \in A,\ t = 1, \ldots, T \tag{2.2.19}$$

$$y_{jt} \in \{0, 1\} \quad \text{for} \quad j \in J,\ t = 1, \ldots, T \tag{2.2.20}$$

$$\tilde{x}_{cijt} \leq \tilde{\beta}_{ct} \quad \text{for} \quad c \in C',\ (i,j) \in AC(c),\ t = 1, \ldots, T \tag{2.2.21}$$

$$\sum_{c \in C'} \sum_{s=t}^{\min\{T, t+p_c-1\}} \tilde{\alpha}_{kcs} \leq 1 \quad \text{for} \quad k = 1, \ldots, K,\ t = 1, \ldots, T \tag{2.2.22}$$

$$\tilde{\beta}_{ct} - \sum_{s=1}^{t} \sum_{k=1}^{K} \tilde{\alpha}_{kcs} \leq 0 \quad \text{for} \quad c \in C',\ t = 1, \ldots, T \tag{2.2.23}$$

$$\sum_{t=1}^{p_c-1} \tilde{\beta}_{ct} = 0 \quad \text{for} \quad c \in C' \tag{2.2.24}$$

$$\sum_{k=1}^{K}\sum_{t=1}^{p_c-1}\tilde{\alpha}_{kct}=0 \qquad \text{for} \quad c\in C' \tag{2.2.25}$$

$$\tilde{\alpha}_{kct}\in\{0,1\},\ \tilde{\beta}_{ct}\in\{0,1\} \qquad \text{for} \quad c\in C',\ k=1,\ldots,K,\ t=1,\ldots,T \tag{2.2.26}$$

Constraint sets (2.2.13)-(2.2.20) and (2.2.22)-(2.2.26) are analogous to constraint sets (2.2.1)-(2.2.6) and (2.2.8)-(2.2.12) in IRLP, respectively. The objective (2.2.13) is to minimize the cumulative weighted distance between the demands and the closest open facilities using available arcs after component installations or initial arcs in the network over the time horizon. Constraint set (2.2.14) requires each demand node to be served by one emergency responder at each time period using the initial arcs or arcs that become available after installation of components. The most important change is in (2.2.21), which ensures that component $c$ in $C'$ can only be used to assign demand node $i$ to facility $j$ if the component $c$ has been installed prior to the time period and the installation of component $c$ shortens the distance between $i$ and $j$ (i.e., $(i,j)\in AC(c)$). Constraint set (2.2.21) links the design part with the recovery part as in IRLP.

As shown in A.1, unit processing times that are identical for all components in $C'$ (i.e.,without loss of generality $p_c=1$ for all $c\in C'$) allow us to remove many variables and constraints, which drastically simplifies the integer programming formulation. In this simplified version of the model, we select $K$ components to install at each time period instead of assigning component installation jobs to individual recovery crews. This simplification results in decreased computational times, even for experiments with long time horizons and large recovery crews.

As in IRLP, the Lagrangian relaxation allows us to split the c-IRLP model into two parts by relaxing constraint set (2.2.21). In the next section, we discuss how we need to adjust the Lagrangian relaxation algorithm we present in Section 2.2.1 to solve the c-IRLP.

**Lagrangian Relaxation and Subgradient Algorithm**

Now, we present the Lagrangian relaxation problem formulation on constraint set (2.2.21). Let $u_{cijt}$ be Lagrangian multiplier for $c \in C',\ (i,j) \in AC(c),\ t = 1, \ldots, T$, analogous to Lagrangian relaxation in Section 2.2.1. Therefore, we briefly highlight new differences.

After simplifying the relaxed formulation, we can write the Lagrangian relaxation problem $L(u)$ as

$$L(u) = \min \sum_{t=1}^{T} \sum_{c \in C'} \sum_{(i,j) \in AC(c)} \left(w_{it} d_{cij} + u_{cijt}\right) \tilde{x}_{cijt} + \sum_{t=1}^{T} \sum_{(i,j) \in A} w_{it} d_{0ij} \tilde{x}_{0ijt} - \sum_{t=1}^{T} \sum_{c \in C'} \sum_{(i,j) \in AC(c)} u_{cijt} \tilde{\beta}_{ct}$$

$$\text{s. t. } (2.2.14) - (2.2.20) \text{ and } (2.2.22) - (2.2.26)$$

The Lagrangian relaxation dual is

$$\max_{u \geq 0} L(u)$$

We solve the Lagrangian relaxation dual problem using a subgradient algorithm as for IRLP. Algorithm 1 can be applied to the c-IRLP with two minor modifications. Line 1 in the Algorithm 1 must change to $L^* = \sum_{t=1}^{T} \sum_{(i,j) \in A} w_{it} d_{0ij}$ and line 5 must change to $\gamma^n_{cijt} := \tilde{x}^n_{cijt} - \tilde{\beta}^n_{ct}$. The remaining parts of the subgradient algorithm in Section 2.2.1 remain the same.

**Lagrangian and Linear Relaxation Heuristic**

We now present a heuristic that constructs a feasible solution for the c-IRLP. We do so by obtaining a feasible solution to the Lagrangian relaxation of the c-IRLP, and enhancing the

feasible solution using the linear relaxation solution of the c-IRLP.

Danna et al. (2005) uses an approach to obtain a feasible solution to a mixed integer programming model better than the current incumbent solution by enhancing the solution using a linear relaxation solution. We use a similar approach. We can obtain an incumbent solution using the Lagrangian relaxation, however, it does not satisfy the constraint set (2.2.21). Contrarily, the linear relaxation solution satisfies all of the constraint sets except the integrality constraints. We combine these two solutions to find a feasible solution that satisfies all of the constraint sets by first identifying the variables that take the same values in the Lagrangian and linear relaxation solutions, and fixing these variables, thus forming a partial solution. Let $\bar{x}, \bar{y}$ denote values of the design decision variables for the Lagrangian relaxation problem solution, and let $\bar{\bar{x}}, \bar{\bar{y}}$ denote values of the design decision variables for the linear relaxation problem solution. Then we define sets $S_1 = \{(c, i, j, t) : \bar{x}_{cijt} = \bar{\bar{x}}_{cijt}\}$ and $S_2 = \{(j, t) : \bar{y}_{jt} = \bar{\bar{y}}_{jt}\}$, which denote the values of $\tilde{x}$ and $y$ variables that have the same values in the Lagrangian and linear relaxation solutions, respectively. Note that the values of $\tilde{x}$ and $y$ are integer in the set $S_1$ and $S_2$. We fix the values of the $\tilde{x}$ and $y$ variables in the c-IRLP for the indexes in the sets $S_1$ and $S_2$, respectively. Then, we solve the c-IRLP that yields a solution that is feasible for the constraint sets (2.2.13)-(2.2.26) and is an upper bound for the optimal objective function. Even though we solve an NP-complete problem, this method can be computationally efficient since many of the variables are fixed in this procedure. For example, in our experiments in the following section, we fix approximately 80 to 90 percent of $\tilde{x}$ variables and 5 to 10 percent of $y$ variables that have the same values in the Lagrangian and linear relaxation solutions. In addition, we use sets $S_1$ and $S_2$ to set starting values for the variables $x$ and $y$, respectively, in the standard implementation. Using the partial solution as a starting point helps the solver obtain an incumbent solution faster than without setting the starting point. Hence, this approach can improve the computation time compare to the computation time of the model using standard implementation.

## 2.3 Computational Results

In this section, we present and analyze computational results using both real-world data representing road infrastructure and emergency medical calls for Hanover County, Virginia, United States and data sets from Beasley's OR Library (Beasley, 2015).

### 2.3.1 Computational Results for IRLP

Computations for IRLP were performed on a computer with a 2.6 GHz Intel Core 5 Duo Processor with 8 GB of RAM. We used CPLEX 12.6.2.0 to solve the integer programming model that was coded in GAMS. Each experiment was run with a 3600-second time limit.

The Hanover County data has $|I| = 125$ demand nodes and $|J| = 16$ fire and rescue stations (available facilities). We assume that our available facilities and demand nodes are located in the center of each grid point. Since disasters are rare, the emergency calls for service observed after a single disaster may be insufficient to represent the anticipated demand for all demand points. Therefore, we use data aggregated over a 31 month period to estimate post-disaster demand, and we assume that the demand that would occur in a short period of time after a disaster is proportional to the aggregated demand data over a long period. This assumption appears to be reasonable based on the data we collected after Hurricane Irene in 2011. We use real distances, $d_{ij}$, in miles, from facility location $j$ to call location $i$ in the disrupted arc set $|A'| = 325$, where $d_{ij} \leq 6$ and in the initial connected network arc set $A$, where $d_{ij} > 6$. In addition, lengthened versions of the arcs in $A'$ are contained in the initial connected network arc set $A$, where $|A| = 2000$. Processing times, $p_{ij}$, are integers randomly generated from a discrete $U[1, 3]$ distribution. We allow $P = 8$ available facilities to be open in each time period. Since our model considers short-term repair of the road network components, we consider the time horizon as a day and vary the number of time periods $T$ and the number of network recovery crews $K$.

We also test the model and algorithm with two data sets, each consisting of 100 demand

nodes from Beasley's OR Library uncapacitated P-median data sets (Pmed1 and Pmed3). The data sets provide a graph, which we use as the initial graph $G = (I, A)$, the number of open facilities $P$, and arc distances associated with each arc. In both data sets, we set $J = I$ and $w_{it}$ are randomly generated from a continuous uniform $U(0, 1)$ distribution for each demand node $i \in I$. We assume $w_{it}$ stays the same at each time period $t = 1, \ldots, T$ for each demand node $i \in I$. The installable arc set $A'$ contains the three shortest arcs for each demand point. The distances of the arcs in $A'$ are equal to the values in the original data set from Beasley's OR Library. Lengthened versions of these arcs are contained in the set of initially available arcs $A$. The distances of the lengthened arcs in $A$ are increased by half of their original distances from Beasley's data for each arc that also appears in $A'$. The distances of the remaining arcs in $A$ are not disrupted, and therefore they are equal to the original distances given in Beasley data. Processing times $p_{ij}$ for each arc $(i, j) \in A'$ are randomly generated from a discrete uniform $U[1, 2]$ distribution. We consider each time horizon as a day and vary the time horizon $T$ and the number of network recovery crews $K$ in the computational experiments as in the Hanover County data experiments.

Tables 2.1 and 2.2 summarize the objective values and running times for the Hanover County data set and for the data sets from Beasley's OR Library, respectively. The $|A|$, $|A'|$ and $|J|$ columns report the number of arcs initially in the network, number of installable arcs, and the number of facility locations, while the columns labeled $K$ and $T$ report the number of recovery crews and the length of the time horizon. The "Lagrangian Relaxation (LR) Lower Bound" column reports the lower bound values obtained from the Lagrangian relaxation and the running time in seconds in parentheses. The LR lower bounds are better than the lower bounds obtained from the linear programming relaxations for all experiments in Tables 2.1 and 2.2. The Lagrangian heuristic identifies upper bounds for the optimal values, which are shown in the "Lagrangian Relaxation (LR) Upper Bound" column. The column "Optimal Solution Using LR Upper Bound" reports the objective function value and the cumulative computation time in parentheses. These solutions are

| $\|A\|$ | $\|A'\|$ | $\|I\|$ | $\|J\|$ | $P$ | $K$ | $T$ | Linear Relaxation Lower Bound | Lagrangian Relaxation (LR) Lower Bound | Lagrangian Relaxation (LR) Upper Bound | Optimal Solution Using LR Upper Bound | Optimal Solution Without Using LR Upper Bound |
|---|---|---|---|---|---|---|---|---|---|---|---|
| 2000 | 325 | 125 | 16 | 8 | 3 | 10 | 39.42 (4) | 42.43 (9) | 49.48 (14) | 45.19 (25) | 45.19 (16) |
| 2000 | 325 | 125 | 16 | 8 | 4 | 10 | 38.75 (3) | 41.81 (12) | 49.06 (16) | 44.44 (49) | 44.44 (35) |
| 2000 | 325 | 125 | 16 | 8 | 5 | 10 | 38.13 (4) | 41.32 (14) | 49.11 (17) | 43.79 **(57)** | 43.79 (83) |
| 2000 | 325 | 125 | 16 | 8 | 3 | 15 | 57.59 (5) | 62.17 (30) | 73.69 (29) | 66.07 **(224)** | 66.07 (674) |
| 2000 | 325 | 125 | 16 | 8 | 4 | 15 | 56.33 (11) | 61.35 (48) | 79.58 (56) | 64.76 **(198)** | 64.76 (967) |
| 2000 | 325 | 125 | 16 | 8 | 5 | 15 | 55.25 (16) | 60.15 (31) | 72.42 (39) | 63.66 **(568)** | 63.66 (1006) |
| 2000 | 325 | 125 | 16 | 8 | 3 | 20 | 75.06 (17) | 81.49 (33) | 97.16 (41) | 86.30 **(272)** | 86.30 (1946) |
| 2000 | 325 | 125 | 16 | 8 | 4 | 20 | 73.17 (24) | 79.90 (46) | 97.00 (55) | 84.38 **(466)** | 84.38 (1946) |
| 2000 | 325 | 125 | 16 | 8 | 5 | 20 | 71.57 (39) | 78.71 (57) | 96.71 (68) | 82.81 **(548)** | 82.81 (793) |
| 2000 | 325 | 125 | 16 | 8 | 3 | 24 | 88.63 (30) | 96.36 (56) | 117.11 (67) | 102.12 **(552)** | 102.12 (1965) |
| 2000 | 325 | 125 | 16 | 8 | 4 | 24 | 86.21 (50) | 94.24 (78) | 117.61 (88) | 99.70 **(372)** | 99.75 (3600) **(Gap** $0.06\%$**)** |
| 2000 | 325 | 125 | 16 | 8 | 5 | 24 | 84.19 (77) | 92.84 (105) | 115.00 (120) | 97.85 **(464)** | 97.95 (3600) **(Gap** $0.17\%$**)** |
| 2000 | 325 | 125 | 16 | 8 | 3 | 30 | 108.43 (67) | 118.46 (95) | 143.62 (107) | 125.27 **(2001)** | 125.99 (3600) **(Gap** $0.6\%$**)** |
| 2000 | 325 | 125 | 16 | 8 | 4 | 30 | 105.19 (152) | 115.86 (194) | 143.88 (209) | 122.27 **(865)** | 124.00 (3600) **(Gap** $1.58\%$**)** |
| 2000 | 325 | 125 | 16 | 8 | 5 | 30 | 102.50 (230) | 113.90 (261) | 144.05 (289) | 119.99 **(1228)** | 120.00 (3600) **(Gap** $0.02\%$**)** |

Table 2.1: Improvements in the optimal solutions for IRLP using Lagrangian upper bounds for the Hanover County data. Computational time, in seconds, is shown in the parentheses. "Optimal Solution Using LR Upper Bound" reports the objective function value and the computation time using CPLEX Lagrangian heuristic upper bound in the branch and bound tree and "Optimal Solution Without Using Upper Bound" reports the optimal objective function value and the computation time when using CPLEX without the Lagrangian heuristic upper bound.

| | $\|A\|$ | $\|A'\|$ | $\|I\|$ | $\|J\|$ | $P$ | $K$ | $T$ | Linear Relaxation Lower Bound | Lagrangian Relaxation (LR) Lower Bound | Lagrangian Relaxation (LR) Upper Bound | Optimal Solution Using LR Upper Bound | Optimal Solution Without Using LR Upper Bound |
|---|---|---|---|---|---|---|---|---|---|---|---|---|
| Pmed1 | 10000 | 300 | 100 | 100 | 5 | 3 | 10 | 28434.87 (157) | 29500.21 (209) | 31960.94 (213) | 30244.43 **(327)** | 30244.43 (1195) |
| | | | | | | 4 | 10 | 27890.37 (173) | 29259.65 (201) | 32060.34 (205) | 29979.35 **(769)** | 29979.35 (887) |
| | | | | | | 5 | 10 | 27484.74 (171) | 29183.47 (231) | 31660.91 (236) | 29793.31 (785) | 29793.31 (562) |
| | | | | | | 3 | 15 | 41577.88 (421) | 43805.66 605) | 47719.55 (611) | 44853.09 **(1086)** | 44853.09 (3171) |
| | | | | | | 4 | 15 | 40843.32 (301) | 43682.06 (346) | 47693.86 (353) | 44509.49 **(1237)** | 44509.49 (2040) |
| | | | | | | 5 | 15 | 40384.06 (245) | 43651.92 (348) | 48254.89 (514) | 44296.61 **(1244)** | 44296.61 (1332) |
| | | | | | | 3 | 20 | 54504.287 (591) | 58289.95 (737) | 63433.44 (624) | 59403.17 (3600) **(Gap** 0.05%**)** | 59443.37 (3600) (Gap 0.18%) |
| | | | | | | 4 | 20 | 53733.75 (477) | 58205.75 (606) | 64102.98 (612) | 59011.63 **(2636)** | 59024.50 (3600) (Gap 0.07%) |
| | | | | | | 5 | 20 | 53274.33 (611) | 58146.70 (736) | 62707.89 (742) | 58798.15 **(2122)** | 58798.15 (2141) |
| Pmed3 | 10000 | 300 | 100 | 100 | 10 | 3 | 10 | 19870.12 (71) | 20772.03 (89) | 22988.81 (91) | 21514.02 **(1260)** | 21514.02 (1381) |
| | | | | | | 4 | 10 | 19356.51 (73) | 20519.53 (94) | 23155.06 (98) | 21325.4 (3420) | 21325.4 (2878) |
| | | | | | | 5 | 10 | 18971.67 (85) | 20397.49 (97) | 23147.13 (100) | 21199.18 (3600) (Gap 0.48%) | 21206.93 (3600) (Gap 0.45%) |
| | | | | | | 3 | 15 | 28777.47 (359) | 30686.42 (580) | 34663.63 (586) | 31947.38 (3600) **(Gap** 0.05%**)** | 32155.81 (3600) (Gap 1.19%) |
| | | | | | | 4 | 15 | 28065.82 (344) | 30531.11 (396) | 34770.12 (402) | 31948.37 (3600) (Gap 1.49%) | 31779.40 (3600) (Gap 0.97%) |
| | | | | | | 5 | 15 | 27603.22 (254) | 30488.25 (299) | 34774.21 (305) | 31308.17 (3600) **(Gap** 0.12%**)** | 31309.97 (3600) (Gap 0.14%) |
| | | | | | | 3 | 20 | 37456.98 (475) | 40710.83 (588) | 46627.35 (595) | 43303.03 (3600) **(Gap** 3.09%**)** | 47968.59 (3600) (Gap 12.5%) |
| | | | | | | 4 | 20 | 36679.15 (338) | 40623.7 (466) | 46216.43 (472) | 42070.64 (3600) **(Gap** 1.15%**)** | 42081.40 (3600) (Gap 1.15%) |
| | | | | | | 5 | 20 | 36214.41 (254) | 40617.78 (388) | 46249.88 (394) | 41438.53 (3600) **(Gap** 0.06%**)** | 41470.72 (3600) (Gap 0.29%) |

Table 2.2: Improvements in the optimal solutions for IRLP using Lagrangian upper bounds for Beasley's data. Computational time, in seconds, is shown in the parentheses. "Optimal Solution Using LR Upper Bound" reports the objective function value and the computation time using CPLEX Lagrangian heuristic upper bound in the branch and bound tree and "Optimal Solution Without Using Upper Bound" reports the optimal objective function value and the computation time when using CPLEX without the Lagrangian heuristic upper bound.

found using the Lagrangian heuristic upper bound as a cut value in the branch and bound tree of the original model. With this improvement, all instances in Table 2.1 were solved to optimality within the 3600-second limit, and the optimality gap of almost all instances decreased within the 3600-second limit in Table 2.2. The last column entitled “Optimal Solution Without Using Upper Bound" reports the optimal objective function value and the computation time in parentheses when using CPLEX without the Lagrangian heuristic upper bound. The computation time in the column “Optimal Solution Using LR Upper Bound” includes the CPLEX time to solve the linear relaxation, to obtain the upper bound using Lagrangian relaxation, and to solve the model. The computation time in the column “Optimal Solution Without Using Upper Bound" only includes the time to calculate the optimal solution for the original model.

The choice of step size in the Lagrangian relaxation is important, since the convergence of the algorithm depends on the step size. We observe that the Polyak step size formula $t_k = \frac{\theta^k(L^\star - L(u^k))}{||\gamma^k||^2}$ (Polyak, 1987) results in a fast convergence in the subgradient algorithm for computational experiments for the Hanover County and Beasley’s OR Library’s data sets.

In Table 2.1, ten of the fifteen experiments solve to optimality within the 3600-second limit without using the upper bound, while in Table 2.2, nine of the eighteen experiments solve optimally within the 3600-second limit without using the upper bound. As we can observe in the Table 2.1 and Table 2.2, CPLEX requires more time to find an optimal solution over the longer time horizons, which is not surprising, since the number of decision variables and the number of constraints increase with the length of the time horizon $T$. Total times using different methods are comparable. Using the upper bound as a cut value in the branch and bound tree improves the computation times for thirteen of the fifteen and eight of the eighteen experiments (shown in boldface) in the two rightmost columns in Table 2.1 and 2.2, respectively. In addition, using the upper bound as a cut value in the branch and bound tree decreases the optimality gap for six out of eighteen experiments

(shown in boldface) in Table 2.2. Also, in the experiment with $T = 10$ and $K = 3$ for the Pmed3 data set, the resulting best integer feasible solution using using the upper bound as a cut value in the branch and bound tree is better than the best integer feasible solution without using upper bound.

Tables 2.1 and 2.2 report algorithm running times and objective function values. We can further examine the solutions produced by the models. To do so we represent the objective function value as the sum of the objective function value recorded in each time period, which captures the minimum cumulative weighted distance

$$z_t = \sum_{(i,j)\in A\cup A'} w_{it} d_{ij} x_{ijt}, \text{ for } t = 1, \ldots, T$$

and $Z = \sum_{t=1}^{T} z_t$.

We compare our results to two static comparison cases that consider a single time period time $T = 0$ and $T = \infty$. To do so we solve the canonical P-median problem with network $G = (I, A)$ for $T = 0$ and with $G = (I, A \cup A')$ for $T = \infty$, which reflect the network when no arcs and all arcs are installed, respectively. We report the objective function values, in Figure 2.1 and the locations of the open facilities in Table 2.3. This allows us to compare emergency responder locations in the model solutions to those prior to recovery efforts in damaged networks ($T = 0$) and in networks that are fully functional ($T = \infty$).

Figure 2.1 shows the values of $z_t$ over the time horizon for the experiment $K = 5$ and $T = 10$ using the Hanover County data set. The objective function value $z_t$ starts with highest value at $t = 0$ (refers to a single time period $T = 0$) since no arcs are installed yet, and it decreases over the time horizon as the network recovery crews finish installing arcs from $A'$, which are then used by the emergency responders to decrease the average distance. The best possible single period objective function value occurs at $t = \infty$ when all arcs are installed.

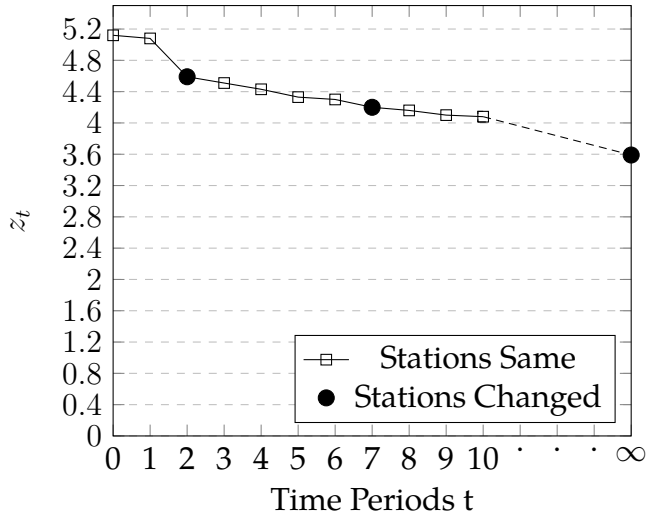


Figure 2.1: Objective function value for IRLP accrued in each time period for $K = 5$ and $T = 10$ for the Hanover County data set, where $t = 0$ represents the objective value without any repair and $t = \infty$ represents the objective value after all arcs are installed.

| | | Time Periods t | | | | | | | | | | |
|---|---|---|---|---|---|---|---|---|---|---|---|---|
| Facilities | T = 0 | 1 | 2 | 3 | 4 | 5 | 6 | 7 | 8 | 9 | 10 | T = ∞ |
| 1 | × | × | | | | | | | | | | × |
| 2 | | | | | | | | | | | | |
| 3 | | | | | | | | | | | | × |
| 4 | × | × | × | × | × | × | × | × | × | × | × | × |
| 5 | | | | | | | | | | | | |
| 6 | × | × | × | × | × | × | × | × | × | × | × | × |
| 7 | × | × | × | × | × | × | × | × | × | × | × | × |
| 8 | × | × | × | × | × | × | × | | | | | |
| 9 | | | | | | | | × | × | × | × | |
| 10 | × | × | × | × | × | × | × | × | × | × | × | × |
| 11 | | | | | | | | | | | | × |
| 12 | | | | | | | | | | | | |
| 13 | | | | | | | | | | | | |
| 14 | × | × | × | × | × | × | × | × | × | × | × | |
| 15 | | | × | × | × | × | × | × | × | × | × | × |
| 16 | × | × | × | × | × | × | × | × | × | × | × | |

Table 2.3: Open Facilities for IRLP for the Hanover County data set in each time period for $K = 5$ and $T = 10$. $T = 0$ shows open facilities using only initial arcs in the network, $T = \infty$ shows open facilities after repairing all arcs.

Table 2.3 shows locations of the open facilities over the time horizon for the instance with $K = 5$ and $T = 10$. The locations of open facilities change two times during this experiment, which are also indicated in Figure 2.1. In time period 2, Facility 1 closes and Facility 15 opens, and in time period 7, Facility 8 closes and Facility 9 opens. By allowing the model to change the location of some of the emergency responders, the average distance between nodes and emergency responders is further reduced between time periods. Hence, changing emergency responder locations improves emergency responders response times during the recovery phase. We observed at most two changes in the locations of the emergency responders in all of the computational experiments reported in Table 2.1 even there is no cost for doing so. In some of our experiments not reported in this study, we observed up to 5 changes in locations when a large portion of the road infrastructure is damaged (i.e., $|A'|$ is large relative to $|A|$).

Figure 3.5 provides a visual representation of the optimal restoration plan for the instance with $K = 5$ and $T = 10$ including the arcs used to assign demand to an emergency responder for time periods 0, 5 and 10. Thin lines show arcs from $A$ and thick lines show installed arcs from $A'$ used in the optimal solution for given time periods. Figure (3.5a) shows the optimal solution with initial arcs in the network selected from $A$. Figure (2.3b) and (2.3c) show the solution after five and ten time periods, respectively, and the thick black lines in these sub-figures illustrate the arcs that have been installed. The number of installed arcs changes depending on the number of recovery crews, the time periods, and processing times of the installed arcs. Our computational experiments suggest that it is best to install arcs that are connected to the most critical facility locations prior to and after emergency responders are located there. As a result, the recovery crews are essentially co-located with the emergency responders. The solutions can help decision-makers decide where to initially locate emergency responders after a disaster strikes, as well as how to move these responders during the recovery phase. The solutions therefore shed light on how to prioritize the installation of arcs in a recovery plan to aid in the delivery of

time-critical services.

### 2.3.2 Computational Results for Component Based IRLP (c-IRLP)

Computations for the c-IRLP were performed on a computer with a 1.4 GHz Intel Core 5 Duo Processor with 4 GB of RAM. We used Gurobi 6.5.2. to solve the integer programming model that was coded in Python. Each experiment was run with a 3600-second time limit.

We use the Hanover County data set as described in Section 2.3.1 for the c-IRLP with $|C'| = 971$ installable components. The sets $AC(c)$ represent the arcs in $A'$ that are shortened when component $c \in C'$ is installed, with $|AC(c)| \leq 5$ and $\cup_{c \in C'} AC(c) = A'$. Processing times for installable components, $p_c$, are integers randomly generated from a discrete $U[1, 5]$ distribution. If the installation of a component affects several arcs, the processing time of the component is assigned as a randomly generated integer from a discrete $U[2, 5]$. As in IRLP, we allow $P = 8$ available facilities to be open in each time period, and we vary the number of time periods $T$ and the number of network recovery crews $K$ in the computational experiments.

Table 2.5 summarizes the objective values and running times for the Hanover County data set. The $|A|$, $|C'|$ and $|J|$ columns report the number of arcs initially in the network, number of installable components, and the number of facility locations, while the columns labeled $K$ and $T$ report the number of recovery crews and the length of the time horizon. The "Lagrangian Relaxation (LR) Lower Bound" column reports the lower bound values obtained from the Lagrangian relaxation and the running time in seconds in parentheses. The LR lower bounds are better than the lower bounds obtained from the linear programming relaxations for all experiments in Table 2.5. We report the upper bound we obtained from Lagrangian and linear relaxation heuristic introduced in Section 2.2.2 in the column "Lagrangian and Linear Relaxation Upper Bound" which yields better upper bounds than the upper bounds using the Lagrangian heuristic. The "Optimal Solution w/ Starting

Partial Feasible Solution" column reports the optimal solution and the computation time when we set starting values for variables $x$ and $y$ for the indexes in the set $S_1$ and $S_2$ that we describe in the Section 2.2.2. Note that the computation time includes the time to compute sets $S_1$ and $S_2$. The last column entitled "Optimal Solution w/ Standard Implementation" reports the optimal objective function value and the computation time in parentheses when solving the model using standard implementation. A time limit of 3600 seconds was imposed for all instances. Six out of nine experiments are solved optimally while three out of nine experiments yielded a solution with an optimality gap of less than 0.26% within the time limit. We observe that using the Lagrangian and linear relaxation heuristic, we obtain an upper bound within $3\%$ of the optimal solution value within 2074 seconds for each experiment. In eight out of nine experiments, computational times of the upper bound are shorter than the computational times of the optimal solution using standard implementation. In addition, when we set starting values for the variables $x$ and $y$ for indexes in $S_1$ and $S_2$, respectively, five out of nine experiments result in faster computation times or an improved gap.

Figure 2.2 shows the values of $z_t$ over the time horizon for the c-IRLP instance with $K = 5$ and $T = 10$ using the Hanover County data set. We observe a decreasing pattern in the objective function value $z_t$ over the time horizon as the recovery crews install components from set $C'$ and then emergency responders use arcs which benefit from the installed components. Table 2.4 shows the locations of the open facilities over the time horizon for same instance. The locations of open facilities change once during this experiment, which are also indicated in Figure 2.2. In time period 3, Facility 14 closes and Facility 3 opens.

Figure 2.4 provides a visual representation of the optimal restoration plan for the instance with $K = 5$ and $T = 10$ including the arcs used to assign demand to an emergency responder for time periods 0, 5 and 10. Thin lines show arcs from $A$ and thick lines show arcs from $A'$ whose distances shorten by using installed components from $C'$ and used in the optimal solution up until that time period. At the end of the time horizon 10, 39

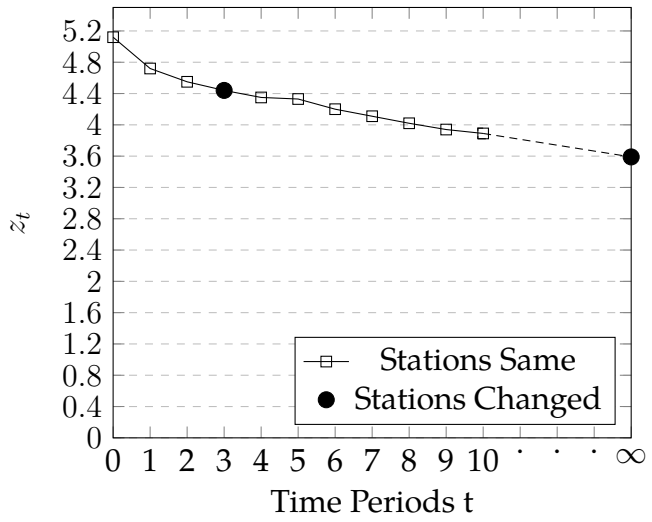


Figure 2.2: Objective function value of the c-IRLP accrued in each time period for $K = 5$ and $T = 10$ for the Hanover County data set, where $t = 0$ represents the objective value without any repair and $t = \infty$ represents the objective value after all components are installed.

| | | Time Periods t | | | | | | | | | | |
|---|---|---|---|---|---|---|---|---|---|---|---|---|
| Facilities | T = 0 | 1 | 2 | 3 | 4 | 5 | 6 | 7 | 8 | 9 | 10 | T = $\infty$ |
| 1 | × | × | × | × | × | × | × | × | × | × | × | × |
| 2 | | | | | | | | | | | | |
| 3 | | | | × | × | × | × | × | × | × | × | × |
| 4 | × | × | × | × | × | × | × | × | × | × | × | × |
| 5 | | | | | | | | | | | | |
| 6 | × | × | × | × | × | × | × | × | × | × | × | × |
| 7 | × | × | × | × | × | × | × | × | × | × | × | × |
| 8 | × | × | × | × | × | × | × | × | × | × | × | |
| 9 | | | | | | | | | | | | |
| 10 | × | × | × | × | × | × | × | × | × | × | × | × |
| 11 | | | | | | | | | | | | × |
| 12 | | | | | | | | | | | | |
| 13 | | | | | | | | | | | | |
| 14 | × | × | × | | | | | | | | | |
| 15 | | | | | | | | | | | | × |
| 16 | × | × | × | × | × | × | × | × | × | × | × | |

Table 2.4: Open Facilities for the c-IRLP for the Hanover County data set in each time period for $K = 5$ and $T = 10$. $T = 0$ shows open facilities using only initial arcs in the network, $T = \infty$ shows open facilities after repairing all components.

| $\|A\|$ | $\|C'\|$ | $\|I\|$ | $\|J\|$ | $P$ | $K$ | $T$ | Linear Relaxation Lower Bound | Lagrangian Relaxation Lower Bound | Lagrangian & Linear Relaxation Upper Bound | Optimal Solution w/ Starting Partial Feasible Solution | Optimal Solution w/ Standard Implementation |
|---|---|---|---|---|---|---|---|---|---|---|---|
| 2000 | 971 | 125 | 16 | 8 | 3 | 25 | 93.52 (43) | 96.93 (82) | 104.49 (196) | 102.35 (219) | 102.35 (176) |
| 2000 | 971 | 125 | 16 | 8 | 4 | 25 | 89.47 (46) | 93.73 (85) | 101.79 (381) | 99.22 **(262)** | 99.22 (281) |
| 2000 | 971 | 125 | 16 | 8 | 5 | 25 | 86.30 (56) | 91.35 (113) | 99.76 (651) | 96.91 **(638)** | 96.91 (1371) |
| 2000 | 971 | 125 | 16 | 8 | 3 | 30 | 109.12 (58) | 113.85 (107) | 123.46 (282) | 120.41 (446) | 120.40 (360) |
| 2000 | 971 | 125 | 16 | 8 | 4 | 30 | 104.22 (102) | 110.01 (163) | 120.27 (629) | 116.78 (978) | 116.78 (217) |
| 2000 | 971 | 125 | 16 | 8 | 5 | 30 | 100.40 (226) | 107.31 (303) | 117.74 (1283) | 114.24 (3600) (Gap 0.11%) | 114.24 (3600) (Gap 0.03%) |
| 2000 | 971 | 125 | 16 | 8 | 3 | 35 | 124.22 (85) | 130.41 (146) | 141.85 (651) | 138.17 **(1093)** | 138.17 (1295) |
| 2000 | 971 | 125 | 16 | 8 | 4 | 35 | 118.01 (187) | 126.04 (278) | 138.21 (1797) | 134.09 (3600) **(Gap 0.01%)** | 134.15 (3600) (Gap 0.05%) |
| 2000 | 971 | 125 | 16 | 8 | 5 | 35 | 114.08 (205) | 123.19 (292) | 135.04 (2074) | 131.08 (3600) **(Gap 0.13%)** | 131.27 (3600) (Gap 0.26%) |

Table 2.5: The optimal solutions and bounds for the c-IRLP for the Hanover County data. Computational time, in seconds, is shown in the parentheses. "Lagrangian and Linear Relaxation Upper Bound" reports the upper bound obtained from the Lagrangian and linear heuristic and the computation time using Gurobi. "Optimal Solution w/ Starting Partial Feasible Solution" reports the optimal objective function value and computation time when we set starting values. "Optimal Solution w/ Standard Implementation" reports the optimal objective function value and the computation time when using the standard implementation with Gurobi.

components were installed and 42 arc distances were shortened using those installed components. The number of installed components changes depending on the number of recovery crews, the time periods, and processing times of the installed components. As in IRLP experiments, the c-IRLP computational experiments suggest that it is best to install components that are beneficial to the most critical facility locations prior to and after emergency responders are located there with a more realistic and practical setting.

## 2.4 Conclusions

In this chapter, we introduce an integrated restoration and location problem (IRLP) and model the interdependencies between critical infrastructure systems and service providers. We study a P-median model variation with the goal of minimizing the cumulative weighted distance between emergency responders and demand nodes over a time horizon. We also introduce the c-IRLP, an extension to this model to approximately model components of disrupted arcs between demand and facility locations. The models can be used to model the delivery of a variety of time-sensitive critical services after a disaster event occurs. The models provide insight into how the activities of the two types of service providers should be coordinated and which network components should be restored sooner during recovery.

We develop integer programming formulations of our models. We introduce Lagrangian relaxation dual problems to obtain a lower bound to the models. A subgradient algorithm is used to solve the Lagrangian relaxation dual problems. Solving the models using Lagrangian relaxation results in a better lower bound than the linear relaxation lower bound in all computational experiments we report. We further develop a Lagrangian heuristic to identify a feasible solution to IRLP model, which provides an upper bound that is used to decrease the size of the branch and bound tree. Using the upper bound obtained from the Lagrangian heuristic, we show an improvement in the computational time of IRLP. For comparison, we also show the time to solve original model without the upper

bounds. Numerical experiments with real-world data sets and with data from Beasley's OR Library are used to examine the quality of the Lagrangian relaxation lower bound and the improvement in IRLP. For the c- IRLP, we develop a Lagrangian and linear relaxation heuristic by using a feasible solution to Lagrangian relaxation of the c-IRLP and enhancing the feasible solution using linear relaxation of the c-IRLP. The resulting upper bound from the Lagrangian and linear relaxation heuristic improved the Lagrangian relaxation heuristic upper bound in all cases tested. We also use this enhanced feasible solution to set starting values for some variables in the standard implementation. This approach helps the solver obtain an incumbent solution faster than without setting starting values, and hence, leads to improved computational times for some experiments. Numerical experiments with real-world data are used to examine the quality of the Lagrangian relaxation lower bound, as well as the Lagrangian and linear relaxation heuristic upper bound.

After an extreme event, damage to infrastructure systems can delay the delivery of essential services. These proposed models and analysis demonstrate the importance of modeling the interdependencies between infrastructure systems and emergency services. Solutions to the models provide a plan for restoring the most critical network components to the models and provide insight into how to deliver essential services during the recovery. We were able to solve most instances in less than one hour of CPU time for Hanover County and Beasley's data sets, which suggests that the models can be used to aid decision makers with emergency response and recovery issues in real-time after a disaster.

There are several directions which the models can be extended. First, other objectives such as coverage are often used to model the quality of service in disaster settings. Second, we could take transportation restrictions under consideration, where both emergency responders and recovery crews can only move to "adjacent" facilities or components in sequential time periods. In the next section, we present a new model that consider coverage objective and also consider relocation restrictions for emergency responders.

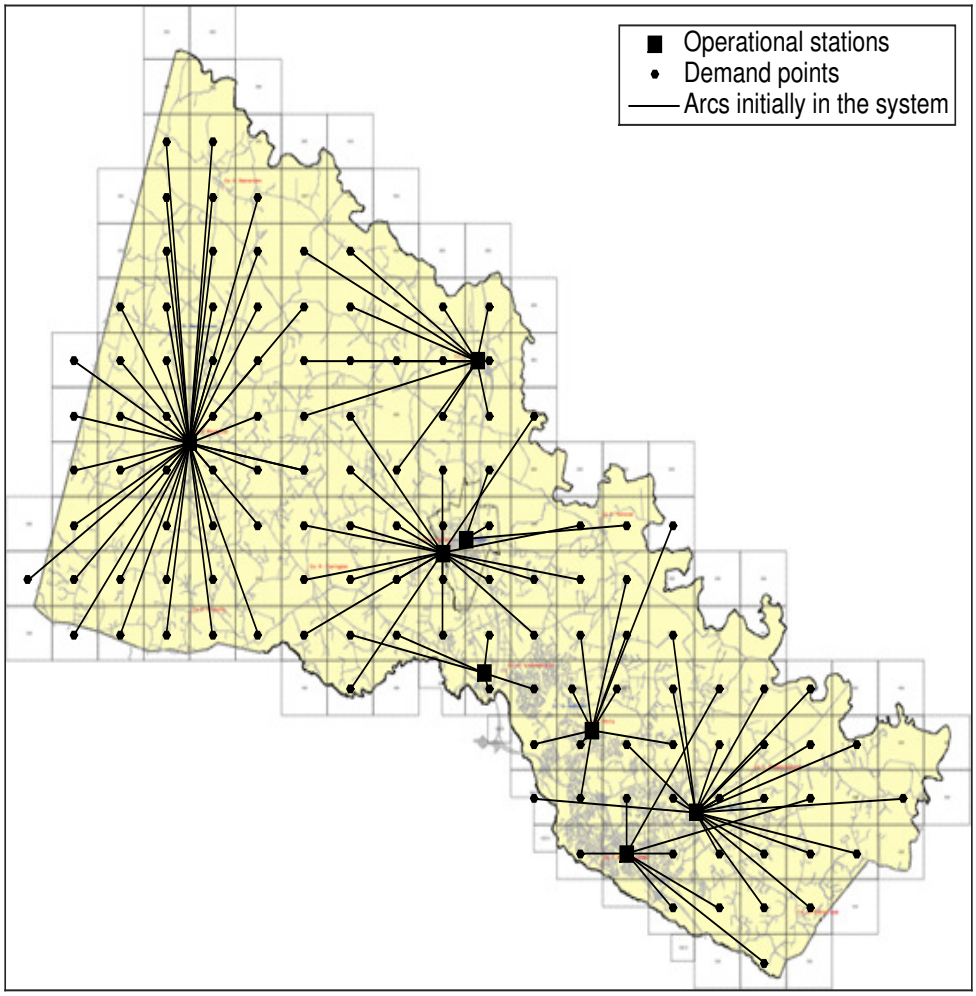


(a) Time period 0

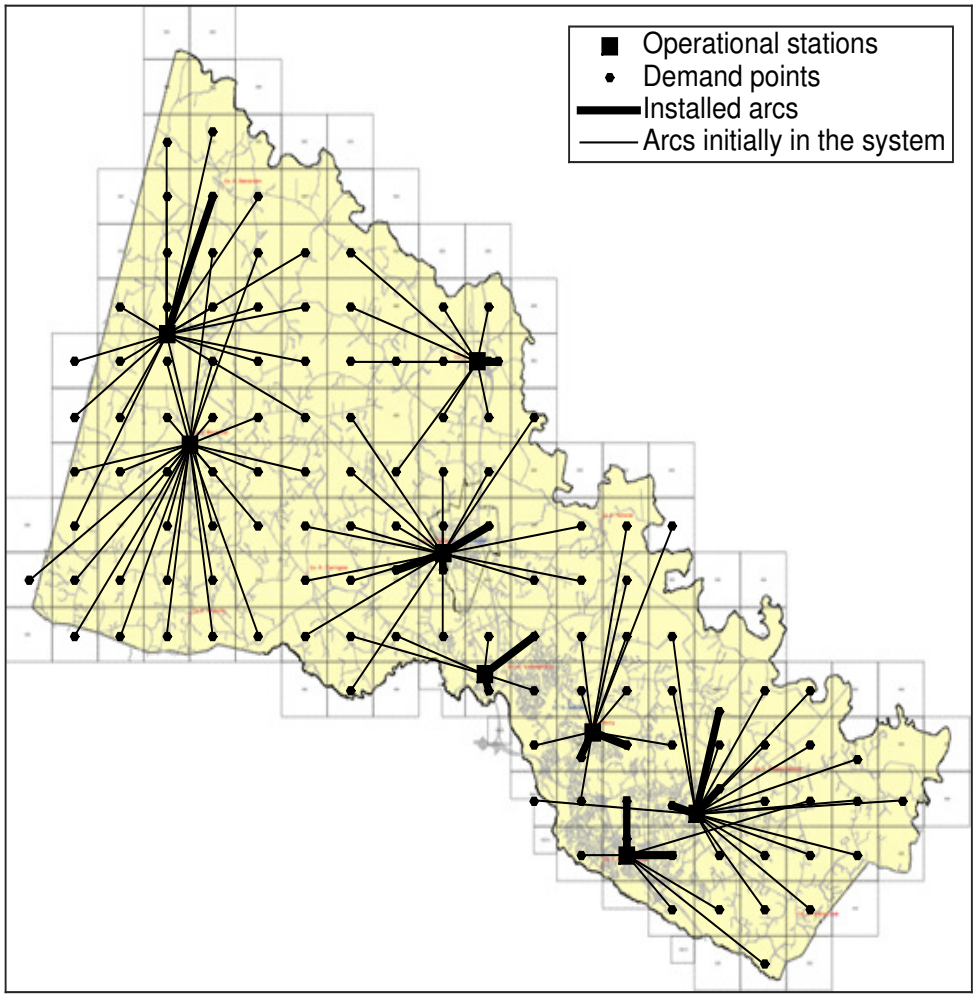


(b) Time period 5

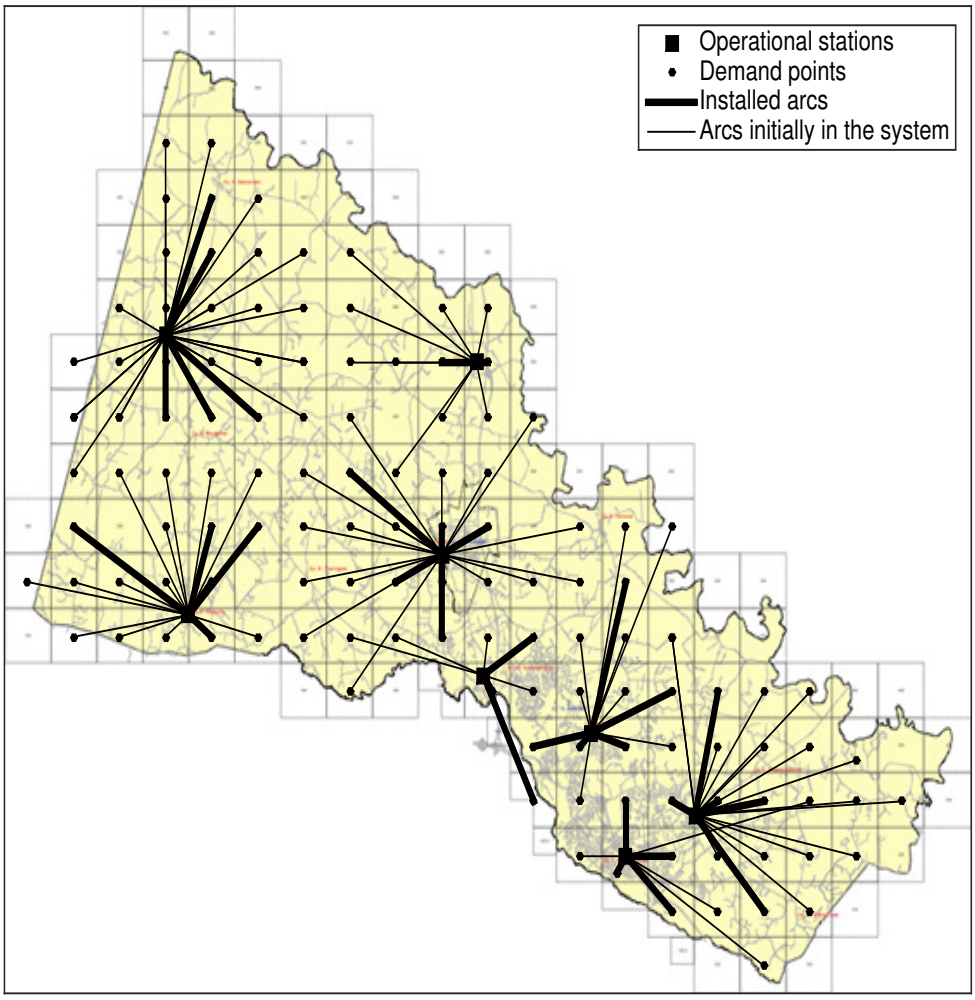


(c) Time period 10

Figure 2.3: The installation of arcs for IRLP for the Hanover County data set for optimal restoration effort $K = 5$ and over the time horizon $T = 10$. Figure (a) shows the solution using initial arcs. The thick arcs represent installed arcs in $A'$ that have been installed up until time periods 5 and 10 in Figures (b) and (c), respectively. The thin arcs represent arcs in $A$ used in the solution.

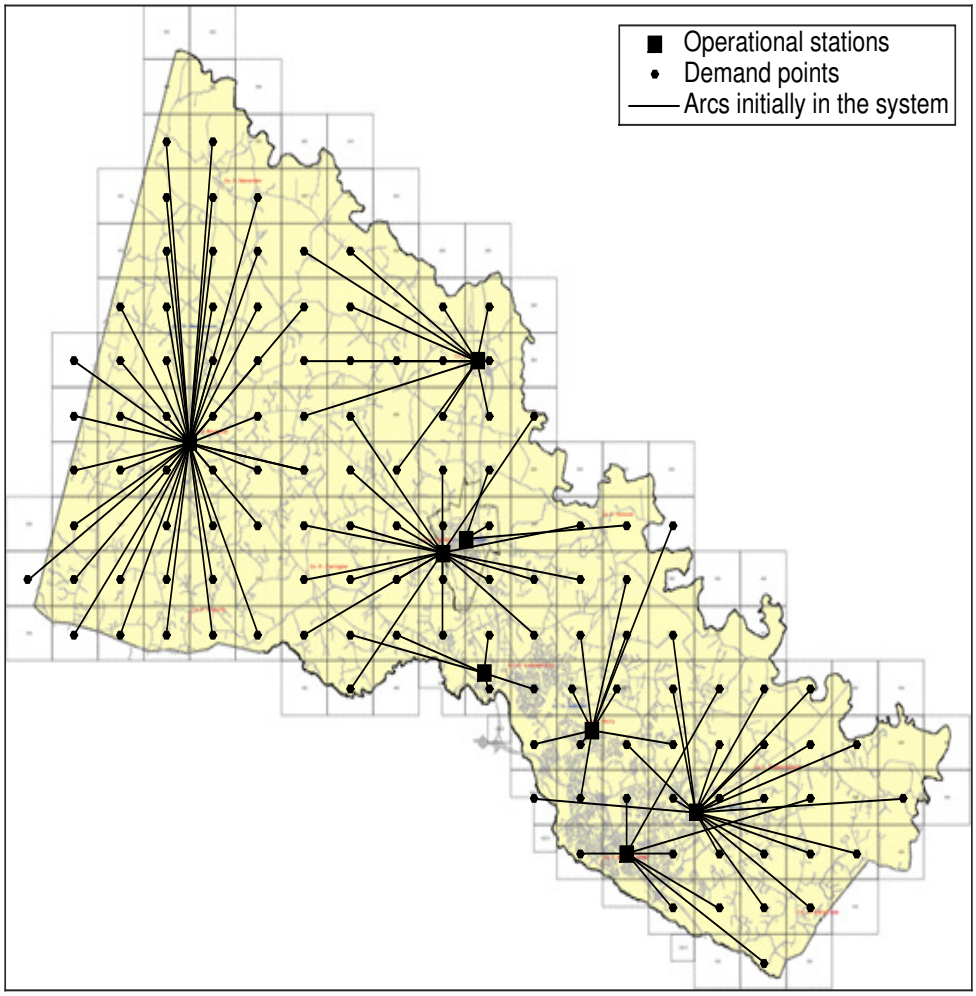


(a) Time period 0

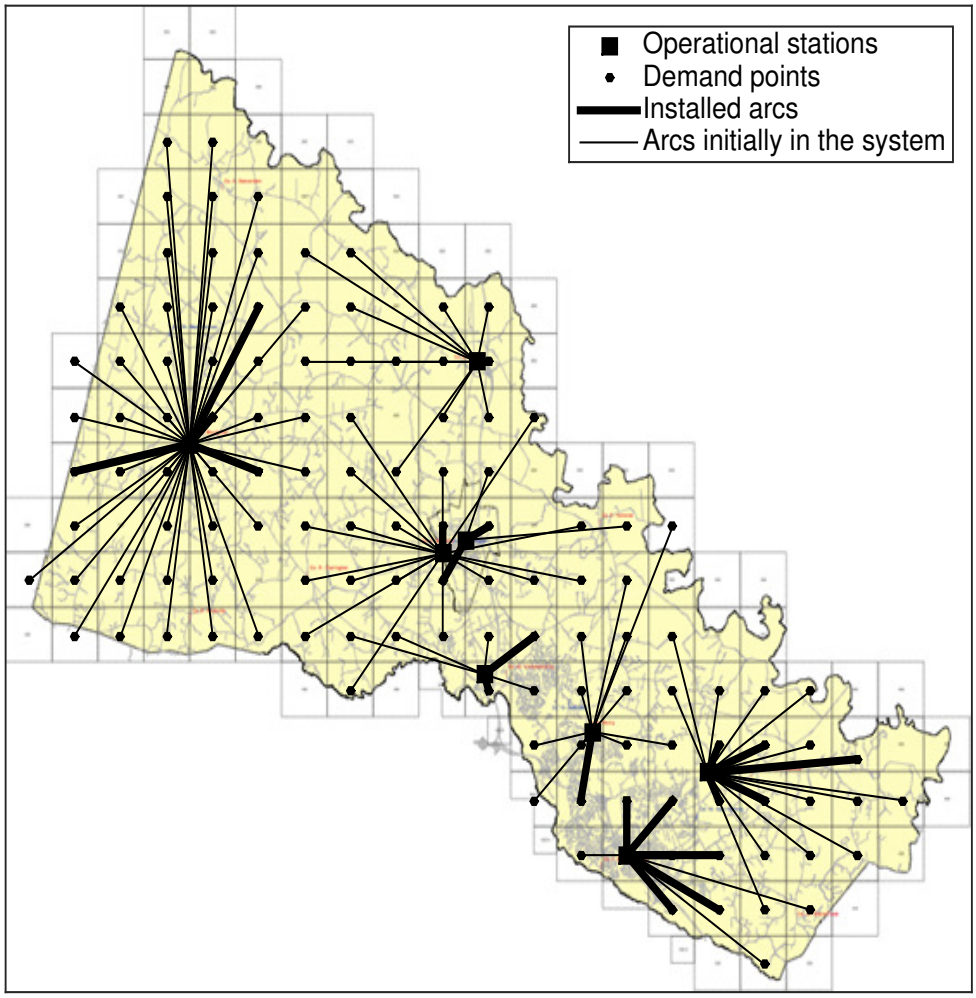


(b) Time period 5

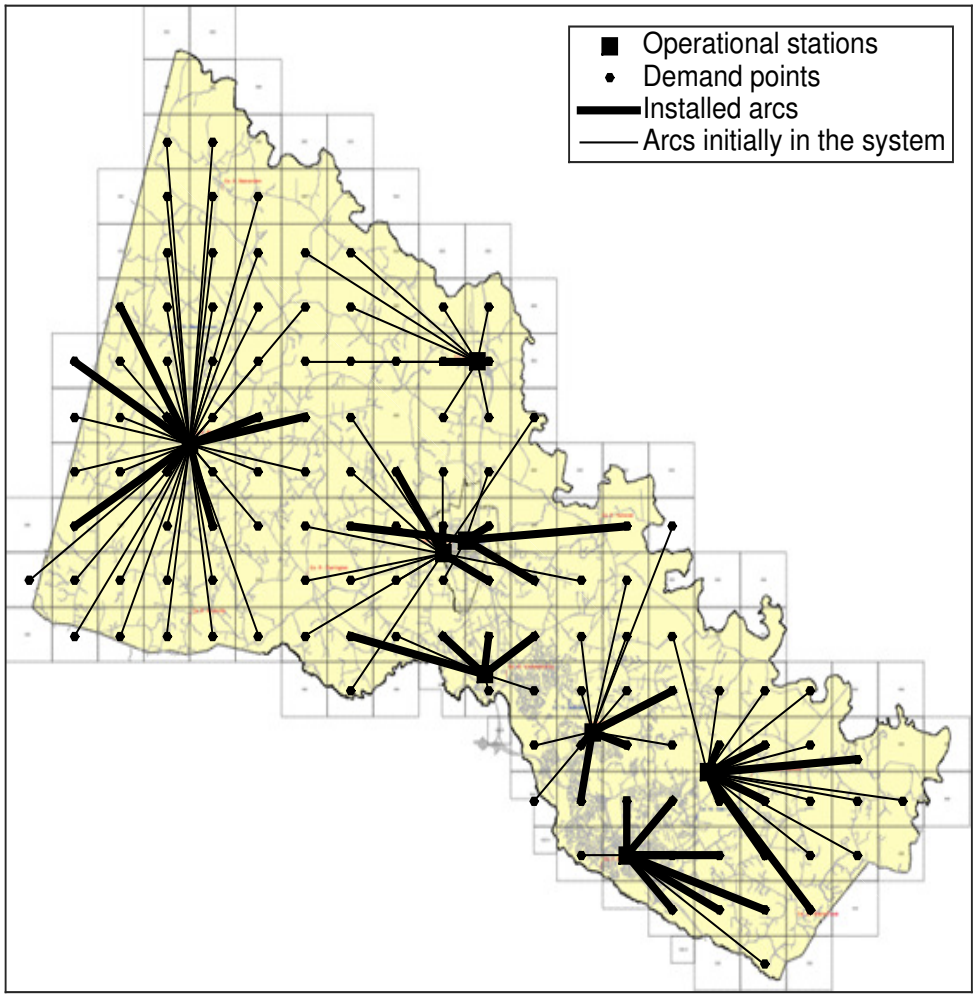


(c) Time period 10

Figure 2.4: The installation of arcs for the c-IRLP for the Hanover County data set for optimal restoration effort $K = 5$ and over the time horizon $T = 10$. Figure (a) shows the solution using initial arcs. The thick arcs in Figure represent installed components in $C'$ that have been installed up until time periods 5 and 10 in Figures (b) and (c), respectively. The thin arcs represent arcs in $A$ used in the solution.

# Chapter 3

# A Maximal Multiple Coverage and Network Restoration Problem for Disaster Recovery

## 3.1 Introduction

After disasters, road infrastructure becomes vital for providing aid and saving disaster victims' lives, as it provides a critical link to emergency services, relief, and evacuation routes. Disaster–related disruptions on the road infrastructure system make it hard to serve emergency calls and provide emergency aid. For example, during Hurricane Sandy, more than half of the road infrastructure system was unavailable (FEMA (2013b)). Following Hurricane Sandy, the Department of Transportation authorized $12.4 billion to repair and reopen roads and rebuild transit assets (FEMA (2013b)). During Hurricane Harvey in 2017, many roadways suffered catastrophic flooding, which resulted in debris on roads, even major highways such as I-10, I-45 and US-59 (Blake and Zelinsky (2018)). The Texas Department of Transportation crews cleared roadways by removing more than 10 million cubic feet of debris in the areas most impacted by the hurricane (Texas Department of

Transportation (2017)). Days before a hurricane reaches a coast, government agencies pre-locate emergency response resources (FEMA (2013a); Furgate (2012)). During disaster response operations, the planning staff decides the priority of roads and streets to allocate local resources (FEMA (2007)). Given the large repair cost and extended damage to road infrastructure, prioritizing the recovery of roadways based upon their importance to emergency services is crucial. The prioritization decisions need more advanced analytical methods to improve the recovery efforts.

During normal operations, emergency responders (e.g., firefighters, police, emergency medical service (EMS) providers) have a certain service region based on travel time to respond to emergency calls (Swersey (1994)). However, during and immediately after disasters, emergency responders located in regions with many disrupted roads cannot respond to demand in their service areas as quickly as during normal operations. Therefore, the locations of emergency responders and the condition of the surrounding the road infrastructure system around their locations have a critical impact on the number of people that can be reached in a timely manner after disasters. The damage to road infrastructure (e.g., from debris or flooding) and the geographic features of the region may limit the movement of emergency responders. Further, first responders and other resources that are staged prior to the disaster may only be able to access certain points of the affected region after the disaster occurs (FEMA (2013a)). As a result, not all the facility locations may be available at the beginning of the disaster recovery operations, and they may become available as road infrastructure is dynamically restored.

We study how to optimally coordinate both road infrastructure restoration (e.g., clearing debris from roads) and emergency response efforts after disasters. The goal of the model is to maximize the multiple coverage of emergency service demand over a time horizon. Due to high volume of emergency service requests after disasters, unavailability of emergency service responders is more likely. We capture this issue by covering emergency service demands multiple times to incorporate backup coverage. In our model, we consider

the road infrastructure system as a network and repair physical components of road infrastructure to restore the network. The model seeks to schedule the restoration of the road infrastructure system over a time horizon and locates emergency responders at facilities. After restoration is completed, the disrupted arcs become available in the network. Emergency responders deliver emergency relief and services more effectively by changing locations as more arcs in the network become available during the recovery process. The model considers limited entry points to the affected region after the disaster as well as restrictions on the movement of the emergency responders during the recovery process that reflect road damage or geographic limitations, two important considerations of emergency response operations. The model consists of three parts. The recovery part models component installations by identical recovery crews over a finite time horizon. The relocation part models the movement of the emergency responders using arcs that are initially available or that become available following restoration. The coverage part captures covering demand points if there are available arcs in the network to do so.

In this study, we make the following contributions:

- We present a maximal multiple coverage and network recovery problem that considers the interdependency between disaster recovery performance of the network recovery crews and emergency service responders. This model studies how to effectively cover emergency demands with backup coverage by locating and relocating emergency responders on a network, subject to relocation restrictions, while recovering a network over a finite time horizon.
- We introduce two heuristics, each of which provides a feasible solution for the problem as well as a lower bound to the optimal objective function value. The first heuristic is based on the Lagrangian relaxation solution procedure and the second heuristic is based on an integer rounding procedure for the linear programming relaxation.
- We present a detailed case study using real world data from Bronx Borough during

Hurricane Sandy. We include computational studies to demonstrate the effectiveness of the heuristics. The solution sheds light on the prioritization of the network restoration and relocation activities of emergency responders after disasters to achieve better emergency demand coverage.

The remaining sections are organized as follows. Section 3.2 presents a literature review. Section 3.3 provides the mathematical formulation of our model and introduces the two heuristics, namely, the Lagrangian and linear relaxation heuristic and the linear relaxation rounding heuristic. Section 3.4 reports computational results obtained by using the heuristics to identify feasible solutions for our model on a realistic case study and discusses the key insights from the analysis. The model solutions identify network recovery plans and the movement of emergency responders on available arcs. In addition, the results give insights into how to relocate emergency responders subject to relocation restrictions to maximize multiple coverage of emergency service demand over the time horizon. Section 3.5 provides concluding remarks.

## 3.2 Literature Review

We present a coverage problem that maximizes the multiple coverage of emergency service demand by locating emergency responders at facilities. Coverage problems are one of the main classes of location problems that consider coverage of service areas based on spatial proximity. Coverage models have been studied extensively by using a wide range of methodological and theoretical developments in the literature and have been applied to public service problems (Murray (2016)).

Toregas et al. (1971) present the first *deterministic* model, the location set covering problem (LSCP), with an objective to minimize the number of facilities to cover all demand points. Given the limited number of resources, covering all demand points could be hard to

achieve. Church and ReVelle (1974) present the maximal covering location problem (MCLP), with the aim of maximizing coverage by locating a fixed number of facilities. However, the LSCP and the MCLP ignore facility unavailability that occurs when an emergency responder cannot cover demand points when the emergency responder is dispatched to a demand point. Several deterministic models consider the multiple coverage of demand points to capture backup coverage. Hogan and ReVelle (1986) introduce a model that considers the secondary coverage of a demand node. Gendreau et al. (1997) present a double coverage location model with two different coverage standards. The model requires all the demand points to be covered by an emergency responder located within $r_2$ time units. In addition, a proportion $\alpha$ of the demand must be within $r_1$ time units of an emergency responder with $r_1 \leq r_2$.

In addition to deterministic models, *probabilistic* models have been developed to capture facility unavailability by explicitly considering busy probabilities and reliabilities of facilities. Daskin (1983) presents the maximal expected covering location problem (MEXCLP), an extension of MCLP. MEXCLP takes into account the probability that a facility is not able to cover the demand. We consider backup coverage to capture facility unavailability by considering multiple coverage instead of considering facility unavailability probabilities, which are typically hard to estimate in disaster settings.

Another stream of papers consider *dynamic* models that relocate facilities (Brotcorne et al. (2003)). Our model considers relocations of emergency responders between facility locations to capture dynamic changes in the network due to arc installation over the time horizon. Gendreau et al. (2001) present a dynamic relocation model with the objective to maximize backup coverage while minimizing relocation costs. Rajagopalan et al. (2008) present another dynamic relocation model that incorporates location–specific busy probabilities as an extension to the queuing probabilistic location set covering problem (Marianov and Revelle (1994)) with multiple periods. The aim of the dynamic set covering location model in Rajagopalan et al. (2008) is to minimize the number of emergency responders

required while meeting predetermined emergency responder availability requirements for dynamic demand environments. Another dynamic model is the time–dependent emergency responder allocation model, which captures travel time and demand site variations due to time of day (Degel et al. (2015)).

Relocation is practical for firefighters and emergency responders. Therefore, most relocation models consider emergency service responders. However, a large number of relocations creates a poor work environment for personnel. Hence, the issue of controlling the number of relocations has arisen in the dynamic coverage model literature by considering relocation cost or an upper limit on the number of location changes (Gendreau et al. (2006)). For example, the model presented by Gendreau et al. (2001) penalizes repeated relocation of the same vehicle to limit the number of relocations. Van Buuren et al. (2012) present a dynamic ambulance relocation model that only allows relocation of idle emergency responders to limit the number of relocations. We consider relocations over a time horizon during a disaster recovery to capture the dynamic change in the network due to recovery. Our model installs network components to enable emergency responders to move between emergency responder locations. Since we consider the recovery efforts over a finite time horizon, decisions regarding how to invest this limited time to install components can be considered a cost of relocating.

The coverage models in all three categories have represented important contributions to location analysis and modeling in a range of problem contexts. In addition, the existing models employ a wide range of methodological and theoretical improvements to develop better solution techniques. Church and ReVelle (1974) present two different heuristics, namely the greedy adding and the greedy adding with substitution algorithms to construct feasible solutions for MCLP. Later, Galvão and ReVelle (1996) solve the Lagrangian relaxation dual of MCLP using a subgradient algorithm by improving upper and lower bounds obtained from the algorithm at each iteration. We present a Lagrangian and linear relaxation heuristic and a linear relaxation rounding heuristic to construct feasible solutions

for the problem. In these heuristics, we compare feasible solutions obtained using different types of neighborhood search algorithms. Vatsa and Jayaswal (2016) present a formulation for a multi-period MCLP with server uncertainty. This model is efficiently solved using Benders decomposition, while a tabu search heuristic is used to identify near-optimal solutions to the models presented in Gendreau et al. (2001, 1997). Recently, Cordeau et al. (2019) propose solving large scale maximal covering problems using branch-and-Benders-cut algorithms.

Sharkey et al. (2015a) present interdependency relationships between infrastructure systems to study the necessary level of coordination for effective restoration efforts across all systems after disasters. We study the interdependency between disaster recovery performance of the network recovery crews and emergency service responders. There are few papers in the literature that study interdependencies of infrastructure systems and network recovery while measuring the performance of the system over a planning horizon. Lee et al. (2007) introduce the interdependent layer network (ILN) model to explicitly model infrastructure interdependencies as a network-flow based model, where interdependent infrastructure systems are networks, and corresponding services are flows. Nurre et al. (2012) introduce the integrated network design and scheduling (INDS) problem to model the restoration services of interdependent infrastructure systems after disruptive events. The INDS problem allows recovery crews to install new arcs and nodes into the network with the objective to maximize the cumulative weighted flow through the network over a time horizon. The recovery part of our model has similar constraints as the model proposed in (Nurre et al. (2012)). Cavdaroglu et al. (2013) extend the INDS problem to multiple interdependent networks with the objective to minimize cost, which includes flow cost, unsatisfied demand cost, and arc installation and assignment costs over the planning horizon of the restoration. Almoghathawi et al. (2019) present a restoration problem for interdependent infrastructure networks with the aim of maximizing the resilience of the networks while minimizing the total restoration cost. Maya Duque et al. (2016)

propose a network repair crew scheduling and routing problem to optimize accessibility to humanitarian relief demand areas, and the model is solved using dynamic programming. Instead of scheduling one repair crew and including precedence relationships between damaged nodes as in Maya Duque et al. (2016), our study considers multiple repair crews, and models the dependency between damaged components by letting several network components benefit from each installation. Recently, Morshedlou et al. (2018) present an integrated vehicle routing problem and infrastructure network restoration crew scheduling problem with the objective to maximize the resiliency of the infrastructure network over a restoration time horizon. Baycik and Sharkey (2019) propose interdiction-based approaches to identify damage in disrupted critical infrastructures by accounting their dependencies to develop inspection plans.

This chapter is an extension to Iloglu and Albert (2018), who formulate a component-based integrated restoration and location problem (c-IRLP) (Iloglu and Albert (2018)), an extension to the P-median problem that models the interdependency between infrastructure systems and service providers as a network. An essential distinction of our model is that we restrict initial emergency responder locations as well as relocations, whereas c-IRLP allows emergency responders to relocate anywhere on the network without restriction. In this way, the model proposed in this chapter generalizes c-IRLP by lifting the assumption that all emergency responders can be located anywhere on the network at any time without restriction. Furthermore, our model considers multiple coverage of emergency service demand to provide backup emergency service during large volume of emergency service requests after disasters, whereas c-IRLP assigns the closest emergency responder to each demand location and does not take backup coverage into account.

## 3.3 The Maximal Multiple Coverage and Network Recovery Problem

In this section, we introduce the maximal multiple coverage and network recovery (MMCaNR) problem for recovering disrupted components in a network while relocating emergency service providers and covering demands, which we formulate as an integer programming model. In the model, we consider a network as a topological structure that consists of nodes and arcs. Nodes in the network represent emergency service demand points and emergency facility locations. Arcs represent the paths between facility locations and demand points and between facility locations. Since we consider the disrupted network after a disaster, there are impassable arcs due to debris or other types of disaster damage. Therefore, the network has disrupted arcs as well as initially available arcs.

The goal of the model is to cover emergency demands with backup coverage by coordinating the recovery activities of two types of service providers: emergency responders and road infrastructure recovery crews. This is accomplished by locating emergency responders at facilities and scheduling crews to repair components in the network over a finite time horizon. We assume disrupted arcs are comprised of one or more *components* (streets), any of which could be disrupted, rendering the arcs unavailable. A single component can be present on multiple paths, and therefore, repairing a component enables multiple disrupted arcs that share the component. Each recovery crew is scheduled to install at most one component into the network at each time period. Not all the facility locations are open at the beginning of the disaster recovery operation horizon due to the conditions of the surrounding road infrastructure, and they become available as the network is dynamically restored. To capture this dynamic change, we restrict emergency responder relocations. Therefore, emergency responders are located at initially available facilities at the beginning of the time horizon. They are relocated in the later time periods using available arcs, including the arcs that become available after a component installation that represent allowable

paths for relocation. The objective is to maximize the cumulative multiple coverage over the time horizon.

Table 3.1 lists all the input sets and parameters. We initially start with a network $G = (I, A \cup E)$, where the nodes in $G$ are the union of demand nodes $D$ and facility locations $J$ (i.e., $I = D \cup J$) and $A \cup E$ is the union of initially available arcs between demand nodes and facility locations $A$, and initially available arcs between facility locations $E$. At the beginning of the time horizon $T$, we let set $J_0 \subseteq J$ represent initially available emergency responder locations. We have four different types of arcs in the network, and each one is represented with a different set: initially available arcs $A \subseteq D \times J$ and disrupted arcs $A' \subseteq D \times J$ between demand nodes and facility locations, and initially available arcs $E \subseteq J \times J$ and disrupted arcs $E' \subseteq J \times J$ between facility locations that capture the paths for relocation.

The model considers component installations to make disrupted arcs in $A'$ and $E'$ available in the network. We do not install disrupted arcs directly, since they represent paths. A component represents a sub-path or a combination of sub-paths that is disrupted, and hence, installation of the component can enable multiple arcs that use the component. We define the set $C'$ as a set of installable components into the network. Since installing a single component can enable arcs in $A'$ and $E'$ such that were disabled due to the disruption of that component, we define a set of components for each disrupted arc in $A'$ and $E'$. We define a set of components $AC(i, j)$ for each $(i, j) \in A'$ such that installation of any component $c \in AC(i, j)$ enables arc $(i, j)$ and allows us to cover demand point $i$ by facility location $j$. Likewise, we define a set of components $EC(j, j')$ for each $(j, j') \in E'$ such that installation of any $c \in EC(j, j')$ allows emergency responders to move between facilities $j$ and $j'$ in either direction. Components are installed by one of the $K$ identical network recovery crews over a finite time horizon $T$. We represent the component installation times with integral parameter $p_c$ for each $c \in C'$. After the installation of component $c \in C'$ is completed: (1) if $c \in AC(i, j)$, the demand point $i \in D$ can be covered by facility location $j$,

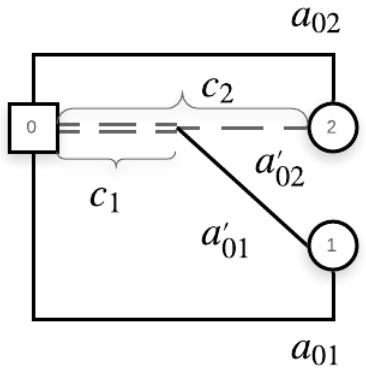


Figure 3.1: The network shows components and arcs relationships with facility location 0 and two demand nodes represented with 1 and 2. The solid lines represent initially available arcs. The dashed lines represent the installable network components.

(2) if $c \in EC(j, j')$, the arc $(j, j') \in E'$ between facility location $j$ and $j'$ becomes available for emergency responder relocations. Note that a component $c \in C'$ can enable multiple disrupted arcs in $A'$ and $E'$.

Figure 3.1 illustrates the relationship between components and arcs with facility location 0 and demand points 1 and 2. The solid lines represent the initially available arcs while dashed lines represent the disrupted components. In Figure 3.1, $c_1$ and $c_2$ represent installable components, with component $c_1$ representing a short segment of the path and $c_2$ representing a longer segment of the path that also includes $c_1$. When component $c_1$ is repaired, a disrupted arc between facility location 0 and the demand point 2 becomes available. When the component $c_2$ is repaired, the disrupted arcs between facility location 0 and demand 1 and the facility location 0 and demand 2 become available.

The model relocates emergency responders over a time horizon to achieve better coverage using the available arcs. If an emergency responder is located at a facility, we call that facility an “open facility." After disasters, not all facilities are open. We model emergency responder relocations over the time as network flows. To do so, we introduce a dummy source node $u$, which is connected by arcs to the initially open locations in $J_0$, and a dummy

sink node $v$, which is connected by arcs to the locations in $J$. The $P$ emergency responders are located at facilities in $J_0$ by moving from the dummy source node $u$ at the beginning of the time horizon. Then emergency responders are relocated in the network at each time period using the available arcs at the time. While there is no cost for relocating emergency responders, the relocation restrictions ensure that relocation times are short. Emergency responders can move to adjacent facility locations using only available arcs. If the arcs for relocating emergency responders are defined as those whose travel times are within a certain time threshold parameter, the relocation times between any pair of facility locations are approximately the same. At the end of the time horizon, emergency responders move to the dummy sink node $v$.

We consider multiple coverage to respond to the large demand volume after disasters in the presence of emergency responder unavailabilities. The model considers $L$ levels of coverage, and a demand point is fully covered if it is covered by $L$ facilities. The objective is to maximize cumulative multiple coverage with weights $w_{it}$ and $\theta_\ell$, where $w_{it}$ represents the demand at node $i$ at time $t$ and $\theta_\ell$ represents the marginal increase in coverage if covered $\ell$ times, $\ell = 1, \ldots, L$. The parameter $\theta_\ell$ is positive and non-increasing with $\sum_{\ell=1}^{L} \theta_\ell = 1$. The full set of input sets and parameters is listed in Table 3.1.

The model has three parts. The recovery part schedules the installation of the components. The relocation part relocates the emergency responders at the facility locations. The coverage part captures the multiple coverage of the emergency service demand. We have three types of binary decision variables, where each corresponds to a different part in the model.

Table 3.1: Input sets and parameters

| **Sets** | |
|---|---|
| $I$ | set of nodes, with $I = D \cup J$ |
| $D$ | set of demand points, with $D \subseteq I$ |
| $J$ | set of facility locations, where $J \subseteq I$ |
| $J_0$ | set of facility locations that are initially open, with $J_0 \subseteq J$ |
| $A$ | set of arcs between demand points and facility locations that are initially available, with $A \subseteq D \times J$ |
| $A'$ | set of disrupted arcs between demand points and facility locations, with $A' \subseteq D \times J$ |
| $E$ | set of arcs between facility locations that are initially available, with $E \subseteq J \times J$ |
| $E'$ | set of disrupted arcs between facility locations, with $E' \subseteq J \times J$ |
| $C'$ | set of components that can be installed to the network |
| $AC(i,j)$ | subset of installable components $c \in C'$ such that location $j$ can cover the demand $i$ after installation of component $c$, for every $(i,j) \in A'$, where $AC(i,j) \subseteq C'$ |
| $EC(j,j')$ | subset of installable components $c \in C'$ such that after installation of component $c \in C$ is completed emergency responders can move between $j$ and $j'$ in both directions for every $(j,j') \in E'$, where $EC(i,j) \subseteq C'$ |
| $u$ | source node |
| $v$ | sink node |
| **Parameters** | |
| $T$ | number of time periods |
| $K$ | number of network recovery crews |
| $p_c$ | processing time to install component $c \in C'$ |
| $w_{it}$ | demand at node $i \in D$ at time $t = 1, \ldots, T$ |
| $P$ | number of emergency responder crews to locate at facility locations |
| $L$ | levels of coverage |
| $\theta_\ell$ | marginal increase in coverage when covered $\ell$ times for $\ell = 1, \ldots, L$ |
| $N_i^A$ | subset of facility locations $j \in J$ such that location $j$ cover the demand $i$ using an initially available arc $(i,j) \in A$ |

The *relocation decision variables* are:

- $y_{j,j',t} = 1$ if an emergency responder located at $j$ at time $t-1$ moves to emergency responder location $j'$, where $(j,j') \in E \cup E'$ at time $t = 1, \ldots, T$, and $0$ otherwise.
- $y_{u,j',0} = 1$ if an emergency responder moves from dummy source node $u$ to emergency responder location $j' \in J_0$ at time $t = 0$, and $0$ otherwise.
- $y_{j,v,T+1} = 1$ if an emergency responder located at $j \in J$ at time $T$ moves to dummy sink node $v$ at time $t = T+1$, and $0$ otherwise.

The *coverage decision variables* are:

- $z_{i\ell t} = 1$ if demand at $i \in D$ is covered by at least $\ell$ levels at time $t = 1, \ldots, T$ for $\ell = 1, \ldots, L$, and 0 otherwise.
- $\delta_{ijt} = 1$ if demand $i \in D$ is covered by emergency responder facility $j \in J$ using disrupted arc $(i, j) \in A'$ that becomes available after a component installation at time $t = 1, \ldots, T$, and 0 otherwise.

The *recovery decision variables* are:

- $\beta_{ct} = 1$ if component $c \in C'$ is operational at time $t = 1, \ldots, T$, and 0 otherwise.
- $\alpha_{kct} = 1$ if network recovery crew $k = 1, \ldots, K$ completes the installation of component $c \in C'$ at time $t = 1, \ldots, T$, and 0 otherwise.

Next, we formulate the model as an integer programming model.

$$Z = \max \sum_{t=1}^{T} \sum_{\ell=1}^{L} \sum_{i \in D} w_{it} \theta_\ell z_{i\ell t} \tag{3.3.1}$$

$$\text{s. t.} \sum_{j' \in J_0} y_{u,j',0} = P \tag{3.3.2}$$

$$\sum_{j':(j,j') \in E \cup E'} y_{j,j',t+1} - \sum_{j':(j',j) \in E \cup E'} y_{j',j,t} = 0 \qquad \text{for} \quad j \in J \setminus \{u, v\} \text{ and } t = 0, \ldots, T \tag{3.3.3}$$

$$\sum_{j \in J} y_{j,v,T+1} = P \tag{3.3.4}$$

$$\sum_{j':(j',j) \in E \cup E'} y_{j',j,t} \leq 1, \qquad \text{for} \quad j \in J,\ t = 1, \ldots, T \tag{3.3.5}$$

$$y_{j,j',t+1} \leq \sum_{c \in EC(j,j')} \beta_{ct} \qquad \text{for} \quad (j, j') \in E',\ t = 1, \ldots, T \tag{3.3.6}$$

$$y_{j,j',t} \in \{0, 1\} \qquad \text{for} \quad (j, j') \in E \cup E',\ t = 1, \ldots, T \tag{3.3.7}$$

$$\sum_{\ell=1}^{L} z_{i\ell t} \leq \sum_{j \in N_i^A} \sum_{j':(j',j) \in E \cup E'} y_{j',j,t} + \sum_{j:(i,j) \in A'} \delta_{ijt} \qquad \text{for} \quad i \in D,\ t = 1, \ldots, T \tag{3.3.8}$$

$$\delta_{ijt} \leq \sum_{j':(j',j) \in E \cup E'} y_{j',j,t} \qquad \text{for} \quad (i, j) \in A',\ t = 1, \ldots, T \tag{3.3.9}$$

$$\delta_{ijt} \leq \sum_{c \in AC(i,j)} \beta_{ct} \quad \text{for} \quad (i,j) \in A',\ t = 1, \ldots, T \tag{3.3.10}$$

$$\delta_{ijt} \in \{0,1\} \quad \text{for} \quad (i,j) \in A',\ t = 1, \ldots, T \tag{3.3.11}$$

$$z_{i\ell t} \in \{0,1\} \quad \text{for} \quad i \in D,\ \ell = 1, \ldots, L,\ t = 1, \ldots, T \tag{3.3.12}$$

$$\sum_{c \in C'} \sum_{s=t}^{\min\{T, t+p_c-1\}} \alpha_{kcs} \leq 1 \quad \text{for} \quad k = 1, \ldots, K,\ t = 1, \ldots, T \tag{3.3.13}$$

$$\beta_{ct} - \sum_{s=1}^{t} \sum_{k=1}^{K} \alpha_{kcs} \leq 0 \quad \text{for} \quad c \in C',\ t = 1, \ldots, T \tag{3.3.14}$$

$$\sum_{t=1}^{p_c} \beta_{ct} = 0 \quad \text{for} \quad c \in C' \tag{3.3.15}$$

$$\sum_{k=1}^{K} \sum_{t=1}^{p_c} \alpha_{kct} = 0 \quad \text{for} \quad c \in C' \tag{3.3.16}$$

$$\alpha_{kct} \in \{0,1\},\ \beta_{ct} \in \{0,1\} \quad \text{for} \quad c \in C', k = 1, \ldots, K,\ t = 1, \ldots, T \tag{3.3.17}$$

The objective $(3.3.1)$ is to maximize the cumulative multiple coverage of emergency demand over the time horizon. The relocation part consists of constraint sets (3.3.2) - (3.3.7), the coverage part consists of constraint sets (3.3.8) - (3.3.12), and the recovery part consists of constraint sets (3.3.13) - (3.3.17). Constraint set (3.3.6) links the relocation and recovery parts, and constraint set (3.3.10) links the coverage and recovery parts. Emergency responder relocations are modeled as network flow constraints in constraint sets (3.3.2)-(3.3.5) over the available arcs in the network at time period $t$. Constraint set $(3.3.2)$ ensures that $P$ emergency responders are located at initially available facilities in $J_0$ by moving from dummy source node $u$ at time period $t = 0$, which reflects limited access points after a disaster. Constraint set (3.3.3) captures relocation restrictions, and it ensures flow-balance to model facility relocations between every consecutive time periods starting from time period $0$ to $T$. Note that for every $j \in J$, $(j,j) \in E$, therefore emergency responders can stay at the same location between consecutive time periods. Constraint set (3.3.4) requires that $P$ emergency responders move from open facilities to dummy sink node $v$ at time period $T + 1$. Constraint set (3.3.5) ensures at most one emergency responder is located at each facility at each time period $t$. At each time period $t$, where $t = 1, \ldots, T$, the locations

of the $P$ emergency responders are given by the set $\{j' \in J : y_{j,j',t} = 1,\ (j,j') \in E \cup E'\}$. Constraint set (3.3.6) requires at least one component in $EC(j,j')$ to be installed for an emergency responder to move from location $j$ to $j'$ if there is no initially an available arc from $j$ to $j'$ in $E$. Constraint set (3.3.7) requires the relocation decision variables to be binary. Note that we can reformulate MMCaNR in a straightforward manner as a static emergency responder coverage location problem by simply replacing $y_{j,j',t}$ with $y_j$ for all $j \in J$ for the case when the relocation of emergency responders is not reasonable.

Constraint set (3.3.8) sets the coverage level for each demand point at each time period $t$ and ensures that for each demand $i \in D$, the total level of coverage is less then the total number of open emergency responder locations.Note that we assume $\theta_\ell$ is non-increasing over $\ell$, with $\sum_{\ell=1}^{L} \theta_\ell = 1$. This assumption ensures that $z_{i1t} \geq z_{i2t} \geq \ldots \geq z_{i\ell t}$ for $i \in D$ and $t = 1, \ldots, T$. If $\theta_\ell$ is not non-increasing over $\ell$, we must add $z_{i1t} \geq z_{i2t} \geq \ldots \geq z_{i\ell t}$ for $i \in D$ and $t = 1, \ldots, T$ as constraints to the model. To cover demand $i$ by a facility using an initially available arc in $A$, the facility must have an emergency responder located at it. To cover demand $i$ by a facility using an initially disrupted arc $(i,j) \in A'$, the arc must be available in the network by installing any component $c \in AC(i,j)$ by that time (captured by constraint set (3.3.10)) and the facility $j$ must have an emergency responder located at it (captured by constraint set (3.3.9)), which means constraint sets (3.3.9) and (3.3.10) both need to be satisfied. Constraint sets (3.3.11) and (3.3.12) require the coverage decision variables to be binary.

Constraint set (3.3.13) ensures that at most one component is installed by each recovery crew in each time period, where $\alpha_{kct} = 1$ means recovery crew $k$ starts installation of component $c \in C'$ at time $t - p_c + 1$ and finishes installation at time $t$. Starting from time $t$, this component can be used by arcs that benefit from the component. Constraint set (3.3.14) requires component $c$ to be operational (i.e., $\beta_{ct} = 1$) after installation of component $c$ is complete. Constraint sets (3.3.15) and (3.3.16) ensure that $\beta_{ct}$ and $\alpha_{kct}$ cannot be set to one before the processing time $p_c$ of component $c$. Constraint set (3.3.17) requires the recovery

decision variables to be binary.

MMCaNR can be trivially extended to a P-median model extension with backup coverage. The P-median variation considers relocating P emergency responders into facilities as network flows while repairing disrupted components in the network over the time horizon. The objective is to minimize the total weighted distance between demand points and the $L$ closest open facilities over the time horizon. This extends c-IRLP presented in Iloglu and Albert (2018) that allows for emergency responder relocations restrictions and requires multiple emergency responder assignments for each demand node.

### 3.3.1 Lagrangian and Linear Relaxation Heuristic

We present a heuristic using Lagrangian and linear programming relaxation of MMCaNR to construct a feasible solution to MMCaNR. Lagrangian relaxation is a common method to solve combinatorial optimization problems by dualizing the constraints that make the problem “hard" to solve (Fisher (2004)). However, the Lagrangian relaxation solution does not satisfy the dualized constraints. We use the linear programming relaxation solution to enhance Lagrangian relaxation solution so that the resulting solution is feasible for MMCaNR.

To construct the feasible solution, we first present the Lagrangian relaxation dual problem and optimize it using a subgradient algorithm. Then we describe a procedure for constructing a feasible solution for MMCaNR using the Lagrangian relaxation dual problem solution and the linear programming relaxation solution.

We first need to choose the constraint set to dualize to generate the Lagrangian relaxation dual of MMCaNR. We apply Lagrangian relaxation to constraint set (3.3.10), which links the coverage part with the restoration part. The objective function in (3.3.1) is then equivalent to:

$$\bar{Z} = \min \left\{ - \sum_{t=1}^{T} \sum_{\ell=1}^{L} \sum_{i \in D} w_{it} \theta_{\ell} z_{i\ell t} \right\}$$

under constraint sets (3.3.2)-(3.3.9) and (3.3.11)- (3.3.17), and we present the Lagrangian relaxation dual problem using objective $\bar{Z}$. Let $u_{ijt}$ be the Lagrangian multiplier for $(i,j) \in A',\ t = 1, \ldots, T$, then we define the Lagrangian relaxation problem as following:

$$L(u) = \min \left[ -\sum_{t=1}^{T} \sum_{\ell=1}^{L} \sum_{i \in D} w_{it} \theta_{\ell} z_{i\ell t} \right] + \sum_{t=1}^{T} \sum_{(i,j) \in A'} u_{ijt} \left[ \delta_{ijt} - \sum_{c \in AC(i,j)} \beta_{ct} \right]$$

$$\text{s. t. } (3.3.2) - (3.3.9) \text{ and } (3.3.11) - (3.3.17)$$

The Lagrangian relaxation dual is:

$$\max_{u \geq 0} \ L(u)$$

We optimize the Lagrangian relaxation dual problem by iteratively solving the dual problem using the subgradient algorithm in (Iloglu and Albert (2018)) with the necessary changes for our model.

We now can construct a feasible solution to MMCaNR by using the similar approach in Iloglu and Albert (2018) by combining the Lagrangian and linear programming relaxation solutions. Let $\bar{y}$ denote values of the decision variables of the relocation part for the Lagrangian relaxation problem solution, and let $\bar{\bar{y}}$ denote values of the decision variables of relocation part for the linear programming relaxation problem solution. Then we define a set $S = \{(j, j', t) : \bar{y}_{jj't} = \bar{\bar{y}}_{jj't}\}$ that consists of the indices where the $y$ variables have the same values in the Lagrangian and linear programming relaxation solutions. We note that the variable $y$ values whose indices belong to set $S$ are integer. Then, we fix the values of the $y$ variable for the indices in the set $S$ in MMCaNR and solve MMCaNR with these fixed values. The solution yields a feasible solution for the constraint sets (3.3.1)-(3.3.17) and provides a lower bound for the optimal objective function value.

MMCaNR is NP-complete since a maximal expected coverage model variation is em-

bedded in it. Fixing the relocation decision variables using the heuristic algorithm results in an efficient lower bound for MMCaNR. For example, in our experiments in the following section, $80 - 90$ percent of $y$ variables have the same values in the Lagrangian and linear programming relaxation solutions and so by fixing these values in the heuristic yields computationally efficient feasible solutions. Next, we present another heuristic algorithm using an integer rounding procedure for the linear programming relaxation of MMCaNR.

### 3.3.2 Linear Relaxation Rounding Heuristic

Many mixed integer programming problems are successfully solved using the idea of fixing a subset of the variables in order to obtain subproblems that are easier to solve (Berthold (2014)). Our model includes a large number of relocation decision variables, which presents a computational challenge when solving MMCaNR. However, only a few of the relocation variables are active in the optimal solutions. To address this issue, we fix the subset of relocation decision variables to their linear relaxation solution values and form a sub–MMCaNR problem that is smaller and easier to solve than MMCaNR. Berthold (2014) introduces an approach based on a relaxation enforced neighborhood search (RENS) for mixed integer nonlinear programs (MINLPs) by rounding linear and nonlinear programming relaxation solutions to construct sub–MINLPs. We use a similar approach to construct and solve sub–MMCaNR problem as in the approach by Berthold (2014).

We first solve the purely continuous linear programming relaxation of MMCaNR and let $y^\star$ denote the linear programming relaxation solution values of the relocation decision variables $y$. We construct the sub–MMCaNR problem by setting the binary relocation decision variables $y_{j',j,t}$, to $0$ if no emergency responder is located at $j$ at time $t$ in the linear programming relaxation of MMCaNR $\left(i.e., \sum_{j':(j',j)\in E\cup E'} y^\star_{j',j,t} = 0\right)$ as in Berthold (2014). Therefore, a neighborhood is defined by fixing the subset of relocation decision variables $y$ values to zero. Then, we search for a feasible solution in the neighborhood

by solving the sub–MMCaNR problem. The solution is feasible for MMCaNR, since the values of the fixed relocation variables in the sub–MMCaNR problem are integer in the linear programming relaxation solution and these relocation variables satisfy all of the constraints set of MMCaNR. Therefore, the resulting solution yields a lower bound on the optimal objective value to MMCaNR.

## 3.4 Computational Results

In this section, we provide a case study where we apply MMCaNR and analyze computational results obtained using real data representing road infrastructure and emergency service demands for the Bronx Borough, New York, United States. We performed computations for MMCaNR and the heuristics on a computer with a 1.4 GHz Intel Core 5 Duo Processor with 4GB of RAM. We used GUROBI 6.5.2. to solve the mixed integer programming model that was coded in Python 2.7.

We first describe the data generation process using the real world data obtained during Hurricane Sandy in the Bronx Borough. As shown in Figure 3.2, the Bronx Borough data is split into $|D| = 276$ demand nodes, each of which corresponds to the center of each census tract. The data includes $|J| = 38$ total facility location nodes; 32 fire and rescue stations (NYC OpenData (2012)) and six hurricane evacuation centers (NYC OpenData (2013)). We use exact coordinates of facility location and demand nodes. The weight $w_{it}$ associated with each demand node $i \in D$ for $t = 1, \ldots, T$ reflects 311 service damage tree complaints associated with the demand node to capture the areas affected by Hurricane Sandy (October 29, 2012 - November 5, 2012) multiplied by the proportional population for the associated demand node's census tract to capture the number of possible service requests. Note that we assume the weight $w_{it}$ is fixed over the time horizon $T$ for each demand node $i \in D$.

More than 500 miles of roadways were affected by Hurricane Sandy in New York City

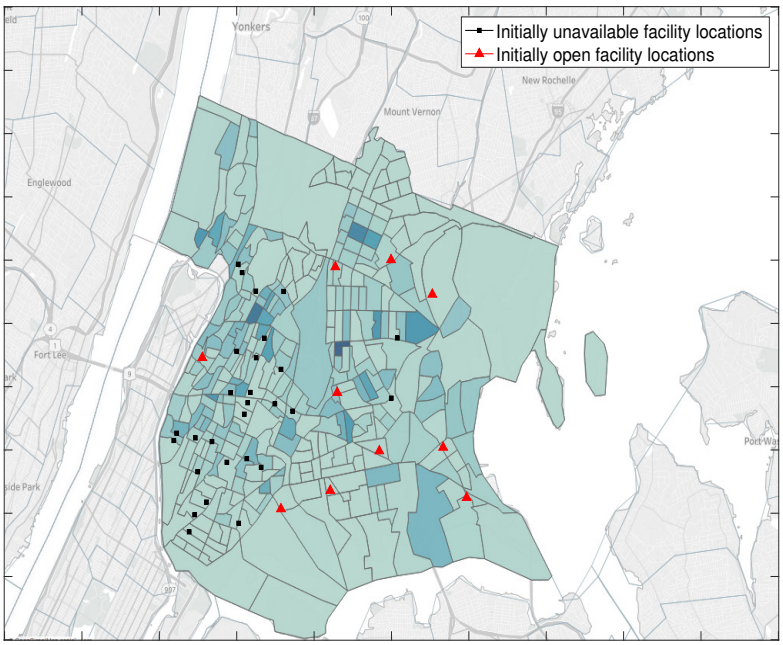


Figure 3.2: Map of our case study showing initially open facility locations (in red $J_0$), and unavailable facility locations (in black $J \backslash J_0$). Population density is shown for each census tract of the Bronx Borough.

due to downed trees and debris on roads (Office of Emergency Management (2014)). Hence, to approximately create the disrupted arc set, we filter only damaged tree complaints from the 311 service requests during Hurricane Sandy. The number of damaged tree complaints in the 311 service requests data vary from 1 to 29. When there are more damaged tree complaints in the same area, we are more certain that a fallen tree has disrupted an arc. Therefore, if both end nodes of a component receive more than five complaints, we assume the arc, which is comprised of the component, is disrupted. Then, we filter the disrupted arcs between demand points and facility locations to the ones that only affect the coverage. To do so, we use real road distances, in miles, to decide a demand node coverage by a facility location using GeoPy package in Python. We set the coverage distance to $0.7$ miles to create set $A'$. A coverage distance of 0.7 miles (in Manhattan distance) approximately represents three avenue blocks, which represents a walkable distance to emergency service

locations in a dense urban region. According to this procedure, we generate $|A'| = 1573$ disrupted arcs between demand and facility location nodes within the coverage distance. We assume that demand–facility arcs $(i, j)$ with fewer than five damaged tree complaints with at most one edge belong to $A$. Then, we generate initial coverage set $N_i^A$ for each $i \in D$ if demand point $i$ is within the 0.7 miles coverage distance from facility location $j$ and $(i, j) \in A$.

We allow emergency responders relocate between facility locations if the distance between locations is less than two miles, since this represents a relocation that can be done in a short amount of time in between consecutive time periods. We generate $|E'| = 466$ disrupted arcs between facility locations with distance less than two miles. Also, we allow 10 facility locations in the coverage area (i.e., within 0.7 miles) with the least damaged tree complaints to be initially open in set $J_0$, since these locations represent entry points that are initially accessible to emergency responders. If each pair of facility locations $j$ and $j'$ are initially open, we assume there is an initially available arc $(j, j')$ in set $E$. Note that for every $j \in J$, $(j, j) \in E$.

Next, we analyze the road infrastructure component-wise for disrupted arcs and create the installable component set $|C'| = 1029$. To generate sets $AC(i, j)$ and $EC(j, j')$, we first calculate up to 10 shortest paths between each $(i, j) \in A'$ with distance less than or equal to 0.7 miles and $(j, j') \in E'$ with distance less than or equal to 2 miles. Then, a component belongs to set $AC(i, j)$ (or $EC(j, j')$) if at least one of the 10 shortest paths between $(i, j) \in A'$ (or $(j, j') \in E'$) becomes available following component installation. Processing time $p_c$ for each installable component $c \in C'$ is generated by combining the real distance and damage severity that reflects the number of complaints, resulting in $1 \leq p_c \leq 4$. We allow $P = 10$ out of $|J| = 38$ facilities to be open by locating emergency responders in each time period. We set $L = 2$ to allow for primary coverage and one level of backup coverage, with $\theta_1 = 0.7$ and $\theta_2 = 0.3$. This allows for most of the benefit to come from primary coverage. Since our model considers short-term recovery of the road network components after disasters, we

consider the time horizon as a day. We vary the number of time periods $T = 8, 12, 18$ to reflect the different work hours per day and the number of recovery crews $K = 1, 2, 3, 4, 5$.

Table 3.2: Feasible and optimal solutions for the Bronx Borough data. Computational time, in seconds, is shown in the parentheses. "Linear Relaxation Rounding Heuristic Solution" reports the feasible solution value obtained using the heuristic and the computation time using GUROBI. "Lagrangian & Linear Relaxation Heuristic Solution" reports the feasible solution value obtained using the heuristic and the computation time using GUROBI and "Optimal Solution Value" reports the optimal solution if the instance is solved optimally within an hour or the best objective function value found in one hour and the computation time to solve MMCaNR using GUROBI.

| $\|A'\|$ | $\|E'\|$ | $\|C'\|$ | $\|D\|$ | $\|J\|$ | $P$ | $T$ | $K$ | Linear Relaxation Rounding Heuristic Solution Value (Time(s)/Gap) | Lagrangian & Linear Relaxation Heuristic Solution Value (Time(s)/Gap) | Optimal Solution Value (Time(s)/Gap) |
|---|---|---|---|---|---|---|---|---|---|---|
| 1573 | 466 | 1029 | 276 | 38 | 10 | 8 | 1 | 909.83 (15s) | 914.58 (31s) | 915.45 (93s) |
| 1573 | 466 | 1029 | 276 | 38 | 10 | 8 | 2 | 1198.62 (47s) | 1198.62 (98s) | 1198.62 (1968s) |
| 1573 | 466 | 1029 | 276 | 38 | 10 | 8 | 3 | 1404.78 (182s) | 1404.78 (99s) | 1406.91 (1372s) |
| 1573 | 466 | 1029 | 276 | 38 | 10 | 8 | 4 | 1539.47 (188s) | 1537.59 (158s) | 1551.31 (622s) |
| 1573 | 466 | 1029 | 276 | 38 | 10 | 8 | 5 | 1647.35 (105s) | 1647.80 (197s) | 1653.84 (998s) |
| 1573 | 466 | 1029 | 276 | 38 | 10 | 12 | 1 | 1618.40 (600s) | 1612.87 (228s) | 1621.56 (3600s/2.52%) |
| 1573 | 466 | 1029 | 276 | 38 | 10 | 12 | 2 | 2136.88 (1644s) | 2132.57 (381s) | 2126.73 (3600s/2.61%) |
| 1573 | 466 | 1029 | 276 | 38 | 10 | 12 | 3 | 2460.48 (1957s) | 2444.38 (532s) | 2457.89 (3600s/0.49%) |
| 1573 | 466 | 1029 | 276 | 38 | 10 | 12 | 4 | 2668.86 (2224s) | 2668.86 (775s) | 2663.35 (3600s/0.81%) |
| 1573 | 466 | 1029 | 276 | 38 | 10 | 12 | 5 | 2794.27 (2694s) | 2795.42 (2078s) | 2797.09 (3600s/0.94%) |
| 1573 | 466 | 1029 | 276 | 38 | 10 | 18 | 1 | 2886.32 (2897s) | 2891.72 (1930s) | 2884.18 (3600s/5.08%) |
| 1573 | 466 | 1029 | 276 | 38 | 10 | 18 | 2 | 3717.60 (3072s) | 3714.44 (2034s) | 3635.79 (3600s/4.16%) |
| 1573 | 466 | 1029 | 276 | 38 | 10 | 18 | 3 | 4174.93 (3589s) | 4167.22 (1666s) | 4134.45 (3600s/1.74%) |
| 1573 | 466 | 1029 | 276 | 38 | 10 | 18 | 4 | 4429.24 (3600s/0.56%) | 4438.35 (3291s) | 4427.57 (3600s/0.70%) |
| 1573 | 466 | 1029 | 276 | 38 | 10 | 18 | 5 | 4573.82 (3600s/0.62%) | 4569.61 (3528s) | 4562.47 (3600s/0.96%) |

We now present the results and insights obtained from solving MMCaNR. Table 3.2 summarizes the objective values and running times for the Bronx Borough data set for applying the heuristic algorithms and solving MMCaNR using GUROBI. The $|A'|$ and $|E'|$ columns report the number of unavailable arcs between demand–facility nodes and between facility–facility nodes, respectively. The column $|C'|$ reports the number of installable components, while column $|D|$ and $|J|$ report the number of demand nodes and facility location nodes. Column $T$ and $K$ report length of the time horizon and number of recovery crews. The "Linear Relaxation Rounding Heuristic Solution Value" column reports the feasible solution obtained using the integer rounding procedure and the running time in seconds in parentheses. The "Lagrangian & Linear Relaxation Heuristic Solution Value"

column reports the feasible solution constructed using the Lagrangian relaxation solution and enhanced with the linear programming relaxation solution and the running time in seconds in parentheses. The "Optimal Solution Value" column reports the optimal solution and the running time in seconds in parentheses if the instance is solved optimally within an hour or the best solution values and the gap found using GUROBI within a one hour time limit. Note that reported gaps in Table 3.2 are the relative MIP optimality gaps found by GUROBI within an hour.

The computation time in the column "Linear Relaxation Rounding Heuristic Solution" includes the time to solve the linear programming relaxation. The computation time in the column "Lagrangian & Linear Relaxation Heuristic Solution" includes the time to solve the linear programming relaxation and the Lagrangian relaxation using the subgradient algorithm. Thus, the total computational time for each heuristic is comparable. We observe that the feasible solutions obtained using the Lagrangian and linear relaxation heuristic are computationally faster than the linear relaxation rounding heuristic to obtain solutions in 12 out of 15 instances in Table 3.2. On the other hand, the linear relaxation rounding heuristic solution values are as good as or better than the Lagrangian and linear relaxation heuristic solution values in the 10 out of 15 instances in Table 3.2.

We examine the optimal solutions produced by MMCaNR by examining the performance of the model at each time period. To do so, we represent the optimal objective function value $Z$ as a sum of the multiple coverage of emergency service demand recorded in each time period, $Z_t, t = 1, ..., T$, with:

$$Z_t = \sum_{\ell=1}^{L} \sum_{i \in D} w_{it} \theta_\ell z_{i\ell t}, \text{ for } t = 1, \ldots, T$$

and $Z = \sum_{t=1}^{T} Z_t$. Figure 3.3 reports $Z_t, t = 1, ..., T$ for MMCaNR instances with $K = 1, 2, 3, 4, 5$ and $T = 8$. Figure 3.3 also reports the coverage values associated with a fully functional network $G^\star$, we use network $G^\star = (I, A \cup A' \cup E \cup E')$, with all arcs initially

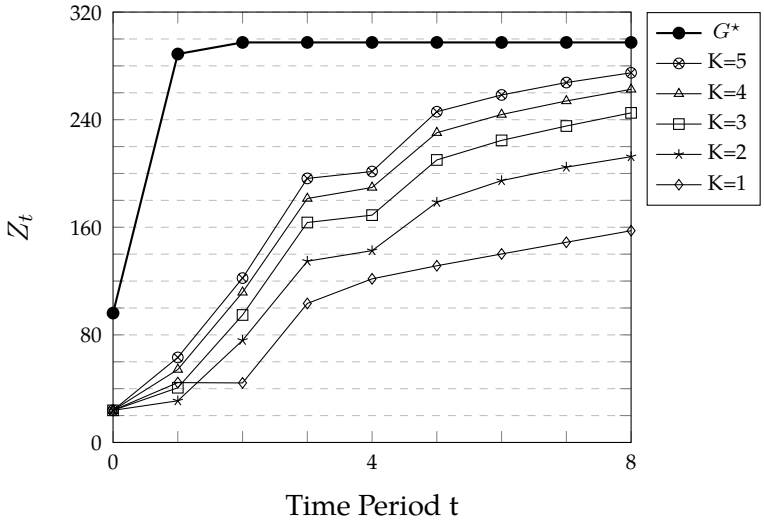


Figure 3.3: Optimal multiple coverage of emergency service demand values for MMCaNR accrued in each time period for $K = 1, 2, 3, 4, 5$, and $T = 8$ for the Bronx Borough data set, where $t = 0$ represents the objective value without any repair. $G^\star$ represents the objective value when the network is fully functional and emergency responders are first located in the initially available facilities then relocated over the time horizon $T = 8$.

available. In $G^\star$, the $P$ emergency responders are initially located in the initially available facilities $J_0$ at time $t = 0$ and are relocated over the time horizon using arcs in $E \cup E'$. The solution found using the fully functional network $G^\star$ provides an upper bound for the optimal objective function.

We report the locations of open facilities in Table 3.3 for $t = 0, \ldots, 8$ and $K = 5$ using the Bronx Borough data set. This allows us to compare the optimal emergency responder locations at $t = 0, \ldots, 8$ to those in the fully functional network $G^\star$.

In Figure 3.3, the multiple coverage recorded using only initially available arcs at $t = 0$ is $Z_0 = 23.89$ and increases over the time horizon as the network crews install new components from $C'$. We observe that the model solution suggests first repairing components that enable emergency responders to move between facility locations in the network using arcs in $E'$. Therefore, at the earlier periods of the time horizon, coverage improvement of the system is slower and also $Z_t$ achieves the same value for the different number of recovery crews. The difference between $Z_t$ for $K = 1$ and $K = 2$ is significant compared to the

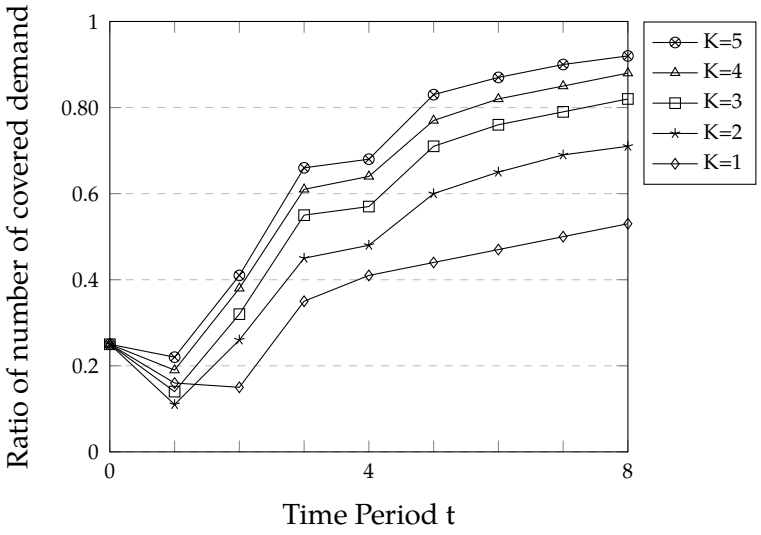


Figure 3.4: Ratio of optimal multiple coverage of emergency service demand values for MMCaNR accrued in each time period for $K = 1, 2, 3, 4, 5$, and $T = 8$ compare to the optimal multiple coverage of emergency service demand values for the fully functional network $G^\star$ for the Bronx Borough data set.

coverage differences between other consecutive number of recovery crews. This occurs, since one recovery crew can repairing one component at a time, and the first components installed tend to be in $E'$ to enable facility locations relocations. Lastly, the best possible emergency service demand coverage value occurs with the fully functional network $G^\star$. Even though the emergency responders are located at initially available facilities in $J_0$ at the beginning of time horizon in the network $G^\star$, relocations can occur using all arcs in $E \cup E'$, since all arcs in $A'$ and $E'$ are initially available. Thus the system reaches its maximal achievable $Z_t$ value at time $t = 2$.

Figure 3.4 illustrates the ratio of the multiple coverage in the optimal MMCaNR solutions ($Z_t$) to the corresponding multiple coverage in the same time period in the fully functional network $G^\star$, which we denote the coverage ratios. Figure 3.4 illustrates the coverage ratios for $t = 1, ..., 8$ and $K = 1, 2, 3, 4, 5$ repair crews. The coverage ratio is 0.25 at the beginning of the time horizon at $t = 0$. When $t = 0$, all emergency responders are located at the same set of locations in $J_0$ in all solutions. However, the solution using the fully functional network $G^\star$ can cover significantly more demand due to all arcs in $A'$ and $E'$ being initially

available. The coverage ratios increase between $t = 1$ and $t = 8$ as network components are repaired. Emergency managers can use this analysis to decide the number of repair crews to achieve certain ratios of coverage.

Figure 3.5 provides a visual representation of the solutions for the instance with $T = 8$ and $K = 5$ including the open facilities and their coverage areas for time periods 0, 4, and 8 as well as the solution to the instance using the fully functional network $G^\star$ at $t = 8$. Figure (3.5a) shows the initial coverage of emergency service demand and initial locations of emergency responders in the network for the optimal solution at time $t = 0$. Figure (3.5b) and (3.5c) show the solution at time periods 4 and 8, respectively. The circles in these sub-figures illustrate the emergency responders' coverage areas. Figure (3.5d) shows the solution with the fully functional network $G^\star$.

We highlight the value of modeling relocation restrictions by comparing the optimal solutions to MMCaNR to the corresponding MMCaNR model without relocation restrictions. To do so, the set the initially available arcs between facility location set is $E = J \times J$ and the set of disrupted arcs between emergency responder locations is $E' = \emptyset$. Table 3.4 reports the open facility locations over the time horizon for instance of MMCaNR without relocation restrictions with $T = 8$ and $K = 5$. These locations can be compared to that in Table 3.3. In Table 3.4, open facility locations at the beginning of the time horizon are shown in the first column represented by $t = 0$. The last column shows the open facility locations in the fully functional network $G^\star$ at $t = 8$. In Table 3.4, each emergency responder is relocated at most two times for a total of 10 relocations across the time horizon, while in the original MMCaNR instance (as reported in Table 3.3), each emergency responder is relocated at most two times for a total of nine relocations across the time horizon. In addition, Table 3.3 indicates that when there are relocation restrictions, there are intermediate facility locations (i.e., facility location $24$ and $34$) used to relocate emergency responders from one location to another if there is no direct arc to do so. There is no need for such intermediate facilities when the movement of emergency responders is unrestricted, as in Table 3.4.

We can compare the facility locations reported in Tables 3.3 and 3.4 to evaluate the relocations at each time period in the disrupted network $G$ with relocation restrictions (Tables 3.3) and without relocation restrictions (Table 3.4) as well as locations of emergency responders in the fully functional network $G^\star$. We call emergency responder locations in the final column of tables as the "ideal" emergency responder locations of the network $G^\star$, since they are the optimal facility locations in the fully functional network $G^\star$. At time $t = 8$, in Table 3.3, eight of the 10 emergency responder locations are the same as the "ideal" emergency responder locations in $G^\star$, and in Table 3.4, seven of the 10 emergency responder locations are the same as the "ideal" emergency responder locations in $G^\star$. The computational results of the original MMCaNR model suggest that it is best to install components that enable disrupted arcs in $E'$ between facility locations earlier in the time horizon and then install components that enable the disrupted arcs in $A'$ between demand points and the open facility locations to increase the emergency service demand coverage.

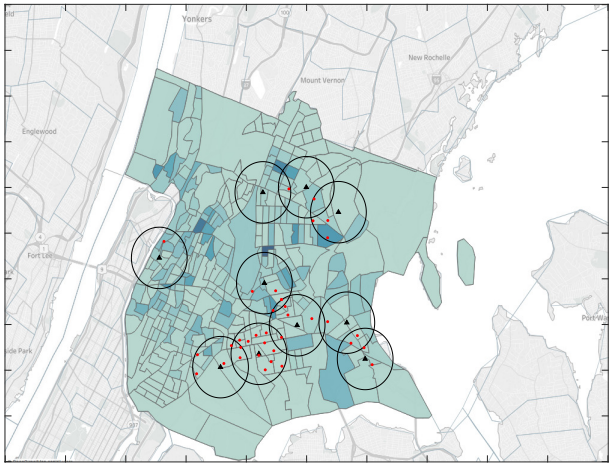

(a) Time period 0

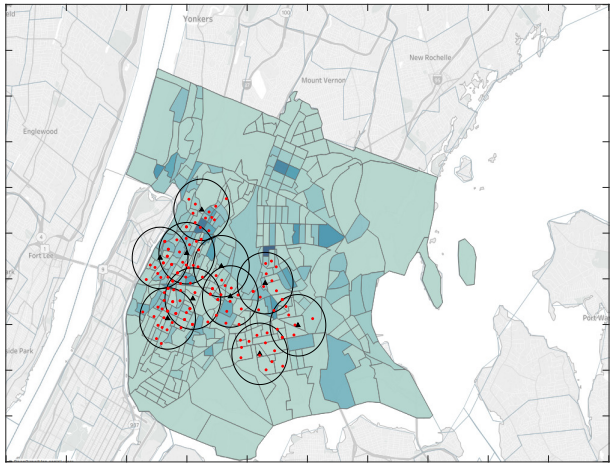

(b) Time period 4

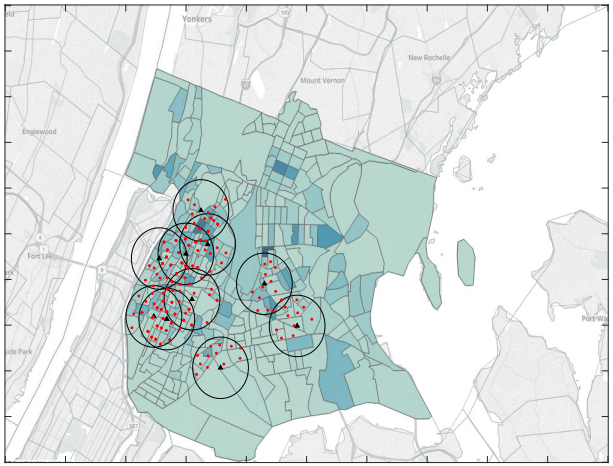

(c) Time period 8

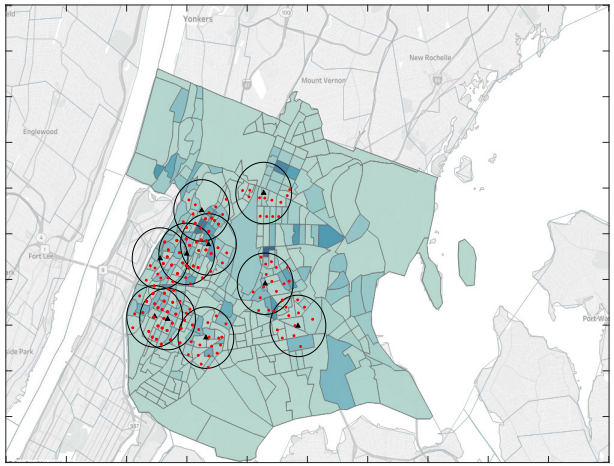

(d) $G^{\star}$ (Fully functional network)



Figure 3.5: MMCaNR emergency responder locations for the Bronx Borough data set with $K = 5$ and over the time horizon $T = 8$. Figure (3.5a) shows the model solution using initial arcs. The triangles represent the open facilities and the circles around them represent the coverage area of given triangles at time periods 4 and 8 in Figures (3.5b), (3.5c) and Figure (3.5d) shows the optimal model solution when the network is fully functional.

Table 3.3: Open facility locations in the optimal solutions to MMCaNR for the Bronx Borough data set in each time period for $T = 8$ and $K = 5$. The second column $t = 0$ shows open facility locations in $J_0$ at the beginning of time horizon. The last column $G^\star$ shows "ideal" facility locations, which are the optimal facility locations for the fully functional network.

| | | Time Periods t | | | | | | | | |
|---|---|---|---|---|---|---|---|---|---|---|
| Facilities | t = 0 | 1 | 2 | 3 | 4 | 5 | 6 | 7 | 8 | $G^\star$ |
| 1 | | | | × | × | × | × | × | × | × |
| 6 | | | | | | × | × | × | × | × |
| 11 | | | | × | × | × | × | × | × | × |
| 16 | × | × | × | | | | | | × | |
| 18 | × | × | × | × | × | × | × | × | × | × |
| 19 | | | × | × | × | × | × | × | × | |
| 22 | | | | | | | | | | × |
| 23 | | | | | | × | × | × | × | × |
| 24 | | | | | × | | | | | |
| 25 | | × | × | × | × | | | | | |
| 26 | | | × | × | × | × | × | × | × | × |
| 29 | × | × | × | × | × | × | × | × | | |
| 30 | × | × | × | × | × | × | × | × | × | × |
| 31 | × | × | × | × | × | × | × | × | × | × |
| 34 | × | × | | | | | | | | × |
| 35 | × | | | | | | | | | |
| 36 | × | × | × | × | | | | | | |
| 37 | × | × | | | | | | | | |
| 38 | × | × | × | | | | | | | |

Table 3.5 summarizes the total number of emergency responder relocations and the total distance associated with these relocations (in miles) for the instances with $T = 8$ and $K = 1, 2, 3, 4, 5$ in the original MMCaNR and the MMCaNR without relocation restrictions. We calculate the total distance of emergency responder relocations by summing the Manhattan distances between facility locations for all emergency responders over the time horizon. Note that in the original MMCaNR instances, we allow emergency responders to relocate between locations if the there is an available arc with a distance less than or equal to two miles. Even though when we remove the relocation restrictions in the MMCaNR without relocation restrictions, the total number of relocations is similar to those of the original MMCaNR. When we remove the relocation restrictions, we observe that emergency responders travel up to six miles between consecutive time periods. Furthermore, the total distances of the relocations are more than double those of the corresponding original

Table 3.4: Open facility locations in the optimal solutions to MMCaNR without relocation restrictions for the Bronx Borough data set in each time period for $T = 8$ and $K = 5$. The second column $t = 0$ shows open facility locations in $J_0$ at the beginning of time horizon. The last column $G^\star$ shows "ideal" facility locations, which are the optimal facility locations for the fully functional network.

| Facilities | t = 0 | 1 | 2 | 3 | 4 | 5 | 6 | 7 | 8 | $G^\star$ |
|---|---|---|---|---|---|---|---|---|---|---|
| 1 | | × | × | × | × | × | × | × | × | × |
| 5 | | × | × | × | × | × | × | × | × | |
| 6 | | × | × | × | × | × | × | × | × | × |
| 11 | | | | | | | | | | × |
| 16 | × | × | | | | | | | | |
| 18 | × | | × | × | × | × | × | × | × | × |
| 19 | | × | × | × | × | × | × | × | × | |
| 22 | | | | × | × | × | × | × | × | × |
| 23 | | × | × | × | × | × | × | × | × | × |
| 25 | | × | × | | | | | | | |
| 26 | | × | × | × | × | × | × | × | × | × |
| 29 | × | × | × | × | × | × | × | × | × | |
| 30 | × | | | | | | | | | × |
| 31 | × | | × | × | × | × | × | × | × | × |
| 34 | × | | | | | | | | | × |
| 35 | × | | | | | | | | | |
| 36 | × | × | | | | | | | | |
| 37 | × | | | | | | | | | |
| 38 | × | | | | | | | | | |

Table 3.5: Comparison of the total number of relocations and the total distance of relocations (in miles) in the original MMCaNR and the MMCaNR without relocation restrictions

| | Total number of relocations | | Total distance of relocations (miles) | |
|---|---|---|---|---|
| K | Original MMCaNR | MMCaNR with no relocation restrictions | Original MMCaNR | MMCaNR with no relocation restrictions |
| 1 | 10 | 10 | 13.32 | 29.43 |
| 2 | 12 | 12 | 17.80 | 24.31 |
| 3 | 11 | 11 | 16.43 | 34.35 |
| 4 | 11 | 11 | 14.97 | 30.28 |
| 5 | 9 | 10 | 14.97 | 29.22 |

MMCaNR instances in four out of five instances. We further study the impact of relocation restrictions in Figure 3.6, which compares the multiple coverage of emergency responders at each time period of the original MMCaNR to the MMCaNR without relocation restrictions for $K = 1, 2, 5$. We observe that there are large differences in the multiple coverage of emergency responders between the two models and that these differences are most accentuated at the beginning of the time horizon.

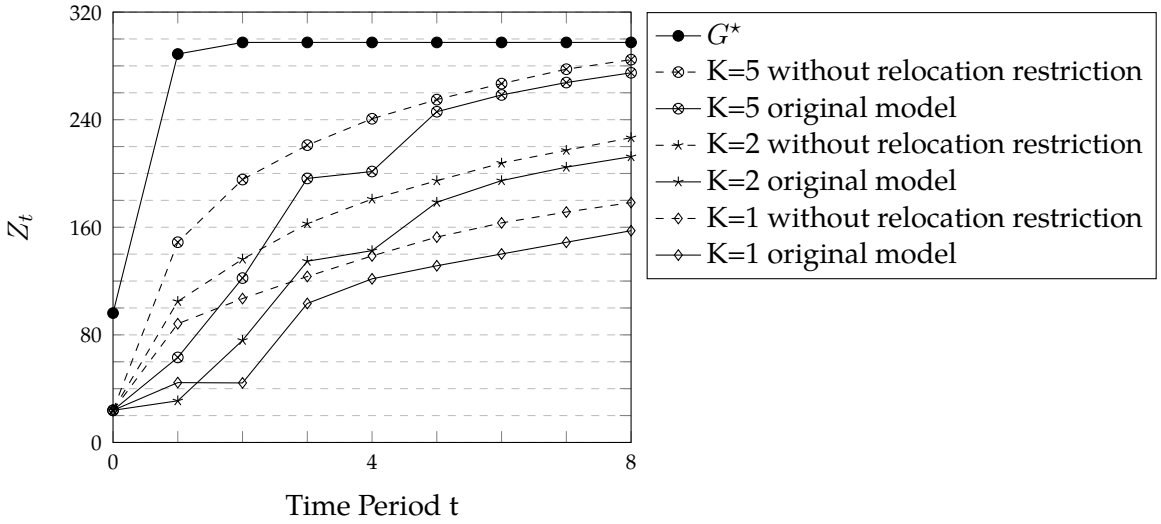


Figure 3.6: Comparison of optimal multiple coverage of emergency service demand values for MMCaNR and MMCaNR without relocation restrictions accrued in each time period for $K = 1, 2, 5$, and $T = 8$ for the Bronx Borough data set, where $t = 0$ represents the objective value without any repair. $G^\star$ represents the objective value when the network is fully functional and emergency responders are first located in the initially available facilities then relocated over the time horizon $T = 8$.

We perform a sensitivity analysis on various parameters of the Bronx Borough data set to understand how the original MMCaNR model solutions change under different inputs and to obtain policy insights. To do so, we create seven model instances based on the Bronx Borough data set that each change one type of input, and we solve MMCaNR with these seven additional data sets with $T = 8$ and $K = 1, 2, 3, 4, 5$ . We describe these model instances as follows.

1. We consider having a different set of initially available locations $J_0$. Here, $J_0$ contains the "ideal" locations associated with the fully functional network $G^\star$, as reported last column in Table 3.3.

2. We consider having a different set of initially available locations $J_0$. Here, $J_0$ contains the $|P|$ most damaged facility locations, where damage is computed as the total number of 311 complaints in the location's coverage area.

3. We consider a component to be disrupted, and hence, installable if both ends of

the component receive three or more complaints in the 311 data (as opposed to five complaints in the original problem instance). This results in a new installable component set $C'$ as well as its corresponding disrupted arc set $A'$.

4. We set relocation distance for emergency responders to one mile (two miles in the initial data set). Shortening the relocation distance changes the set of initially available arcs between facilities $E$ and the set of disrupted arcs between facility locations $E'$.

5. We consider $L = 3$ levels of coverage with $\theta_1 = 0.5, \theta_2 = 0.3$ and $\theta_3 = 0.2$.

6. We consider a coverage distance of 1.0 mile when determining the subset of facility locations that cover demand at $i \in I$, captured by $N_i^A, i \in I$.

7. We consider locating $P = 8$ emergency responders.

We report the optimal multiple coverage of emergency service accrued in each time period for each case. We illustrate the multiple coverage in each time period for the first four sets of model instances in Figure 3.7 and for the last three sets of model instances in Figure 3.8. We also compare each instance to the multiple coverage associated with its corresponding fully functional network $G^*$. Note that the first four sets of model instances in Figure 3.7 have the same multiple coverage values associated with the fully functional network $G^*$ at time $t = 8$ as in the original problem instance, whereas the last three sets of instances in Figure 3.8 have different multiple coverage values associated with the fully functional network $G^*$ as in the original problem instance (as reported in Figure 3.3).

Figure 3.7 illustrates the multiple coverage in each time period for instance sets 1 – 4. Figures 3.7a and 3.7b illustrate the results when we change the set of initially available facility locations, $J_0$. Figure 3.7a illustrates the case when the "ideal" locations are initially available (i.e., $J_0 = \{1, 6, 11, 18, 22, 23, 26, 30, 31, 34\}$). In this case, the total number of relocations decreases to six with $K = 5$ recovery crews and time horizon $T = 8$, since the facilities are already located in "ideal" locations. Nine of the ten open facility locations

at $t = 8$ are same as those in the second last column in Table 3.3. Figure 3.7b illustrates the case when the 10 initial facility locations are those with the most damage complaints (i.e., $J_0 = \{3, 6, 9, 10, 11, 13, 14, 20, 21, 23\}$). We observe that the multiple coverage is higher in Figure 3.7b than in Figure 3.3 across all time periods. This occurs, since there is a high weight at the demand points near these initially available facility locations (i.e., $w_{it}$ values), which allows more demand to be covered without having to relocate facilities. The change in the initially open facility location set results in 10 relocations over the time horizon $T = 8$ with $K = 5$ recovery crews. When we compare the open facility locations at the end of time horizon, we observe that three are different than those in Table 3.3. In Figure 3.7a and 3.7b, we observe that we can achieve better coverage in Figure 3.7b for each different number of repair crews $K = 1, 2, 3, 4, 5$.

Figure 3.7c shows the multiple coverage in each time period, when we redefine the installable set of components. In this case, we have more installable components than in the original problem instance. These additional components have short recovery times, since recovery times are proportional to the damage severity (which reflects the number of complaints) and the distance. As a result, more components can be repaired in a short amount of time, and we observe that the multiple coverage in each time period for the given number of recovery crew is slightly higher in some time periods than in Figure 3.3. Figure 3.7d reports the multiple coverage in each time period when we reduce the relocation distance for emergency responders to one mile (as compared to two miles in the initial data set). This further restricts the emergency responders' movement in the network by reducing the size of both $E$ and $E'$. As a result, emergency responders require more time periods to move to desirable facility locations, which results in a lower multiple coverage at the end of time horizon $T = 8$ compare to Figure 3.3.

Figure 3.8 illustrates the multiple coverage in each time period for instances $4$–$7$. Figure 3.8a shows the multiple coverage in each time period when we set the coverage level to $L = 3$, with primary coverage and two levels of backup coverage (as compared to two

total levels of coverage in the initial data set). We set the weights to $\theta_1 = 0.5, \theta_2 = 0.3$ and $\theta_3 = 0.2$. We observe that nine of the ten open facilities at the end of time horizon $t = 8$ are the same as in the original data and reported in Table 3.3. Additionally, the overall multiple coverage is lower in all time periods, since two levels of backup coverage are desired. Figure 3.8b shows the multiple coverage in each time period when we set the coverage distance to one mile (as compared to 0.7 miles in the initial data set).Since an open emergency responder location can cover larger area, we observe higher overall multiple coverage levels as compared to the initial data set as reported in Figure 3.3. We observe that when we consider three levels of coverage, eight of 10 open facility locations at the end of time horizon $T = 8$ are same as the open facility locations reported in Table 3.3. Figure 3.8c shows the multiple coverage in each time period with $P = 8$ open facility locations (as compared to $P = 10$ in the original data set). As expected, decreasing the number of open facility locations results in lower multiple coverage compared to that of the original data set as reported in Figure 3.3. We observe that six out of eight open facility locations are same as the open facility locations reported in Table 3.3 at $t = 8$.

The number of recovery crews, the time horizon, and processing times of the installed components affect the number of installed components. The number of installed components affects the total number of covered demand nodes in all levels and levels of the coverage. Our computational experiments suggest that the best recovery strategy is to install components that are connected to the most critical open facility locations. Therefore, the recovery crews are relocated with the emergency responders using the available arcs in the network. Our model solutions assist decision–makers to decide the relocations of emergency responders and the schedule of recovery crews to improve the emergency service demand coverage during disaster recovery process. As a result, the solutions provide guidance to prioritize the installation of network components to deliver time–sensitive services more effectively during the disaster recovery phase.

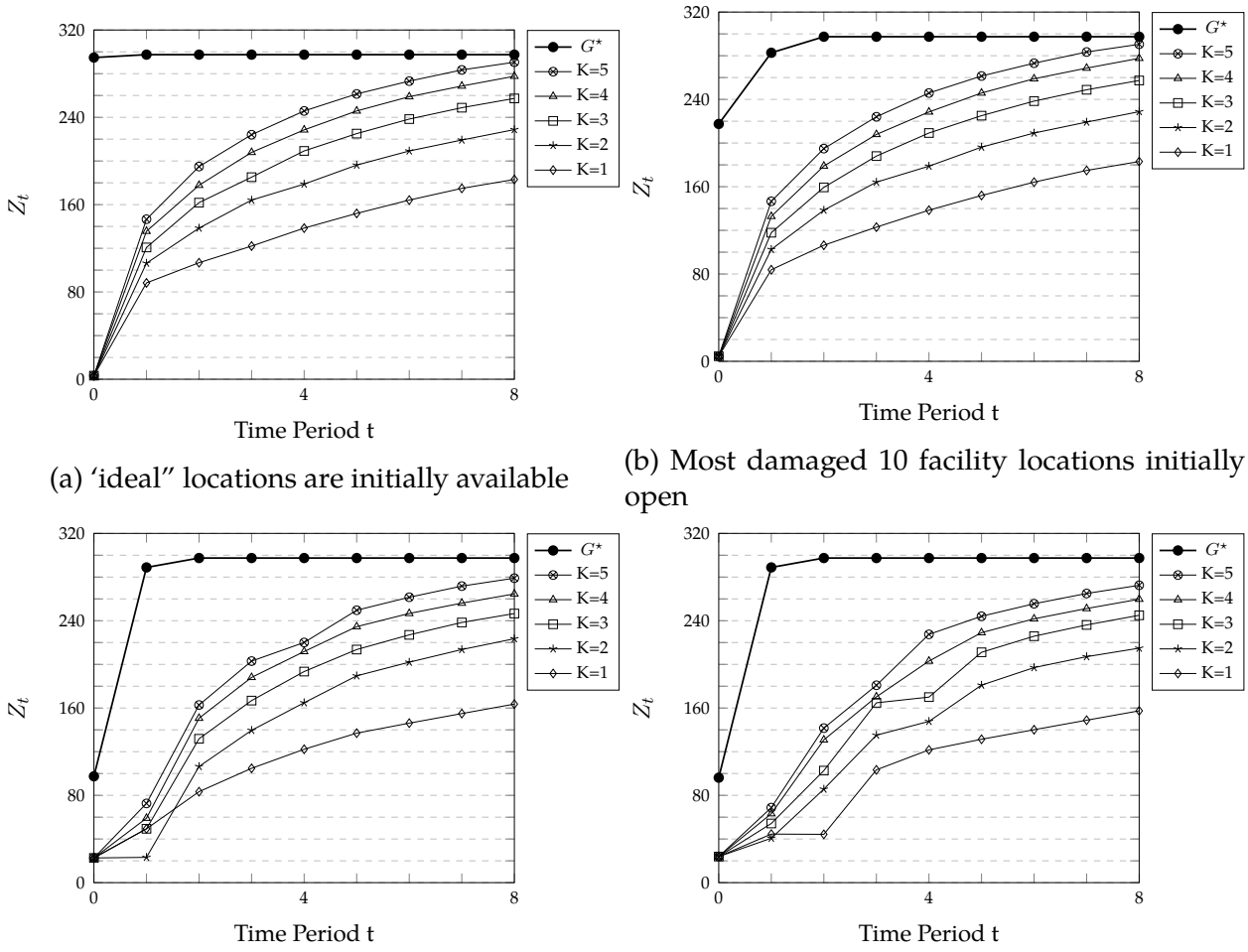


(a) 'ideal" locations are initially available

(b) Most damaged 10 facility locations initially open

(c) Additional installable components

(d) Relocation restriction 1 mile

Figure 3.7: Optimal multiple coverage of emergency service demand values for MMCaNR with the different initial parameters accrued in each time period for $K = 1, 2, 3, 4, 5$, and $T = 8$ for the Bronx Borough data set, where $t = 0$ represents the objective value without any repair. $G^\star$ represents the objective value when the network is fully functional and emergency responders are first located in the initially available facilities then relocated over the time horizon $T = 8$.

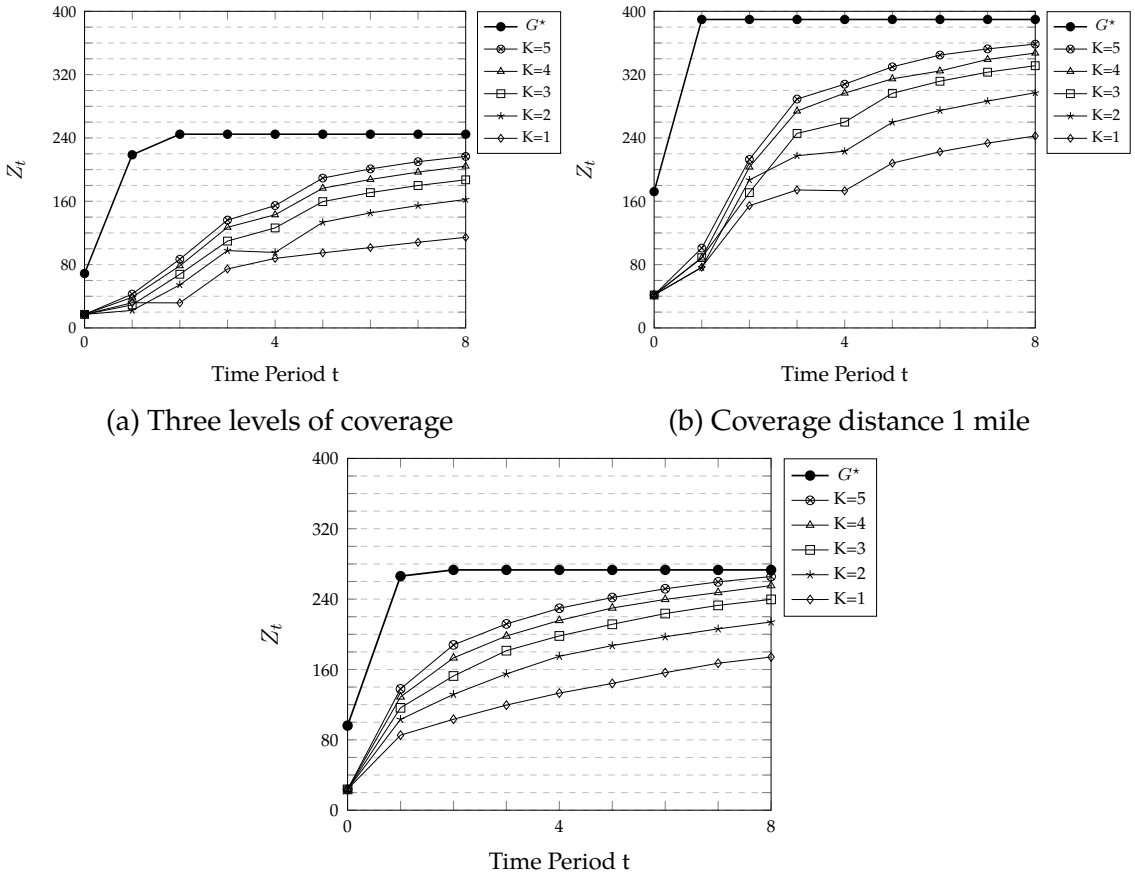


(a) Three levels of coverage

(b) Coverage distance 1 mile

(c) P = 8

Figure 3.8: Optimal multiple coverage of emergency service demand values for MMCaNR with the different initial parameters accrued in each time period for $K = 1, 2, 3, 4, 5$, and $T = 8$ for the Bronx Borough data set, where $t = 0$ represents the objective value without any repair. $G^\star$ represents the objective value when the network is fully functional and emergency responders are first located in the initially available facilities then relocated without no relocation restriction over the time horizon $T = 8$.

## 3.5 Conclusions

Disruptions in road infrastructure can delay the delivery of emergency service and relief demand. In this chapter, we introduce a maximal multiple coverage and network restoration problem (MMCaNR) for recovery and restoration of infrastructure systems after disasters with the goal of maximizing cumulative multiple coverage of emergency service demand over the time horizon. MMCaNR considers the interdependency between road infrastructure and emergency services. While solutions to the problem provide a plan

for restoring the most critical network components, the problem also relocates emergency responders using available arcs to improve the cumulative multiple coverage of emergency service demand. Further, MMCaNR solutions can be used to measure the emergency service demand coverage after disasters.

We develop an integer programming formulation for our model. We introduce a Lagrangian and linear relaxation heuristic and a linear relaxation rounding heuristic. Each heuristic identifies a feasible solution to MMCaNR. We examine the quality of heuristics using real world data set belongs to the Bronx Borough during Hurricane Sandy. In our computational experiments, we observe that the feasible solutions obtained using the Lagrangian relaxation based heuristic are computationally faster, while the linear relaxation rounding heuristic yields better feasible solutions. These observations suggest that the model and heuristics can contribute effective emergency service demand coverage and network recovery in real–time after a disaster.

# Chapter 4

# Facility Location and Restoration Games

## 4.1 Introduction

Infrastructures such that telecommunication, transportation, water, power, and other fundamental systems and services are critical for the security, economy, and social well-being of the nation (Rinaldi et al. (2001)). Effective services of infrastructure systems during recovery efforts, especially following the natural and man-made disasters, requires accounting for the interdependencies of these systems. The complexity of the interconnections and the multi-agent ownership of the infrastructure systems, with different systems owned by private and public agencies, complicates the restoration of essential services during the disaster recovery (Rinaldi et al. (2001)).

Hurricane Sandy, for example, severed power distribution lines, damaged open air substations, flooded basements with transformers and backup generators, and inundated underground substations and subway lines, which often host electrical cables. The damage to power infrastructure created power outages to more than 8 million customers across 21 states, which required several weeks to fully restore. Restoration of power involved removing trees from downed power lines, repairing distribution lines, installing utility poles as well as other tasks. The total 80 utility companies responsible for electricity

generation and distribution could not handle the recovery of the interconnected power grid with their in-house resources (Henry and Ramirez-Marquez (2016)). Resources from other agencies in the US contributed resources for restoration. Hurricane Sandy highlighted the need for procedures to restore infrastructure systems with multiple infrastructure owners and disaster managers. One of the possible improvements is "mutual aid" or "mutual assistance" program that allow companies to share resources to meet their collective needs during disaster recovery (Keogh and Sharon (2015)). This recommendation is echoed by the Department of Homeland Security, describes ways to improve coordination and response structures to build preparedness for disasters. The report recommends nongovernmental parties, including private sector/industry partners in responding to disasters and a new emergency support function to support coordination mechanisms between the government and the infrastructure owners (FEMA (2019)). This is the central issue studied in this chapter.

Infrastructure systems with multiple owners can be modeled as a multi-layer network with each system represented by a layer of the network and the interdependencies between systems by connections between layers (Sharkey et al. (2015b)). After a disaster, each system owner seeks to provide their own services more efficiently by restoring network components (Sharkey et al. (2015b)). In this chapter, we study facility location and restoration games on a two-layer network, in which each network layer belongs to a player who represents an infrastructure owner/manager. Each network layer consists of facility location and demand nodes as well as the edges between them. There are disrupted facility locations and disrupted edges between facility locations and demand points. We consider the recovery of disaster damage in facilities, connections between the facilities and the demand points in and between the layers by allowing infrastructure owners to open facilities and recover/install edges within and between network layers. The network owners want to minimize the total cost to satisfy their own demand, and therefore the main goals of the network owners are aligned. However, owners may be unwilling to coordinate the recovery

efforts to achieve their objectives together, which results in solutions that do not benefit the most possible customers (Nisan et al. (2007)).

The purpose of this chapter is to model the recovery efforts of interdependent infrastructure systems after disasters and the coordination with each other under the control of a governmental agency using non-cooperative game theory by accounting for interdependencies between systems. We consider single-shot facility location and restoration games to model short-term recovery efforts of infrastructure systems after disasters. The games could represent the first day of network recovery. In the games, the two-layer network has two types of edges: intra- and inter-edges. *Intra-edges* (within each player's layer) connect a player's demand nodes to the player's facility location nodes. *Inter-edges* (between layers) connect a player's demand nodes to the other player's facility location nodes. The inter-edges capture network interdependencies and shared network components. In addition to the initially available edges in the network, there are disrupted edges due to a disaster. Each player can recover intra-edges within their layer or inter-edges between layers, which allow these edges to be used in the network by players. Each player can only recover intra- and inter-edges that are connected to their own facilities. An edge between a facility node and a demand node belongs to the player who owns the facility. If an edge is disrupted, the owner of the edge responsible for recovering. If a player uses an inter-edge to satisfy their demand, the player pays a fee to the player who owns the inter-edge, in addition to the cost of using the inter-edge. Each player has a budget to install intra- or inter-edges in the two-layer network. The goal of each player is to minimize the total cost to satisfy demand in their own network using facilities in both layers using available intra- and inter-edges.

We consider a central decision maker/government authority (not an infrastructure owner) as a kind of third player in the games who sets the recovery funding budget and allocates it to the two players for their recovery efforts according to the optimal solution of a centralized model. The centralized model captures the location of facilities, assigns facilities to demand using available edges, and installs new edges in the two-layer network with

one decision maker and provides a social welfare solution. The objective is to minimize the total cost of satisfying the demand of both players. Infrastructure owners can include decisions in which the players use each other's facilities to satisfy their demand. However, due to the multi-agent ownership of the interdependent infrastructure systems, we cannot guarantee that players will obey the central decision maker during their disaster recovery efforts. Therefore, we present non-cooperative facility location and restoration games to capture the coordination between multi-agent owned systems and a government agency. We present a mechanism that provides incentives to players as inter-edge usage fees to achieve a pure Nash equilibrium in the games that aligns with the social welfare solutions.

### 4.1.1 Illustrative Example

We present a simplified example to show that by setting appropriate inter-edge fees, a centralized model solution becomes one of the pure Nash equilibria in the game. Figure 4.1 illustrates an example, where each player has one facility location and one demand on their network layer. We consider Player 1, who owns facility A and demand 1; and Player 2, who owns facility B and demand 2. There are only available edges in this example and no disrupted edges. Players 1 and 2 want to satisfy their demand using facility A or facility B. Player 1 needs to pay 5 units to open Facility A and Player 2 needs to pay 10 units to open facility B. Player 1 needs to pay a cost for using edge $a_{1A} = 9$ or edge $a_{1B} = 1$ to satisfy demand 1. Player 2 needs to pay a cost for using edge $a_{2B} = 3$ or edge $a_{2A} = 1$ to satisfy demand 2. Table 4.1 shows the social welfare solution (in italic) without fees for using inter-edges as well as the pure Nash equilibrium solutions (in boldface) without fees for using inter-edges. In the social welfare strategy that captures the optimal solution of the centralized model, Player 2 opens facility B and shares the facility with Player 1. Hence, Player 1 satisfies demand 1 using Player 2's facility B and inter-edge $(1, B)$, and Player 2 opens facility B and satisfies demand 2 with intra-edge $(2, B)$.

Next, we include inter-edge usage fees in addition to the other costs in the example in

Table 4.1, and we show how inter-edge usage fees change the Nash equilibrium solutions. In Table 4.2a, Player 1 needs to pay a 14 units fee to use inter-edge $(1, B)$ and Player 2 needs to pay a 14 units fee to use inter-edge $(2, A)$. In Table 4.2b, we change the fees for using the inter-edge $(1, B)$ to $10$ units and $(2, A)$ to $15$ units. In Table 4.2, each cell represents the total cost to satisfy demand of a player, where total cost includes the cost of opening a facility, the cost of assigning demand, and the fee for using inter edges payed to the other player (if applicable) for Player 1 and Player 2, respectively and excludes the fee received from the other player for serving the other player's demand with inter edges (if applicable). We observe that in Table 4.2a, in the pure Nash equilibrium strategy, Player 1 opens Facility A and uses intra-edge $(1, A)$ to satisfy Demand 1, Player 2 opens Facility B and uses intra-edge $(2, B)$ to satisfy Demand 2. So, the players satisfy their demand using their own facilities. In Table 4.2a, the social welfare solution is not a pure Nash equilibrium. Further, the total payoffs of both players is 27, which is almost double of the social welfare solution value. When we change the inter-edge usage fees as in Table 4.2b, we observe that the social welfare solution in which Player 1 uses inter-edge $(1, B)$ and Player 2 opens Facility B and uses intra-edge $(2, B)$ is a pure Nash equilibrium. In this example, we observe that the inter-edge usage fees change the Nash equilibrium as well as the total cost to satisfy demand for each player. Therefore, by setting appropriate inter-edge fees, it is possible for the players to make decisions in a way that aligns with the social welfare solution. In this chapter, we present a mechanism to set the fees to achieve the social welfare solution as a Nash equilibrium.

### 4.1.2 Contributions

We establish a game-theoretic framework to provide a fundamental understanding of a class of facility location and restoration problems in a non-cooperative setting with two players as a two-layer network. In the games, each player wants to minimize the cost to satisfy their own demand.

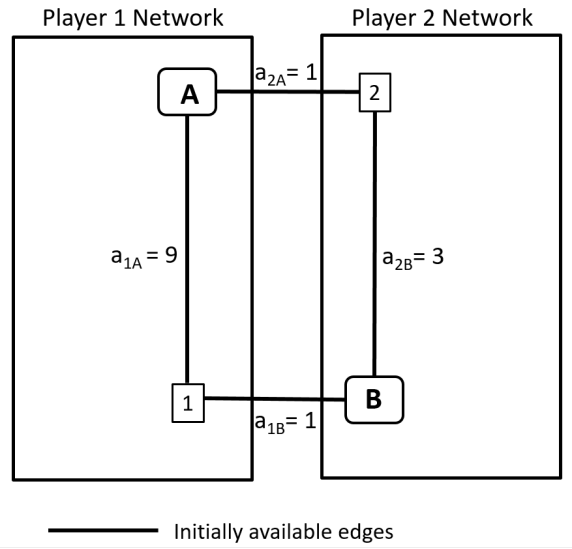


Figure 4.1: An example with Facility A and Demand 1 for Player 1 and Facility B and Demand 2 for Player 2. The cost to open Facility A is 5 and B is 10. The cost to use arc $a_{1A}$ = 9, $a_{1B}$ = 1, $a_{2B}$ = 3, $a_{2A}$ = 1. Note that in this example, all edges are initially available.

Table 4.1: The table represents the total cost payed by each player to satisfy their demand, which includes cost of opening facility and cost of assigning demand for the given strategy for Player 1 and Player 2, respectively. A boldface cell represents pure Nash equilibrium solution, an italic and boldface cell represents the social welfare solution and also a pure Nash equilibrium solution.

| | | Player 2 | | |
|---|---|---|---|---|
| | | open $B$, use $a_{2B}$ | open $B$, use $a_{2A}$ | use $a_{2A}$ |
| Player 1 | open $A$, use $a_{1A}$ | $(14, 13)$ | $(14, 11)$ | **(14, 1)** |
| | open $A$, use $a_{1B}$ | $(6, 13)$ | $(6, 11)$ | $(\infty, 1)$ |
| | use $a_{1B}$ | ***(1, 13)*** | $(1, \infty)$ | $(\infty, \infty)$ |

First, we present a centralized model, where a centralized decision maker/government authority considers satisfying the demand of both players using available edges as well as recovering edges in the two-layer network. The goal of the centralized decision maker is to provide a social welfare solution by minimizing the total cost to satisfy all the demand in the two-layer network. The central decision maker splits the recovery budget between players according to the social welfare solution.

We present two versions of the game under two different setting on how the centralized decision maker splits the recovery budget. In the first version of the game, the central

Table 4.2: The table represents the total cost, including fees for using inter-edges, payed by each player to satisfy their demand. Each cell represents the total cost, which includes cost of opening facility, cost of assigning demand, fee for using inter edges payed to other player (if applicable) and excludes fee received from the other player for serving the other player's demand with inter edges (if applicable). For the given strategy for Player 1 and Player 2, a boldface cell represents the social welfare, an italic cell represents a pure Nash equilibrium solution.

(a) Player 1 needs to pay a 14 unit fee to use inter-edge $(1, B)$ and Player 2 needs to pay a 14 unit fee to use inter-edge $(2, A)$.

| | | Player 2 | | |
|---|---|---|---|---|
| | | open $B$, use $a_{2B}$ | open $B$, use $a_{2A}$ | use $a_{2A}$ |
| Player 1 | open $A$, use $a_{1A}$ | **(14,13)** | $(0, 25)$ | $(0, 15)$ |
| | open $A$, use $a_{1B}$ | $(20, -1)$ | $(6, 11)$ | $(\infty, 15)$ |
| | use $a_{1B}$ | *(15, -1)* | $(15, \infty)$ | $(\infty, \infty)$ |

(b) Player 1 needs to pay a 10 unit fee to use inter-edge $(1, B)$ and Player 2 needs to pay a 15 unit fee to use inter-edge $(2, A)$.

| | | Player 2 | | |
|---|---|---|---|---|
| | | open $B$, use $a_{2B}$ | open $B$, use $a_{2A}$ | use $a_{2A}$ |
| Player 1 | open $A$, use $a_{1A}$ | $(14, 13)$ | $(-1, 26)$ | $(-1, 16)$ |
| | open $A$, use $a_{1B}$ | $(16, 3)$ | $(1, 16)$ | $(\infty, 16)$ |
| | use $a_{1B}$ | ***(11, 3)*** | $(11, \infty)$ | $(\infty, \infty)$ |

decision maker provides recovery budget to players to install inter-edges as well as intra-edges. In the second version, the central decision maker provides a recovery budget to players to install only intra-edges. We show that both non-cooperative games are potential games and that a pure Nash equilibrium always exists by constructing a potential function for the games. A game is a *potential game* if it admits a potential function. The *potential function* is a function in which a change in a single player's utility function value due to a strategy deviation results in the same amount of change in the potential function (Lã et al. (2016)).

Additionally, we compare the Nash equilibrium solutions to the social welfare solutions. To measure the effectiveness of the equilibria, we use common concepts of non-cooperative game theory, namely, the price of stability and the price of of anarchy. The *price of stability* is defined as the ratio between the best objective function value of a Nash equilibrium and

the social welfare solution (Tardos and Wexler (2007)). The *price of anarchy* is defined as the ratio between the worst-case objective function value of a pure Nash equilibrium and the social welfare solution (Roughgarden (2009)). Under certain conditions, we provide a bound for the price of stability for the games.

In the games, both players want to minimize the cost to satisfy their own demand during their disaster recovery efforts. This leads to a selfish setting in which each player makes decisions subject to their own objective and constraints. However, a social welfare solution may include recovering inter-edges and sharing facilities with the other player and result in lower overall costs than either player can achieve alone during the disaster recovery. To encourage players to share facilities, to recover and use inter-edges, we present a mechanism design, which decides inter-edge usage fees using an inverse mixed integer optimization procedure. Every iteration in the inverse optimization procedure requires solving an integer programming problem. As a result, for large problem instances, the inverse optimization procedure may not be practical. We provide an $\alpha$-approximation algorithm to determine fees for using inter-edges. We prove that when players use the fees obtained from the inverse optimization procedure, the optimal solution of the centralized model is a pure Nash equilibrium, and when players use $\alpha$-approximation algorithm fees the optimal solution of the centralized model is an $\alpha$-approximate pure Nash equilibrium.

We illustrate the models and algorithms with a case study that captures the recovery of telecommunications networks following an ice storm that causes to massive telecommunication network outages. The example uses Chicago telecommunication infrastructure companies. Computational results show the effectiveness of the mechanism designs to achieve a Nash equilibrium, which aligns with the social welfare solution.

The remainder of this chapter is organized as follows. Section 4.2 presents the most relevant literature for the facility location and restoration games. Section 4.3 summarizes the mathematical formulations for the centralized model and the non-cooperative facility

location and restoration games. Section 4.4 develops a potential function for the facility location and restoration games and proves the existence of a pure Nash equilibrium using the potential function. Section 4.5 analyzes the price of stability. Section 4.6 presents the mechanism design using an inverse optimization method and $\alpha$-approximation algorithm to set inter-edge usage fees. Section 4.7 presents a case study for two telecommunication companies in Chicago, IL, USA. Section 4.8 presents concluding remarks.

## 4.2 Literature Review

Interdependency relationships between infrastructure systems effect disaster recovery of the systems (Rinaldi et al. (2001)). Lee et al. (2007) model the interdependencies and interconnections of the systems explicitly as a multi-layer network in a centralized decision-making environment. Considering the recovery of infrastructure systems together by including interdependencies can ensure a rapid restoration of the systems, however multi-agent ownership of infrastructure systems make this centralized recovery idea inefficient. Sharkey et al. (2015a) consider different decision-making environments of interdependent infrastructure restoration, such as centralized, decentralized, and information-sharing decision-making environments, and they address the impact of information-sharing in a decentralized decision-making environment. They then introduce interdependent integrated network design and scheduling problems to model the recovery of interdependent infrastructure systems.

Few papers in the literature consider how to recover interdependent infrastructure systems after disasters in a decentralized decision-making environment. The design of large networks with independent service owners such as telecommunication and power networks has been modeled using network formation games, where the independent owners selfishly optimize the quality or cost of their individual service (Tardos and Wexler (2007)). Chen and Zhu (2016) present a two-layer interdependent network game, in which

each player adds or removes intra-edges within their network and inter-edges between the two networks within their budget to maximize algebraic connectivity. Ehsani et al. (2015) present a bounded budget network creation game in which each player creates edges to other players with a fixed budget. Similarly, we consider that each player recovers inter-edges, which are used by the other player in addition to intra-edges, which are used by the player who recovers them within their specific budget. Smith et al. (2017) present interdependent network recovery games with the goal of minimizing recovery cost. Further, they consider a best-case decentralized model, which allows controllers to develop a full recovery plan and negotiate until all parties reach a point where no one wants to deviate from their plan.

Another stream of literature considers facility location problems. While deterministic facility location models are studied extensively in the literature (Snyder and Daskin (2005); Wang et al. (2003); Wolsey et al. (1990)), there are some studies that consider game theoretical settings for facility location problems. There are two types of facility location games: cooperative (Goemans and Skutella (2004); Liu et al. (2016); Verdonck et al. (2016)) and non-cooperative (Cardinal and Hoefer (2010); Carvalho Rodrigues and Xavier (2017)). Some models consider a customer-centered context, where costs are allocated to the customers such that no coalition of customers has an incentive to build their own facilities (Goemans and Skutella (2004); Liu et al. (2016)). Verdonck et al. (2016) focus on transportation carrier collaboration in which the goal is to share facilities (distribution centers) between participating carriers while minimizing cost and improving distribution efficiency. Similarly, our model permits players to share facilities to satisfy their demand and share costs by imposing inter-edge fees. Capacitated facility location games (Carvalho Rodrigues and Xavier (2017)) consider sharing facility opening costs with and without a cost-sharing scheme for the facilities that are used by multiple players.

Our non-cooperative game is a potential game, which is a game with a potential function. A potential function is defined on the set of strategies in the game, such that the equilibria of

the game are given by the local optima of the potential function (Tardos and Wexler (2007)). The advantages of potential games include the existence of pure equilibria, convergence of best response dynamics, and a bound on the price of stability (Tardos and Wexler (2007)). Slikker (2001) studies coalition formation models and shows that under certain conditions the coalition formation model is a potential game. Qi et al. (2018) present a distributed resource scheduling potential game to coordinate severe interference in a dense cellular network.

The price of stability is a common concept used to measure the effectiveness of equilibria and considers the ratio between the best Nash equilibrium and the social welfare solution. Dhamal et al. (2018) present a two-player resource allocation game and show that the PoS can be bounded under certain conditions. Abeliuk et al. (2016) propose an interdependent scheduling game in which each player schedules a set of services. For a special case of the model, they provide bounds on the PoS. Anshelevich et al. (2008) study the PoS for network design and network cost allocation problems. Bloch and Jackson (2006) analyze the stability concepts for modeling network formation.

Lastly, we present mechanism design methods for the facility location and restoration game. A mechanism design idea using inverse optimization is used by Houghtalen et al. (2011) and Agarwal and Ergun (2008) for a cargo carrier alliance. These papers compute incentives for carriers who join the alliance using an inverse optimization technique for their linear programming models. Several studies consider inverse optimization technique for mixed integer linear programming. Duan and Wang (2011) present heuristic algorithms for the inverse mixed integer linear programming algorithm. Wang (2009) proposes cutting plane algorithms for the inverse mixed integer linear programming problem. Primal-dual algorithms are widely used within the area of approximation algorithms. Buchbinder and Naor (2009) present online primal-dual algorithms for covering and packing problems. Jain and Vazirani (1999) present approximation algorithms for metric facility location and P-median problems using the primal-dual scheme.

## 4.3 Mathematical formulations of the centralized model and facility location and restoration games

In this section, we present facility location and restoration games with two players in a two-layer network. First, we present a centralized model, where a centralized decision maker/government authority considers opening facilities, satisfying the demand of both players using available edges as well as recovering edges in the two-layer network. The goal of the centralized decision maker is to provide a social welfare solution by minimizing the total cost to satisfy all the demand in the two-layer network. The social welfare solution may include collaborative recovery decisions such as recovering or using inter-edges or sharing facilities. Due to the multi-agent ownership of the infrastructure systems, it is not guaranteed that players/infrastructure owners follow the social welfare solution and collaborate. Second, we introduce a non-cooperative game setting to include the strategic interactions between the two players. In the game, the central decision maker can be viewed as a third player who allocates the recovery budget between two players according to the social welfare solution.

We establish two different control settings of the central decision maker in splitting the recovery budget, namely strict control and limited control. Thus, we introduce two non-cooperative versions of the facility location and restoration game, namely *the strict control facility location and restoration* (SC-FLR) and *the limited control facility location and restoration* (LC-FLR).

In SC-FLR, the central decision maker provides recovery budget to players and allows them to install intra-and inter-edges. We call this version strict control since the central decision maker needs to ensure that each player installs inter-edges as well as intra-edges with the given budget and other player uses the inter-edges according to the social welfare solution. To do that, the central decision maker can allocate crews to install inter-edges

according to the social welfare solution or requires strict agreements from the players to install inter-edges as in the social welfare solution. Without a strict control, when we consider the selfish nature of the privately-owned infrastructure managers, players, they do not necessarily consider the social welfare during their disaster recovery efforts. Hence players may install only intra-edges using the given recovery budget or a player may not use the inter-edges, which are installed by the other player. Therefore, considering that players install inter-edges as well as intra-edges with the given recovery budget may be too optimistic. We later prove that there is always a pure Nash equilibrium to SC-FLR, in which none of the players uses recovered inter-edges. Possibility of a Nash equilibrium with self-interested behavior causes a suboptimality in the two-layer network recovery, which is measured by the price of anarchy that is the ratio between the worst-case objective function value of a pure Nash equilibrium and the social welfare solution (Roughgarden (2009)). To deviate from this issue, we formulate LC-FLR. In LC-FLR, the central decision maker provides each player a recovery budget to only install intra-edges, but players can use initially available inter-edges as well as installed and initially available intra-edges.

In the games, we have two players in the player set $N = \{1, 2\}$ that represent infrastructure owners. We start with a two-layer network $G = (V, E)$, where the node set $V$ is the union of demand set $D$ and facility location set $F$ (i.e., $V = D \cup F$). The edge set $E = A \cup I$ is the union of initially available intra-and inter-edge set $A$ and the recoverable intra-and inter-edge set $I$. Note that $D = D_1 \cup D_2$, where $D_1$ and $D_2$ are the set of demand nodes for Players 1 and 2, respectively. The facility location set $F$ is the union of pairwise disjoint facility location node sets $F_1$ and $F_2$ for Player 1 and 2,respectively, where $F = F_1 \cup F_2$. The edge set $E$ is the union of pairwise disjoint sets of intra-edge sets $E_1$ and $E_2$ for the edges within the layers of Players 1 and 2, where $E_1 \subset D_1 \times F_1$ and $E_2 \subset D_2 \times F_2$, and inter-edge sets $E_{12}$ and $E_{21}$ (i.e., $E = E_1 \cup E_2 \cup E_{12} \cup E_{21}$). Inter-edge set $E_{12}$ represents edges from the demand set of Player 1 to the facility location set of Player 2, where $E_{12} \subset D_1 \times F_2$, while inter-edge set $E_{21}$ represents edges from the demand set of Player 2 to the facility

location set of Player 1, where $E_{21} \subset D_2 \times F_1$. Note that Players n, where $n \in N$ can recover any intra-edges within their individual layer $G_n = (V_n, E_n)$ and any inter-edges, which are connected to any facility locations of Player $n$.

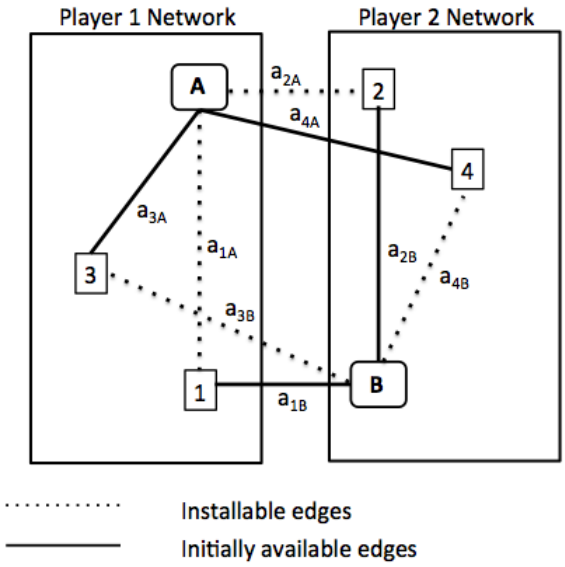


Figure 4.2: The two-layer network with facility location and demand location nodes, initially available intra-and inter-edges, and installable intra-and-inter edges for each player.

In the games, players form network by recovering intra- and inter-edges with a budget $B^n$ given by the central decision maker for each Player $n \in N$. Each disrupted edge $(u, v)$ has a cost $p_{uv}$ to recover, which is payed by the player who owns facility $v$. In addition, for each facility $v \in F_n$, $n \in N$, there is an opening cost $f_v$ payed by the player who owns facility location $v$. Note that the opening costs can be considered as the costs for recovering the disrupted facility locations during disaster recovery efforts. Facility locations that are not disrupted can be modelled with no opening costs, i.e., $f_v = 0$. If Player $n$ uses an intra- or inter-edge to satisfy demand $u \in D_n$ with any facility $v \in F$, Player n pays cost $c_{uv}$. If Player $n$ uses an inter-edge to satisfy demand $u \in D_n$ with other facility that belongs to the other player, Player n pays a fee $d_{uv}$ to the other player. The goal of each player is to minimize the total cost to satisfy their demand captured by $D_n$. To do so, Player 1 opens facilities from facility location nodes $F_1$, recovers intra- or inter-edges from the set $E_1 \cap I$

or $E_{21} \cap I$ and Player 2 opens facilities from facility location nodes $F_2$, recovers intra- or inter-edges from the set $E_2 \cap I$ or $E_{12} \cap I$, then each Player $n \in N$ assigns their demand $u \in D_n$ to any open facilities $v \in F$ using an available edge $(u, v)$. The full set of input sets and parameters is listed below.

Table 4.3: Input sets and parameters

| **Sets** | |
|---|---|
| $N$ | set of players {1,2} |
| $I$ | set of recoverable intra- and inter-edges |
| $A$ | set of initially available intra– and inter–edges |
| $D_n$ | set of demand nodes for Player $n \in N$, where $D_n = V_n \cap D$ and $D_1 \cap D_2 = \emptyset$, $D = D_1 \cup D_2$ |
| $F_n$ | set of facility location nodes for Player $n \in N$, where $F_n = V_n \cap F$, $F_1 \cap F_2 = \emptyset$, $F = F_1 \cup F_2$ |
| $E_n$ | set of intra-edges for Player $n \in N$ |
| $E_{12}$ | set of inter-edges $(u, v)$ used by Player 1 and fees are collected by Player 2, where $u \in D_1$, $v \in F_2$ |
| $E_{21}$ | set of inter-edges $(u, v)$ used by Player 2 and fees are collected by Player 1, where $u \in D_2$, $v \in F_1$ |
| **Parameters** | |
| $f_v$ | cost for opening a facility at location $v \in V \cap F$ (payed by the player who owns facility location $v$) |
| $c_{uv}$ | cost for assigning demand $u \in V \cap D$ to facility $v \in V \cap F$ using an initially available intra-or inter-edge (payed by the player who owns demand $u$) |
| $d_{uv}$ | fee for satisfying demand $u \in D$ using the inter-edge $(u, v) \in E_{12} \cup E_{21}$ (payed by the player who owns demand $u$) |
| $p_{uv}$ | cost for recovering edge $(u, v) \in I$ (payed by the player who owns the facility location $v$) |
| $B^n$ | budget for player $n \in N$ to recover intra- and inter-edges |

We first present a centralized model, where a centralized decision maker/government authority seeks to a social welfare solution by minimizing the overall cost to satisfy demand of both players and decides how to split the recovery budget between players according to the solution. Also, we use the social welfare solution to asses the quality of Nash equilibria, which we present later. Note that the centralized model includes the decision variables of both of the players and the central decision maker decides for both players.

The *decision variables* for the centralized model:

- $y_v^n = 1$ if facility $v \in F_n$ is open, 0 otherwise, $n \in N$.
- $x_{uv}^n = 1$ if demand $u \in D_n$ is connected to facility $v \in F$, and 0 otherwise, $n \in N$.
- $\beta_{uv}^n = 1$ if edge $(u, v) \in I$, where $u \in D$ and $v \in F_n$ is recovered, and 0 otherwise, $n \in N$.

We formulate the centralized model as an integer programming model as follows.

$$\min \sum_{n\in N}\sum_{v\in F_n} f_v y_v^n + \sum_{n\in N}\sum_{(u,v)\in E_n} c_{uv}x_{uv}^n + \sum_{(u,v)\in E_{12}} c_{uv}x_{uv}^1 + \sum_{(u,v)\in E_{21}} c_{uv}x_{uv}^2 \tag{4.3.1}$$

$$\text{s.t} \sum_{v:(u,v)\in E} x_{uv}^n = 1 \text{ for } u \in D_n,\ n \in N \tag{4.3.2}$$

$$y_v^n - x_{uv}^n \geq 0 \text{ for } (u,v) \in E_n, n \in N \tag{4.3.3}$$

$$y_v^1 - x_{uv}^2 \geq 0 \text{ for } (u,v) \in E_{21} \tag{4.3.4}$$

$$y_v^2 - x_{uv}^1 \geq 0 \text{ for } (u,v) \in E_{12} \tag{4.3.5}$$

$$\beta_{uv}^n - x_{uv}^n \geq 0 \text{ for } (u,v) \in E_n \cap I, n \in N \tag{4.3.6}$$

$$\beta_{uv}^2 - x_{uv}^1 \geq 0 \text{ for } (u,v) \in E_{12} \cap I \tag{4.3.7}$$

$$\beta_{uv}^1 - x_{uv}^2 \geq 0 \text{ for } (u,v) \in E_{21} \cap I \tag{4.3.8}$$

$$\sum_{n\in N}\sum_{(u,v)\in E_n\cap I} p_{uv}\beta_{uv}^n + \sum_{(u,v)\in E_{12}\cap I} p_{uv}\beta_{uv}^2 + \sum_{(u,v)\in E_{21}\cap I} p_{uv}\beta_{uv}^1 \leq B \tag{4.3.9}$$

$$y_v^n \in \{0,1\} \text{ for } v \in F_n, n \in N \tag{4.3.10}$$

$$x_{uv}^1 \in \{0,1\} \text{ for } (u,v) \in E_1 \cup E_{12} \tag{4.3.11}$$

$$x_{uv}^2 \in \{0,1\} \text{ for } (u,v) \in E_2 \cup E_{21} \tag{4.3.12}$$

$$\beta_{uv}^n \in \{0,1\} \text{ for } (u,v) \in I, n \in N \tag{4.3.13}$$

The objective (4.3.1) is to minimize the total cost to satisfy the demand of both players. The total cost includes the cost of opening facilities and the cost of using edges to satisfy demand. Constraint set (4.3.2) requires each demand node $u \in D_n$ to be served by one facility $v \in F$. Note that in the centralized model, we do not consider any additional fees for using inter-edges, since we assume the central decision maker has the full control in the two-layer network. Constraint sets (4.3.3), (4.3.4) and (4.3.5) ensure that only open facilities serve demand nodes using available edges in the two layer network. Constraint sets (4.3.6),

(4.3.7) and (4.3.8) ensure that a recovered edge $(u, v)$ is available to serve demand $u$ by facility $v$. Constraint (4.3.9) requires the total cost to recover intra-edges $E_n \cap I$ for $n \in N$, inter-edges $E_{21} \cap I$ and $E_{12} \cap I$ to be within the budget $B$.

The central decision maker has a certain amount of recovery funding budget $B$ and according to the optimal solution of the centralized model, the central decision maker splits the budget $B$ to $B^1$ for Player 1 and $B^2$ for Player 2, where $B = B^1 + B^2$. Later, each player uses their own budget, which is decided by the central decision maker in the two different version of the non-cooperative game. Constraint sets (4.3.10), (4.3.11), (4.3.12) and (4.3.13) require decision variables of Player 1 and Player 2 to be binary.

Next, we present *the strict control facility location and restoration game* (SC-FLR) and *the limited control facility location and restoration game* (LC-FLR). In the both games, players make their own decisions and the government allocates the recovery budget to each player.

In SC-FLR, the government authority ensures that players install inter-edges that aligns with the social welfare solution by setting strict control on players. To do so, the government authority either allocates resources directly to install inter-edges or requires strict agreements from the players to install inter-edges according to the social welfare solution. We present the mixed integer programming formulation of the model for Player 1, the other player's model follows exactly same by replacing the decision variables $y^1, x^1, \beta^1, y^2, x^2$, and $\beta^2$ with $y^2, x^2, \beta^2, y^1, x^1$, and $\beta^1$, respectively.

$$SC\text{-}FLR : \min \sum_{v \in F_1} f_v y_v^1 + \sum_{(u,v) \in E_1} c_{uv} x_{uv}^1 + \sum_{(u,v) \in E_{12}} (c_{uv} + d_{uv}) x_{uv}^1 - \sum_{(u,v) \in E_{21}} d_{uv} x_{uv}^2 \quad (4.3.14)$$

$$\text{s.t} \sum_{v \in F} x_{uv}^1 = 1 \text{ for } u \in D_1 \quad (4.3.15)$$

$$y_v^1 - x_{uv}^1 \geq 0 \text{ for } (u, v) \in E_1 \quad (4.3.16)$$

$$y_v^1 - x_{uv}^2 \geq 0 \text{ for } (u, v) \in E_{21} \quad (4.3.17)$$

$$y_v^2 - x_{uv}^1 \geq 0 \text{ for } (u,v) \in E_{12} \tag{4.3.18}$$

$$\beta_{uv}^1 - x_{uv}^1 \geq 0 \text{ for } (u,v) \in E_1 \cap I \tag{4.3.19}$$

$$\beta_{uv}^2 - x_{uv}^1 \geq 0 \text{ for } (u,v) \in E_{12} \cap I \tag{4.3.20}$$

$$\beta_{uv}^1 - x_{uv}^2 \geq 0 \text{ for } (u,v) \in E_{21} \cap I \tag{4.3.21}$$

$$\sum_{(u,v)\in E_1 \cap I} p_{uv}\beta_{uv}^1 + \sum_{(u,v)\in E_{21} \cap I} p_{uv}\beta_{uv}^1 \leq B^1 \tag{4.3.22}$$

$$y_v^1 \in \{0,1\} \text{ for } v \in F_1 \tag{4.3.23}$$

$$x_{uv}^1 \in \{0,1\} \text{ for } (u,v) \in E_1 \cup E_{12} \tag{4.3.24}$$

$$\beta_{uv}^1 \in \{0,1\} \text{ for } (u,v) \in (E_1 \cup E_{21}) \cap I \tag{4.3.25}$$

The objective (4.3.14) is to minimize the total cost to satisfy Player 1's demand. The total cost includes the cost of opening facilities, the cost of using edges to satisfy Player 1's demand, the fee payed to Player 2 to use inter-edges to serve Player 1's demand and the fee gained from Player 2 for using inter-edges, which are connected to Player 1's facility location nodes. Constraint set (4.3.15) requires each demand node $u \in D_1$ to be served by one facility $v \in F$ using the initially available intra- or inter-edges or recovered intra- or inter-edges. Constraint sets (4.3.16), (4.3.17) and (4.3.18) ensure that only open facilities serve demand nodes using available edges in the two-layer network. Constraint sets (4.3.19), (4.3.20), and (4.3.21) ensure that a recovered edge $(u,v)$ is available to serve demand $u$ by facility $v$. Constraint (4.3.22) requires the total cost to recover intra-edges $E_1 \cap I$ and inter-edges $E_{21} \cap I$ to be within the budget $B^1$. Constraint sets (4.3.23), (4.3.24) and (4.3.25) require the decision variables of Player 1 to be binary. In this formulation, the objective function and feasible solution region of Player 1 depend on the decisions $(y_v^2, x_{uv}^2, \beta_{uv}^2)$ of Player 2. SC-FLR ensures that each player receives a strictly positive benefit from interdependency relationships if they make their decisions regarding to recovering and using inter-edges according to the social welfare solution.

In the absence of a strict control agreement, the government authority has limited control on players and allocates the recovery budget between two players by recognizing that players recover only their individual networks with the given recovery funding budget. We introduce LC-FLR in which players are not installing inter-edges but they can install intra-edges and use initially available intra- and inter-edges.

Next, we present the integer programming formulation for LC-FLR. The main mathematical formulation difference between SC-FLR and LC-FLR is as follows. Since there is always a pure Nash equilibrium, in which neither of the players uses recovered inter-edges, we set recovery decision $\beta^1_{uv} = 0$ for $(u,v) \in E_{21} \cup I$ and $\beta^2_{uv} = 0$ for $(u,v) \in E_{12} \cup I$ in LC-FLR. The constraints that include these variables become redundant, and therefore they are omitted in the formulation. We present the limited control facility location and restoration game model for Player 1, the other player's model follows exactly same by replacing the decision variables $y^1, x^1, \beta^1, y^2$, and $x^2$ with $y^2, x^2, \beta^2, y^1$, and $x^1$, respectively.

$$LC\text{-}FLR: \min \sum_{v \in F_1} f_v y^1_v + \sum_{(u,v) \in E_1} c_{uv} x^1_{uv} + \sum_{(u,v) \in E_{12} \cap A} (c_{uv} + d_{uv}) x^1_{uv} - \sum_{(u,v) \in E_{21} \cap A} d_{uv} x^2_{uv} \tag{4.3.26}$$

$$\text{s.t} \sum_{v:(u,v) \in E} x^1_{uv} = 1 \text{ for } u \in D_1 \tag{4.3.27}$$

$$y^1_v - x^1_{uv} \geq 0 \text{ for } (u,v) \in E_1 \tag{4.3.28}$$

$$y^1_v - x^2_{uv} \geq 0 \text{ for } (u,v) \in E_{21} \cap A \tag{4.3.29}$$

$$y^2_v - x^1_{uv} \geq 0 \text{ for } (u,v) \in E_{12} \cap A \tag{4.3.30}$$

$$\beta^1_{uv} - x^1_{uv} \geq 0 \text{ for } (u,v) \in E_1 \cap I \tag{4.3.31}$$

$$\sum_{(u,v) \in E_1 \cap I} p_{uv} \beta^1_{uv} \leq B^1 \tag{4.3.32}$$

$$y^1_v \in \{0,1\} \text{ for } v \in F_1 \tag{4.3.33}$$

$$x^1_{uv} \in \{0,1\} \text{ for } (u,v) \in E_1 \cup (E_{12} \cap A) \tag{4.3.34}$$

$$\beta^1_{uv} \in \{0,1\} \text{ for } (u,v) \in E_1 \cap I \tag{4.3.35}$$

The objective functions and constraint sets (4.3.27) - (4.3.31) are analogous to (4.3.15) - (4.3.19). Since we set $\beta^1_{uv} = 0$ for $(u,v) \in E_{21} \cap I$ and $\beta^2_{uv} = 0$ for $(u,v) \in E_{12} \cap I$, constraint sets (4.3.20)-(4.3.21) become redundant and we modify constraint (4.3.22) to yield constraint (4.3.32), which requires the total cost to install intra-edges $E_1 \cap I$ to be within the budget $B^1$. Constraint sets (4.3.33), (4.3.34) and (4.3.35) require decision variables of Player 1 to be binary.

Note that the results and definitions in the next sections can be applied to both SC-FLR and LC-FLR. The difference between two versions is that in the limited control version, we assume $\beta^1_{uv} = 0$ for $(u,v) \in E_{21} \cap I$ and $\beta^2_{uv} = 0$ for $(u,v) \in E_{12} \cap I$. Equivalently, in LC-FLR, we assume $E_{21} \cap I = \emptyset$ and $E_{12} \cap I = \emptyset$.

## 4.4 Existence of a Pure Nash equilibrium

In this section, we prove the existence of a pure Nash equilibrium for SC-FLR by constructing a potential function and proving that the game is a potential game.

Let's assume that a strategy $z_n$ of Player n is composed of $(y^n, x^n, \beta^n)$, where $y^n$ represents the open facilities, $x^n$ represents demand-facility assignments using edges in the network, and $\beta^n$ represents installed intra- or inter-edges by player $n$, for $n \in N$ for SC-FLR. Let $S_n$ be the set of strategies for Player n, and $n \in N$. Then we can define SC-FLR with 2 players as $(S_1 \times S_2, u)$, where $S_1 \times S_2$ is the set of strategy profiles of players and $u = (u_1(z_1, z_2), u_2(z_1, z_2))$ is the payoff function, which we define as follows.

$$u_1(z_1, z_2) = \sum_{v \in F_1} f_v y^1_v + \sum_{(u,v) \in E_1} c_{uv} x^1_{uv} + \sum_{(u,v) \in E_{12}} (c_{uv} + d_{uv}) x^1_{uv} - \sum_{(u,v) \in E_{21}} d_{uv} x^2_{uv}, \tag{4.4.1}$$

$$u_2(z_1, z_2) = \sum_{v \in F_2} f_v y_v^2 + \sum_{(u,v) \in E_2} c_{uv} x_{uv}^2 + \sum_{(u,v) \in E_{21}} (c_{uv} + d_{uv}) x_{uv}^2 - \sum_{(u,v) \in E_{12}} d_{uv} x_{uv}^1, \quad (4.4.2)$$

Note that the payoff for each player is exactly same as the objective function of SC-FLR and depends on the strategy profile chosen by the player as well as the strategy profile chosen by the other player. Next, we provide the definition of a pure Nash equilibrium and a potential function, then we prove that SC-FLR is a potential game.

**Definition 5.** *(**Pure Nash equilibrium**) A strategy profile $z^* \in S$ is a pure Nash equilibrium if no unilateral deviation in strategy by any single player is profitable for that player, i.e.,*

$$z_1 \in S_1 : u_1(z_1^*, z_2^*) \leq u_1(z_1, z_2^*)$$

$$z_2 \in S_2 : u_2(z_1^*, z_2^*) \leq u_2(z_1^*, z_2).$$

**Definition 6.** *(**Potential Game**) A game is an exact potential game if and only if a potential function $\phi$ exists for $\hat{z}_1, z_1 \in S_1$, $\hat{z}_2, z_2 \in S_2$ such that*

$$\phi(\hat{z}_1, z_2) - \phi(z_1, z_2) = u_1(\hat{z}_1, z_2) - u_1(z_1, z_2)$$

$$\phi(z_1, \hat{z}_2) - \phi(z_1, z_2) = u_2(z_1, \hat{z}_2) - u_2(z_1, z_2).$$

**Theorem 1.** *The facility location and restoration game is a potential game with the potential function*

$$\phi(z_1, z_2) = \sum_{n \in N} \Big( \sum_{v \in F_n} f_v y_v^n + \sum_{(u,v) \in E_n} c_{uv} x_{uv}^n \Big) + \sum_{(u,v) \in E_{12}} (c_{uv} + d_{uv}) x_{uv}^1 + \sum_{(u,v) \in E_{21}} (c_{uv} + d_{uv}) x_{uv}^2$$

*for $z_1 \in S_1$, $z_2 \in S_2$.*

*Proof.* We first need to show that

$$\phi(\hat{z}_1, z_2) - \phi(z_1, z_2) = u_1(\hat{z}_1, z_2) - u_1(z_1, z_2)$$

for all $\hat{z}_1 \in S_1$ and $\hat{z}_2 \in S_2$. First, we consider the change in the potential function, when Player 1 changes the current strategy $z_1$ to any other strategy $\hat{z}_1 \in S_1$.

$$\begin{aligned}
&\phi(\hat{z}_1, z_2) - \phi(z_1, z_2) \\
&:= \left[ \sum_{v \in F_1} f_v \hat{y}_v^1 + \sum_{(u,v) \in E_1} c_{uv} \hat{x}_{uv}^1 + \sum_{(u,v) \in E_{12}} (c_{uv} + d_{uv}) \hat{x}_{uv}^1 + \sum_{v \in F_2} f_v y_v^2 + \sum_{(u,v) \in E_2} c_{uv} x_{uv}^2 + \sum_{(u,v) \in E_{21}} (c_{uv} + d_{uv}) x_{uv}^2 \right] \\
&- \left[ \sum_{v \in F_1} f_v y_v^1 + \sum_{(u,v) \in E_1} c_{uv} x_{uv}^1 + \sum_{(u,v) \in E_{12}} (c_{uv} + d_{uv}) x_{uv}^1 + \sum_{v \in F_2} f_v y_v^2 + \sum_{(u,v) \in E_2} c_{uv} x_{uv}^2 + \sum_{(u,v) \in E_{21}} (c_{uv} + d_{uv}) x_{uv}^2 \right] \\
&= \sum_{v \in F_1} f_v (\hat{y}_v^1 - y_v^1) + \sum_{(u,v) \in E_1} c_{uv} (\hat{x}_{uv}^1 - x_{uv}^1) + \sum_{(u,v) \in E_{12}} (c_{uv} + d_{uv}) (\hat{x}_{uv}^1 - x_{uv}^1)
\end{aligned}$$

Next, we consider the change in the utility function of Player 1, when Player 1 changes the current strategy to $\hat{z}_1 \in S_1$.

$$\begin{aligned}
u_1(\hat{z}_1, z_2) - u_1(z_1, z_2) &= \left[ \sum_{v \in F_1} f_v \hat{y}_v^1 + \sum_{(u,v) \in E_1} c_{uv} \hat{x}_{uv}^1 + \sum_{(u,v) \in E_{12}} (c_{uv} + d_{uv}) \hat{x}_{uv}^1 - \sum_{(u,v) \in E_{21}} d_{uv} x_{uv}^2 \right] \\
&\quad - \left[ \sum_{v \in F_1} f_v y_v^1 + \sum_{(u,v) \in E_1} c_{uv} x_{uv}^1 + \sum_{(u,v) \in E_{12}} (c_{uv} + d_{uv}) x_{uv}^1 - \sum_{(u,v) \in E_{21}} d_{uv} x_{uv}^2 \right] \\
&= \sum_{v \in F_1} f_v (\hat{y}_v^1 - y_v^1) + \sum_{(u,v) \in E_1} c_{uv} (\hat{x}_{uv}^1 - x_{uv}^1) + \sum_{(u,v) \in E_{12}} (c_{uv} + d_{uv}) (\hat{x}_{uv}^1 - x_{uv}^1)
\end{aligned}$$

We show that $\phi(\hat{z}_1, z_2) - \phi(z_1, z_2) = u_1(\hat{z}_1, z_2) - u_1(z_1, z_2)$ for Player 1. We can easily apply the analogous argument for Player 2. □

We provide a pure Nash equilibrium for SC-FLRs, which is the global minimum of

the potential function $\phi$ (Rosenthal (1973)). To show that, suppose $(z_1^\star, z_2^\star)$ is the global minimum of the potential function $\phi$. Then for $z_1 \in S_1$ and $z_2 \in S_2$, we have following inequalities.

$$\phi(z_1^\star, z_2^\star) - \phi(z_1, z_2^\star) \leq 0 \tag{4.4.3}$$

$$\phi(z_1^\star, z_2^\star) - \phi(z_1^\star, z_2) \leq 0 \tag{4.4.4}$$

By definition of the potential function, we have the following equalities.

$$\phi(z_1^\star, z_2^\star) - \phi(z_1, z_2^\star) = u_1(z_1^\star, z_2^\star) - u_1(z_1, z_2^\star) \tag{4.4.5}$$

$$\phi(z_1^\star, z_2^\star) - \phi(z_1^\star, z_2) = u_2(z_1^\star, z_2^\star) - u_2(z_1^\star, z_2) \tag{4.4.6}$$

Therefore,

$$u_1(z_1^\star, z_2^\star) - u_1(z_1, z_2^\star) \leq 0 \tag{4.4.7}$$

$$u_2(z_1^\star, z_2^\star) - u_2(z_1^\star, z_2) \leq 0 \tag{4.4.8}$$

By Definition 5, $(z_1^\star, z_2^\star) \in S$ is a pure Nash equilibrium.

**Remark 2.** *We observe that there is always a pure Nash equilibrium, in which none of the players uses installed inter-edges. As a result, for the pure Nash equilibrium strategy that consider installing inter-edges, which are not used by the players, we can construct another pure Nash equilibrium strategy with the same payoffs by considering no installation of inter-edges. In other words, for every pure Nash equilibrium strategy $z_1 = (y_1, x_1, \beta_1) \in S_1$ for Player 1 and $z_2 = (y_2, x_2, \beta_2) \in S_2$ for Player 2 in SC-FLR, where $\beta_{uv}^1 > x_{uv}^2$ or $\beta_{uv}^2 > x_{uv}^1$ for $(u, v) \in E_{12} \cup E_{21}$, setting $\tilde{\beta}_{uv}^1 = x_{uv}^2$ and $\tilde{\beta}_{uv}^2 = x_{uv}^1$ for $(u, v) \in E_{12} \cup E_{21}$ gives another pure Nash equilibrium $(\tilde{z}_1, \tilde{z}_2)$ with the same payoffs for both players, where $\tilde{z}_1 = (y_1, x_1, \tilde{\beta}_1) \in S_1$ and $\tilde{z}_2 = (y_2, x_2, \tilde{\beta}_2) \in S_2$.*

**Theorem 3.** *There exists a pure Nash equilibrium strategy $z_1^\star = (y_1, x_1, \beta_1) \in S_1$ for Player 1 and $z_2^\star = (y_2, x_2, \beta_2) \in S_2$ for Player 2 with $\beta_{uv}^n = 0$ for every $(u, v) \in (E_{12} \cup E_{21}) \cap I$ in SC-FLR.*

*Proof.* Let us assume that $(z_1^\star, z_2^\star) \in S$ is a pure Nash equilibrium for LC-FLR, that means $\beta_{uv}^n = 0$ for every $(u, v) \in (E_{12} \cup E_{21}) \cap I$. We want to show that $(z_1^\star, z_2^\star)$ is also a pure Nash equilibrium for SC-FLR. To do that we need to prove neither of the players have any other strategies to deviate from $(z_1^\star, z_2^\star)$ in SC-FLR. We prove it by contradiction. Let us assume that $(z_1^\star, z_2^\star)$ is not a pure Nash equilibrium for SC-FLR. That means without loss of generality Player 1 has a strategy $\bar{z}_1 \in S_1$, where

$$u_1(z_1^\star, z_2^\star) > u_1(\bar{z}_1, z_2^\star). \tag{4.4.9}$$

By assumption $(z_1^\star, z_2^\star) \in S$ is a pure Nash equilibrium for LC-FLR. LC-FLR does not consider installing inter-edges by players, so $\beta_{uv}^n = 0$ for every $(u, v) \in (E_{12} \cup E_{21}) \cap I$. Since Player 2 does not change the strategy in the inequality (4.4.9), inter-edges, which can be installed by Player 2 are still uninstalled (i.e., $\beta_{uv}^2 = 0$ for $(u, v) \in E_{12} \cap I$). As a result, strategy $\bar{z}_1$ cannot consider using an installable inter-edge from set $E_{12} \cap I$. In addition, since no installed inter-edge used in the strategy $z_2^\star$, by considering Remark 2, the strategy $\bar{z}_1$ can be converted to a new feasible strategy for Player 1 with the better payoff for Player 1. This contradicts with the assumption that $(z_1^\star, z_2^\star) \in S$ is a pure Nash equilibrium for LC-FLR. We conclude that $(z_1^\star, z_2^\star)$ is a pure Nash equilibrium for the SC-FLR with $\beta_{uv}^n = 0$ for every $(u, v) \in (E_{12} \cup E_{21}) \cap I$. □

## 4.5 The Facility Location and Restoration Game and the Centralized Model

In this section, we introduce the *Price of Stability* (PoS), which is an important concept for efficiency analysis and show that we can bound the PoS. The PoS measures the ratio between the best possible total payoffs of the pure Nash equilibrium solution and the social welfare solution. We use the *potential function method* to bound PoS by appling Theorem 19.13 in Nisan et al. (2007). Theorem 4 provides an upper bound on the POS for any SC-FLR instance, where the bound is a function of the problem instance input parameters. Note that since the pure Nash equilibrium that minimizes the potential function $\phi$ may not be the best pure Nash equilibrium, the bound is not always tight (Tardos and Wexler (2007)). We recognize that our PoS bound in Theorem 4 can be arbitrarily large.

Let $C(z_1, z_2)$ be the objective function and $(\bar{z}_1, \bar{z}_2) = (\bar{y}^1, \bar{x}^1, \bar{\beta}^1, \bar{y}^2, \bar{x}^2, \bar{\beta}^2)$ be the optimal solution for the centralized model, where

$$C(z_1, z_2) = \sum_{n \in N} \sum_{v \in F_n} f_v y_v^n + \sum_{n \in N} \sum_{(u,v) \in E_n} c_{uv} x_{uv}^n + \sum_{(u,v) \in E_{12}} c_{uv} x_{uv}^1 + \sum_{(u,v) \in E_{21}} c_{uv} x_{uv}^2 \qquad (4.5.1)$$

Thus, the social welfare solution value is $C(\bar{z}_1, \bar{z}_2)$.

**Theorem 4.** *In SC-FLR, PoS is bounded by* $M + 1$*, where*

$$M = \begin{cases} M^\star, & \text{if } d_{uv} > c_{uv} \text{ and } c_{uv} > 0 \text{ for } (u,v) \in E_{12} \cup E_{21} \\ 1, & \text{if } d_{uv} \leq c_{uv} \text{ and } d_{uv} > 0 \text{ for } (u,v) \in E_{12} \cup E_{21} \\ 0, & \text{if } d_{uv} = 0 \text{ for } (u,v) \in E_{12} \cup E_{21} \end{cases}$$

*and*

$$M^\star = \max\{\frac{d_{uv}}{c_{uv}} \text{ for } (u,v) \in E_{12} \cup E_{21}\}.$$

*Proof.* Nisan et al. (2007) prove that if there is a potential function $\phi$ for a potential game, and that for any strategy $(z_1, z_2)$, the inequality

$$\frac{C(z_1, z_2)}{A} \leq \phi(z_1, z_2) \leq B \cdot C(z_1, z_2) \tag{4.5.2}$$

holds for some constants $A, B \geq 0$, where $(z_1, z_2)$ is a strategy from the strategy set $S_1 \times S_2$ and $C(z_1, z_2)$ is the social welfare solution for strategy $(z_1, z_2)$, then the price of stability is at most $A \cdot B$. We need to prove that

$$\frac{1}{A} \cdot C(z_1, z_2) \leq \phi(z_1, z_2) \leq B \cdot C(z_1, z_2) \tag{4.5.3}$$

holds for the facility location and restoration game with the potential function $\phi$ for any possible $(z_1, z_2) \in S_1 \times S_2$ for $A = 1$ and $B = M + 1$, where

$$M = \begin{cases} M^\star, & \text{if } d_{uv} > c_{uv} \text{ and } c_{uv} > 0 \text{ for } (u,v) \in E_{12} \cup E_{21} \\ 1, & \text{if } d_{uv} \leq c_{uv} \text{ and } d_{uv} > 0 \text{ for } (u,v) \in E_{12} \cup E_{21} \\ 0, & \text{if } d_{uv} = 0 \text{ for } (u,v) \in E_{12} \cup E_{21} \end{cases}$$

and

$$M^\star = \max\{\frac{d_{uv}}{c_{uv}} \text{ for } (u,v) \in E_{12} \cup E_{21}\}.$$

Let $(z_1^\star, z_2^\star)$ be the strategy that minimizes $\phi$ and $(z_1^\star, z_2^\star)$ be a pure Nash equilibrium for the facility location and restoration game. Let $(\bar{z}_1, \bar{z}_2)$ be the optimal solution of the centralized model.

$$C(z_1^\star, z_2^\star) = \sum_{n \in N} \sum_{v \in F_n} f_v y^{\star n}_v + \sum_{n \in N} \sum_{(u,v) \in E_n} c_{uv} x^{\star n}_{uv} + \sum_{(u,v) \in E_{12} \cup E_{21}} c_{uv} x^{\star n}_{uv} \tag{4.5.4}$$

$$\leq \sum_{n \in N} \sum_{v \in F_n} f_v y^{\star n}_v + \sum_{n \in N} \sum_{(u,v) \in E_n} c_{uv} x^{\star n}_{uv} + \sum_{(u,v) \in E_{12}} (c_{uv} + d_{uv}) x^{\star 1}_{uv} + \sum_{(u,v) \in E_{21}} (c_{uv} + d_{uv}) x^{\star 2}_{uv}$$

$$= \phi(z_1^\star, z_2^\star) \tag{4.5.5}$$

Therefore,

$$C(z_1^\star, z_2^\star) \leq \phi(z_1^\star, z_2^\star),$$

which implies $A = 1$. Furthermore, the definition of $(z_1^\star, z_2^\star)$ implies that

$$\phi(z_1^\star, z_2^\star) \leq \phi(\bar{z}_1, \bar{z}_2)$$

Let

$$M^\star = \max\{\frac{d_{uv}}{c_{uv}} \text{ for } (u,v) \in E_{12} \cup E_{21}\}$$

and

$$M = \begin{cases} M^\star, & \text{if } d_{uv} > c_{uv} \text{ and } c_{uv} > 0 \text{ for } (u,v) \in E_{12} \cup E_{21} \\ 1, & \text{if } d_{uv} \leq c_{uv} \text{ and } d_{uv} > 0 \text{ for } (u,v) \in E_{12} \cup E_{21} \\ 0, & \text{if } d_{uv} = 0 \text{ for } (u,v) \in E_{12} \cup E_{21} \end{cases}$$

Then we have

$$\begin{aligned} \phi(z_1^\star, z_2^\star) &= \sum_{n\in N}\sum_{v\in F_n} f_v {y^\star}_v^n + \sum_{n\in N}\sum_{(u,v)\in E_n} c_{uv} {x^\star}_{uv}^n + \sum_{(u,v)\in E_{12}} (c_{uv}+d_{uv}) {x^\star}_{uv}^1 + \sum_{(u,v)\in E_{21}} (c_{uv}+d_{uv}) {x^\star}_{uv}^2 \\ &\leq \sum_{n\in N}\sum_{v\in F_n} f_v y_v^n + \sum_{n\in N}\sum_{(u,v)\in E_n} c_{uv} \bar{x}_{uv}^n + \sum_{(u,v)\in E_{12}} (c_{uv}+d_{uv}) \bar{x}_{uv}^1 + \sum_{(u,v)\in E_{21}} (c_{uv}+d_{uv}) \bar{x}_{uv}^2 \\ &\leq \sum_{n\in N}\sum_{v\in F_n} f_v \bar{y}_v^n + \sum_{n\in N}\sum_{(u,v)\in E_n} c_{uv} \bar{x}_{uv}^n + \sum_{(u,v)\in E_{12}} (c_{uv}+Mc_{uv}) \bar{x}_{uv}^1 + \sum_{(u,v)\in E_{21}} (c_{uv}+Mc_{uv}) \bar{x}_{uv}^2 \end{aligned} \tag{4.5.6}$$

$$\begin{aligned} &\leq \sum_{n\in N}\sum_{v\in F_n} f_v \bar{y}_v^n + \sum_{n\in N}\sum_{(u,v)\in E_n} c_{uv} \bar{x}_{uv}^n + \sum_{(u,v)\in E_{12}} (M+1)c_{uv} \bar{x}_{uv}^1 + \sum_{(u,v)\in E_{21}} (M+1)c_{uv} \bar{x}_{uv}^2 \\ &\leq (M+1)\Big( \sum_{n\in N}\sum_{v\in F_n} f_v \bar{y}_v^n + \sum_{n\in N}\sum_{(u,v)\in E_n} c_{uv} \bar{x}_{uv} + \sum_{(u,v)\in E_{12}\cup E_{21}} c_{uv} \bar{x}_{uv} \Big) \\ &\leq (M+1) \cdot C(\bar{z}_1, \bar{z}_2) \end{aligned} \tag{4.5.7}$$

This computation gives us $B = M + 1$. As a result, PoS is at most $M + 1$. □

We observe that if $d_{uv} \leq c_{uv}$ for all $(u,v) \in E_{12} \cup E_{21}$, the PoS is bounded by 2. Further, if $d_{uv} = 0$ for all $(u,v) \in E_{12} \cup E_{21}$, the PoS is bounded by 1 that means the social welfare solution is a Nash equilibrium. Next, we prove that.

**Corollary 5.** *If $d_{uv} = 0$ for $(u,v) \in E_{12} \cup E_{21}$, any solution of the centralized model is a pure Nash equilibrium.*

*Proof.* Let's assume that $(\bar{z}_1, \bar{z}_2) = (\bar{y}^1, \bar{x}^1, \bar{\beta}^1, \bar{y}^2, \bar{x}^2, \bar{\beta}^2)$ is an optimal solution of the centralized model and not a Nash equilibrium. That means, there exists a strategy $(\tilde{z}_1, \bar{z}_2) = (\tilde{y}^1, \tilde{x}^1, \tilde{\beta}^1, \bar{y}^2, \bar{x}^2, \bar{\beta}^2)$ such that

$$u_1(\bar{z}_1, \bar{z}_2) = \sum_{v \in F_1} f_v \bar{y}_v^1 + \sum_{(u,v) \in E_1} c_{uv} \bar{x}_{uv}^1 + \sum_{(u,v) \in E_{12}} (c_{uv} + d_{uv}) \bar{x}_{uv}^1 - \sum_{(u,v) \in E_{21}} d_{uv} \bar{x}_{uv}^2 \tag{4.5.8}$$

$$> \sum_{v \in F_1} f_v \tilde{y}_v^1 + \sum_{(u,v) \in E_1} c_{uv} \tilde{x}_{uv}^1 + \sum_{(u,v) \in E_{12}} (c_{uv} + d_{uv}) \tilde{x}_{uv}^1 - \sum_{(u,v) \in E_{21}} d_{uv} \bar{x}_{uv}^2 \tag{4.5.9}$$

$$> u_1(\tilde{z}_1, \bar{z}_2) \tag{4.5.10}$$

Since $d_{uv} = 0$ for $(u,v) \in E_{12} \cup E_{21}$,

$$u_1(\bar{z}_1, \bar{z}_2) = \sum_{v \in F_1} f_v \bar{y}_v^1 + \sum_{(u,v) \in E_1} c_{uv} \bar{x}_{uv}^1 + \sum_{(u,v) \in E_{12}} c_{uv} \bar{x}_{uv}^1$$

$$> \sum_{v \in F_1} f_v \tilde{y}_v^1 + \sum_{(u,v) \in E_1} c_{uv} \tilde{x}_{uv}^1 + \sum_{(u,v) \in E_{12}} c_{uv} \tilde{x}_{uv}^1$$

$$> u_1(\tilde{z}_1, \bar{z}_2)$$

That means

$$
\begin{aligned}
&u_1(\bar{z}_1, \bar{z}_2) + u_1(\bar{z}_1, \bar{z}_2) = \\
&\sum_{v \in F_1} f_v \bar{y}_v^1 + \sum_{(u,v) \in E_1} c_{uv} \bar{x}_{uv}^1 + \sum_{(u,v) \in E_{12}} c_{uv} \bar{x}_{uv}^1 + \sum_{v \in F_2} f_v \bar{y}_v^2 + \sum_{(u,v) \in E_2} c_{uv} \bar{x}_{uv}^2 + \sum_{(u,v) \in E_{21}} c_{uv} \bar{x}_{uv}^2 \\
&= C(\bar{z}_1, \bar{z}_2) > u_1(\tilde{z}_1, \bar{z}_2) + u_1(\tilde{z}_1, \bar{z}_2) \\
&= \sum_{v \in F_2} f_v \bar{y}_v^2 + \sum_{(u,v) \in E_2} c_{uv} \bar{x}_{uv}^2 + \sum_{(u,v) \in E_{21}} c_{uv} \tilde{x}_{uv}^2 + \sum_{v \in F_2} f_v \bar{y}_v^2 + \sum_{(u,v) \in E_2} c_{uv} \bar{x}_{uv}^2 + \sum_{(u,v) \in E_{21}} c_{uv} \tilde{x}_{uv}^2 \\
&> C(\tilde{z}_1, \bar{z}_2)
\end{aligned}
$$

This means the objective function value of the centralized model with $(\tilde{z}_1, \bar{z}_2)$ is strictly smaller than the optimal solution $(\bar{z}_1, \bar{z}_2)$ of the centralized model, which is a contradiction. We can conclude that with $d_{uv} = 0$ for $(u, v) \in E_{12} \cup E_{21}$, any central optimal solution is a pure Nash equilibrium. □

We provide pure Nash equilibria for the games by using two different ways and compare them in Section 4.7. The first Nash equilibrium is found by minimizing the potential function. The second one is by using best response dynamics. In *the best-response dynamics method*, each player continually improves their solution in response to changes made by the other player. It is a dynamic behavior of a process in which each player updates the strategy based on the best-response to the current situation. Further, in any finite potential game, best response dynamics always converge to a pure Nash equilibrium (Nisan et al. (2007)).

## 4.6 Strict Control Facility Location and Restoration Games and Mechanism Designs

In this section, we provide a mechanism to set, inter-edge usage fees, which motivate players to make their recovery and demand-facility assignment decisions according to the social welfare solution. Even though in Theorem 5, we show that without inter-edge usage fees, the social welfare solution is a Nash equilibrium. Players/infrastructure managers may not willing to install inter-edges just for the other players and consider the social welfare during their disaster recovery efforts. We need to provide motivation for players to install inter-edges according to the social welfare solution. The inter-edge usage fees motivate players to choose collaborative decisions in the non-cooperative game setting.

First, we present a mechanism design algorithm based on an inverse optimization. The main idea of the inverse optimization is to find values of the parameters that make a known feasible solution to the optimal solution by perturbing the parameters as small as possible (Heuberger (2004)). In our case, we want to achieve the social welfare solution in the players' individual problems by perturbing the inter-edge usage fees. Inverse optimization has many practical applications. One of the most common areas is government applications, for example, designing a mechanism to calculate incentives for advocating renewable energy (Duan and Wang (2011)). Another area is motivating the collaboration of privately owned companies. For example, Houghtalen et al. (2011) and Agarwal and Ergun (2008) present a mechanism design using an inverse optimization technique for their linear programming models to encourage cargo carriers to collaborate. We consider the inverse optimization idea for SC-FLR, which is modelled using a mixed integer programming.

In our inverse optimization mechanism design algorithm, we apply the cutting plane algorithm presented by Wang (2009) for our facility location and restoration games to decide inter-edge usage fees. We prove that using the inter-edge usage fees obtained from

the inverse optimization mechanism, the games result in a Nash equilibrium that aligns with the social welfare solution. Every iteration in the inverse optimization procedure requires solving an integer programming problem. As a result, for large problem instances, the inverse optimization method may be impractical. Thus, we provide another mechanism design algorithm based on $\alpha$-approximate algorithm, which requires solving a linear programming problem and so is computationally more efficient for larger instances. However, we prove that when players use the $\alpha$-approximation algorithm fees the social welfare solution becomes an $\alpha$-approximate pure Nash equilibrium, not a pure Nash equilibrium.

The $\alpha$-approximation algorithm is based on the duality theory. This algorithm considers that the strong duality conditions are satisfied within a multiplicative factor $\alpha$. At the end, the algorithm has $\alpha$ as its approximation guarantee.

Both of the mechanism design algorithms use dual constraints. We first construct the linear relaxation of the SC-FLR formulation and the dual of the linear relaxation of the SC-FLR formulation. To do that, we first rearrange the formulation as follows. We fix Player 2's decision variables to the optimal solution values of the centralized model $(\bar{y}^2, \bar{x}^2)$ in Player 1's problem. When we fix the dependent variables in the Player 1's problem, we implicitly set $\beta = x$ for $(u, v) \in E_{12}$, and $\beta$ variables become redundant. As a result, we remove the constraint sets (4.3.20), (4.3.21), and (4.3.25). Further, we replace the $\beta$ variables with $x$ variables in constraint set (4.3.22). The linear relaxation of Player 1's problem is as follows.

$$LR\text{-}SC\text{-}FLR : \min \sum_{v \in F_1} f_v y_v^1 + \sum_{(u,v) \in E_1} c_{uv} x_{uv}^1 + \sum_{(u,v) \in E_{12}} (c_{uv} + d_{uv}) x_{uv}^1 - \sum_{(u,v) \in E_{21}} d_{uv} \bar{x}_{uv}^2 \tag{4.6.1}$$

$$\text{s.t} \sum_{v:(u,v) \in E} x_{uv}^1 = 1 \text{ for } u \in D_1 \tag{4.6.2}$$

$$x^1_{uv} - y^1_v \leq 0 \text{ for } (u,v) \in E_1 \tag{4.6.3}$$

$$\bar{x}^2_{uv} - y^1_v \leq 0 \text{ for } (u,v) \in E_{21} \tag{4.6.4}$$

$$x^1_{uv} - \bar{y}^2_v \leq 0 \text{ for } (u,v) \in E_{12} \tag{4.6.5}$$

$$\sum_{(u,v)\in E_1 \cap I} p_{uv} x^1_{uv} + \sum_{(u,v)\in E_{21}\cap I} p_{uv}\bar{x}^2_{uv} \leq B^1 \tag{4.6.6}$$

$$y^1_v \geq 0 \text{ for } v \in F_1 \tag{4.6.7}$$

$$x^1_{uv} \geq 0 \text{ for } (u,v) \in E_1 \cup E_{12} \tag{4.6.8}$$

Next, we present the dual of LR-SC-FLR for Player 1, in which $\pi^1_u$ represents dual variables associated with constraint set (4.6.2), $\gamma^1_{uv}$ with constraint sets (4.6.3), (4.6.4), and (4.6.5), and $\delta^1$ with constraint set (4.6.6).

$$\max \sum_{u\in D_1} \pi^1_u - \sum_{(u,v)\in E_{12}} \bar{y}^2_v \gamma_{uv} + \sum_{(u,v)\in E_{21}} \bar{x}^2_{uv}\gamma_{uv} - \big(B^1 + \sum_{(u,v)\in E_{21}\cap I} p_{uv}\bar{x}^2_{uv}\big)\delta^1 \tag{4.6.9}$$

$$\pi^1_u + \gamma^1_{uv} \leq c_{uv} \quad \text{for} \quad (u,v) \in E_1 \cap A \tag{4.6.10}$$

$$\pi^1_u + \gamma^1_{uv} \leq c_{uv} + d_{uv} \quad \text{for} \quad (u,v) \in E_{12} \tag{4.6.11}$$

$$\pi^1_u + \gamma^1_{uv} + \delta^1 p_{uv} \leq c_{uv} \quad \text{for} \quad (u,v) \in E_1 \cap I \tag{4.6.12}$$

$$-\sum_{u\in D} \gamma^1_{uv} \leq f_v \quad \text{for} \quad v \in F_1 \tag{4.6.13}$$

$$\pi^1_u \; free \quad \text{for} \quad u \in D_1 \tag{4.6.14}$$

$$\gamma^1_{uv} \leq 0 \quad \text{for} \quad (u,v) \in E_1 \cup E_{12} \cup E_{21} \tag{4.6.15}$$

$$\delta^1 \leq 0 \tag{4.6.16}$$

### 4.6.1 Mechanism design based on the cutting plane algorithm for the inverse integer programming

Next, we present a mechanism design method based on the cutting plane algorithm for the inverse integer programming (Wang (2009)). In this cutting plane algorithm, the strong duality conditions of the linear programming are relaxed. The algorithm can be applied to solve inverse optimization of the mixed integer linear programming problems with slight modification (Wang (2009)). In the algorithm, we start with the set of known extreme points $S = \emptyset$, then dynamically update $S$ at each iteration until we achieve the desired solution as an optimal solution. To do that, we define a new objective function for Player 1's individual problem as

$$Z_1[d](y^1, x^1) := \sum_{v \in F_1} f_v y_v^1 + \sum_{(u,v) \in E_1} c_{uv} x_{uv}^1 + \sum_{(u,v) \in E_{12}} (c_{uv} + d_{uv}) x_{uv}^1,$$

where $f_v$ and $c_{uv}$ are the coefficients of the original facility location and restoration model that are not being perturbed.

The goal of Algorithm 2 is to find the coefficient $d_{uv}$ for $(u, v) \in E_{12}$ that minimizes the $L_1$ norm distance between the initial objective coefficients $d^0$ and $d_{uv}$ weighted with the positive vector parameter $w$ such that the centralized model optimal solution $(\bar{y}^1, \bar{x}^1)$ becomes optimal for the Player 1's individual problem with the objective function $Z_1[d]$. Algorithm 2 terminates in a finite number of iterations (Wang (2009)). Note that the inverse optimization algorithm provides us fees $d_{uv}^\star$ for using inter-edges $(u, v) \in E_{12}$. We apply the same algorithm for the problem of Player 2 with the objective $Z_2[d](y^2, x^2) := \sum_{v \in F_2} f_v y_v^2 + \sum_{(u,v) \in E_2} c_{uv} x_{uv}^2 + \sum_{(u,v) \in E_{21}} (c_{uv} + d_{uv}) x_{uv}^2$ and obtain the fees $d_{uv}^\star$ for using inter-edges $(u, v) \in E_{21}$.

Next, we prove that the social welfare solution becomes a pure Nash equilibrium when we use the fees obtained from the Algorithm 2. However, our games can accept other

**Algorithm 2** Wang's (2009) Cutting Plane Algorithm for Solving the Inverse Integer Programming Problem applied for Player 1's individual problem with the objective function $Z_1[d]$

1: **Initialize:**
Let the optimal solution of the centralized model be $(\bar{y}^1, \bar{x}^1)$ for Player 1
Initialize parameter $d^0$
Initiate an empty set $S = \emptyset$

2: Solve (4.6.17) and let $(d^\star, \pi^\star, \alpha^\star, \delta^\star)$ be an optimal solution for (6.17).

$$\min_{d,\pi,\alpha,\delta} w^T ||d^0 - d||_1 \tag{4.6.17}$$

$$\text{s.t. } Z_1[d](\bar{y}^1, \bar{x}^1) \leq Z_1[d](\tilde{y}^1, \tilde{x}^1),\ (\tilde{y}^1, \tilde{x}^1) \in S \tag{4.6.18}$$

and constraint sets (4.6.10) - (4.6.16).

3: Let $(\tilde{y}^1, \tilde{x}^1)$ be an optimal extreme point solution for the SC-FLR such that

$$(\tilde{y}^1, \tilde{x}^1) = \text{argmin}\{ \sum_{v \in V_1 \cap F} f_v y_v^1 + \sum_{(u,v) \in E_1} c_{uv} x_{uv}^1 + \sum_{(u,v) \in E_{12}} (c_{uv} + d_{uv}) x_{uv}^1$$

s.t. constraint sets $(4.6.2) - (4.6.6)$, and $y_v^1 \in \{0,1\}$ for $v \in F_1, x_{uv}^1 \in \{0,1\}$ for $(u,v) \in E_1 \cup E_{12}$

If $Z^1[d^\star](\bar{y}^1, \bar{x}^1) \leq Z^1[d^\star](\tilde{y}^1, \tilde{x}^1)$ then stop. Otherwise, $S := S \cup (\tilde{y}^1, \tilde{x}^1)$ and go to Step 2.

4: **return** Estimated objective function coefficient $d^\star$.

equilibria, which do not align with the social welfare solution. Later, we use these fees in the best response dynamics and in the potential function to obtain pure Nash equilibria for the games.

**Proposition 6.** *The social welfare solution becomes a a pure Nash equilibrium for SC-FLR with fees obtained from Algorithm 2.*

*Proof.* Let us assume $(\bar{y}^1, \bar{x}^1, \bar{y}^2, \bar{x}^2)$ be the optimal solution of the centralized model. Without loss of generality, we prove that $(\bar{y}^1, \bar{x}^1)$ is a pure Nash equilibrium. When we apply Algorithm 2 for Player 1, we obtain fees $d_{uv}^\star$ for $(u,v) \in E_{12}$, which makes the optimal solution of the centralized model $(\bar{y}^1, \bar{x}^1)$ optimal for Player 1's problem with the objective function $Z_1[d^\star]$. For any strategy $\tilde{z}^1$ the following equality holds, where $\tilde{z}_1 = (\tilde{y}_1, \tilde{x}_1, \tilde{\beta}_1) \in S_1$,

$\tilde{z}_1 = (\bar{y}_1, \bar{x}_1, \bar{\beta}_1) \in S_1$, and $\bar{z}_2 = (\bar{y}_2, \bar{x}_2, \bar{\beta}_2) \in S_2$.

$$Z_1[d^\star](\bar{y}^1, \bar{x}^1) = \sum_{v \in F_1} f_v \bar{y}_v^1 + \sum_{(u,v) \in E_1} c_{uv} \bar{x}_{uv}^1 + \sum_{(u,v) \in E_{12}} (c_{uv} + d_{uv}^\star) \bar{x}_{uv}^1 \tag{4.6.19}$$

$$\leq \sum_{v \in F_1} f_v \tilde{y}_v^1 + \sum_{(u,v) \in E_1} c_{uv} \tilde{x}_{uv}^1 + \sum_{(u,v) \in E_{12}} (c_{uv} + d_{uv}^\star) \tilde{x}_{uv}^1 \tag{4.6.20}$$

Therefore, we can conclude the following inequalities.

$$u_1(\bar{z}_1, \bar{z}_2) = \sum_{v \in F_1} f_v \bar{y}_v^1 + \sum_{(u,v) \in E_1} c_{uv} \bar{x}_{uv}^1 + \sum_{(u,v) \in E_{12}} (c_{uv} + d_{uv}^\star) \bar{x}_{uv}^1 - \sum_{(u,v) \in E_{21}} d_{uv}^\star \bar{x}_{uv}^2 \tag{4.6.21}$$

$$\leq \sum_{v \in F_1} f_v \tilde{y}_v^1 + \sum_{(u,v) \in E_1} c_{uv} \tilde{x}_{uv}^1 + \sum_{(u,v) \in E_{12}} (c_{uv} + d_{uv}^\star) \tilde{x}_{uv}^1 - \sum_{(u,v) \in E_{21}} d_{uv}^\star \bar{x}_{uv}^2 \tag{4.6.22}$$

$$\leq u_1(\tilde{z}_1, \bar{z}_2) \tag{4.6.23}$$

A similar result follows for Player 2. Therefore, we prove that $(\bar{z}_1, \bar{z}_2)$ is a pure Nash equilibrium for SC-FLR. □

### 4.6.2 Mechanism design based on the $\alpha$-approximation algorithm

In Algorithm 2, we solve a mixed integer programming problem in every iteration in Step 3. This can be a disadvantage to obtain fast convergence in the algorithm, especially for large instances. We provide another mechanism design algorithm based on an $\alpha$-approximation algorithm, where parameter $\alpha \geq 1$. The algorithm minimizes the total perturbation in the initial inter-edge fees while holding the strong duality conditions with a relaxation factor $\alpha$ and satisfying duality constraints with the perturbed fees. At the end, the algorithm has $\alpha$ as its approximation is guaranteed (Jain and Vazirani (1999)). First, we define perturbed fees $d_{uv} = d_{uv}^0 - e_{uv} + g_{uv}$, where $d_{uv}^0$ are the initial inter-edge fees and $e_{uv}, g_{uv} \geq 0$ for $(u, v) \in E_{12} \cup E_{21}$ as variables in the algorithm. Note that $f_v$ and $c_{uv}$ are not perturbed.

The formulation of the $\alpha$-approximation algorithm is as follows.

$$\min \sum_{(u,v)\in E_{12}\cup E_{21}} \theta(e_{uv}+g_{uv}) \tag{4.6.24}$$

$$\pi_u^1-\gamma_{uv}^1 \le c_{uv} \quad \text{for} \quad (u,v)\in E_1\cap A \tag{4.6.25}$$

$$\pi_u^1-\gamma_{uv}^1 \le c_{uv}+d_{uv}^0-e_{uv}+g_{uv} \quad \text{for} \quad (u,v)\in E_{12} \tag{4.6.26}$$

$$\pi_u^1-\gamma_{uv}^1-\delta^1 p_{uv} \le c_{uv} \quad \text{for} \quad (u,v)\in E_1\cap I \tag{4.6.27}$$

$$\sum_{u\in D}\gamma_{uv}^1 \le f_v \quad \text{for} \quad v\in F_1 \tag{4.6.28}$$

$$\pi_u^1 \text{ free} \quad \text{for} \quad u\in D_1 \tag{4.6.29}$$

$$\gamma_{uv}^1 \le 0 \quad \text{for} \quad (u,v)\in E_1\cup E_{12}\cup E_{21} \tag{4.6.30}$$

$$\delta^1 \le 0 \tag{4.6.31}$$

$$\pi_u^2-\gamma_{uv}^2 \le c_{uv} \quad \text{for} \quad (u,v)\in E_2\cap A \tag{4.6.32}$$

$$\pi_u^2-\gamma_{uv}^2 \le c_{uv}+d_{uv}^0-e_{uv}+g_{uv} \quad \text{for} \quad (u,v)\in E_{21} \tag{4.6.33}$$

$$\pi_u^2-\gamma_{uv}^2-\delta^2 p_{uv} \le c_{uv} \quad \text{for} \quad (u,v)\in E_2\cap I \tag{4.6.34}$$

$$\sum_{u\in D}\gamma_{uv}^2 \le f_v \quad \text{for} \quad v\in F_2 \tag{4.6.35}$$

$$\pi_u^2 \text{ free} \quad \text{for} \quad u\in D_2 \tag{4.6.36}$$

$$\gamma_{uv}^2 \le 0 \quad \text{for} \quad (u,v)\in E_2\cup E_{12}\cup E_{21} \tag{4.6.37}$$

$$\delta^2 \ge 0 \tag{4.6.38}$$

$$\begin{aligned}&\sum_{v\in F_1} f_v\bar{y}_v^1+\sum_{(u,v)\in E_1} c_{uv}\bar{x}_{uv}^1+\sum_{(u,v)\in E_{12}}(c_{uv}+d_{uv}^0-e_{uv}+g_{uv})\bar{x}_{uv}^1-\sum_{(u,v)\in E_{21}}(d_{uv}^0-e_{uv}+g_{uv})\bar{x}_{uv}^2\\ \le&\alpha\Big[\sum_{u\in D_1}\pi_u^1-\sum_{(u,v)\in E_{12}}\bar{y}_v^2\gamma_{uv}^1+\sum_{(u,v)\in E_{21}}\bar{x}_{uv}^2\gamma_{uv}^1-\big(B^1+\sum_{(u,v)\in E_{21}\cap I}p_{uv}\bar{x}_{uv}^2\big)\delta^1\Big]\end{aligned} \tag{4.6.39}$$

$$\sum_{v\in F_2} f_v\bar{y}_v^2 + \sum_{(u,v)\in E_2} c_{uv}\bar{x}_{uv}^2 + \sum_{(u,v)\in E_{21}} (c_{uv} + d_{uv}^0 - e_{uv} + g_{uv})\bar{x}_{uv}^2 - \sum_{(u,v)\in E_{12}} (d_{uv}^0 - e_{uv} + g_{uv})\bar{x}_{uv}^1$$

$$\leq \alpha\big[\sum_{u\in D_2} \pi_u^2 - \sum_{(u,v)\in E_{21}} \bar{y}_v^1\gamma_{uv}^2 + \sum_{(u,v)\in E_{12}} \bar{x}_{uv}^1\gamma_{uv}^2 - \big(B^2 + \sum_{(u,v)\in E_{12}\cap I} p_{uv}\bar{x}_{uv}^1\big)\delta^2\big] \quad (4.6.40)$$

$$d_{uv}^0 - e_{uv} + g_{uv} \geq 0 \quad \text{for} \quad (u,v) \cup E_{12} \cup E_{21} \quad (4.6.41)$$

$$e_{uv} \geq 0 \quad \text{for} \quad (u,v) \in E_{12} \cup E_{21} \quad (4.6.42)$$

$$g_{uv} \geq 0 \quad \text{for} \quad (u,v) \in E_{12} \cup E_{21} \quad (4.6.43)$$

The objective of the algorithm is to minimize the weighted total perturbation, $\theta||d_{uv}^0 - d_{uv}||_1 = \sum_{(u,v)\in E_{12}\cup E_{21}} \theta(e_{uv} + g_{uv})$ in the initial fees $d^0$ weighted with the positive parameter $\theta$. The dual constraint sets for Player 1 are (4.6.25)-(4.6.31) and the dual constraint sets for Player 2 are (4.6.32)-(4.6.38). The constraint sets (4.6.39) and (4.6.40) ensure that strong duality conditions are relaxed by $\alpha$ for Player 1 and Player 2, respectively. Constraint sets (4.6.41), (4.6.42) and (4.6.43) require $d_{uv} = d_{uv}^0 - e_{uv} + g_{uv}$, $e_{uv}$ and $g_{uv}$ to be non-negative for $(u,v) \in E_{12} \cup E_{21}$.

We solve $\alpha$-approximation linear programming problem optimally and obtain ($\pi^\star$, $\gamma^\star$, $\delta^\star$, $e^\star$, $g^\star$). Then, we observe that the optimal solution of the centralized model $(\bar{y}^1, \bar{y}^2, \bar{x}^1, \bar{x}^2)$ is an $\alpha$-approximate pure Nash equilibrium with the fees $d_{uv}^\star = d_{uv}^0 - e_{uv}^\star + g_{uv}^\star$ for $(u,v) \in E_{12} \cap E_{21}$. Next, we prove this observation holds. However, there might be other $\alpha$-approximate pure Nash equilibria, which are different than the social welfare solution. Later, we use these fees in the best response dynamics and in the potential function to obtain $\alpha$-approximate pure Nash equilibria for SC-FLR.

**Proposition 7.** *The centralized model optimal solution $(\bar{y}^1, \bar{x}^1, \bar{y}^2, \bar{x}^2)$ is an $\alpha$-approximate pure Nash equilibrium with the fees $d^\star$ obtained from $\alpha$-approximation optimal solution.*

*Proof.* Without loss of generality, we prove Theorem 7 for Player 1 and the proof for Player

2 follows analogously.

Let $(\pi^{\star 1}, \gamma^{\star 1}, \delta^{\star 1}, d^{\star})$ be optimal solution of $\alpha$-approximation linear programming problem for Player 1, where $d^{\star}_{uv} = d^{0}_{uv} - e^{\star}_{uv} + g^{\star}_{uv}$ $(u,v) \in E_{12} \cap E_{21}$. We can write the following inequality since constraint set (4.6.39) should be satisfied.

$$\begin{aligned} u_1(\bar{z}_1, \bar{z}_2) = & \sum_{v \in F_1} f_v \bar{y}^1_v + \sum_{(u,v) \in E_1} c_{uv} \bar{x}^1_{uv} + \sum_{(u,v) \in E_{12}} (c_{uv} + d^{\star}_{uv}) \bar{x}^1_{uv} - \sum_{(u,v) \in E_{21}} d^{\star}_{uv} \bar{x}^2_{uv} \\ \leq & \alpha \big[ \sum_{u \in D_1} \pi^{\star 1}_u - \sum_{(u,v) \in E_{12}} \bar{y}^2_v \gamma^{\star 1}_{uv} + \sum_{(u,v) \in E_{21}} \bar{x}^2_{uv} \gamma^{\star 1}_{uv} - \big( B^1 + \sum_{(u,v) \in E_{21} \cap I} p_{uv} \bar{x}^2_{uv} \big) \delta^{\star 1} \big] \end{aligned}$$

Let $(\tilde{y}^1, \tilde{x}^1)$ be the optimal solution for the LR-SC-FLR problem of Player 1. Using strong duality, we have the following inequality.

$$\begin{aligned} & \alpha \big[ \sum_{u \in D_1} \pi^{\star 1}_u - \sum_{(u,v) \in E_{12}} \bar{y}^2_v \gamma^{\star 1}_{uv} + \sum_{(u,v) \in E_{21}} \bar{x}^2_{uv} \gamma^{\star 1}_{uv} - \big( B^1 + \sum_{(u,v) \in E_{21} \cap I} p_{uv} \bar{x}^2_{uv} \big) \delta^{\star 1} \big] \\ \leq & \alpha \big[ \sum_{v \in F_1} f_v \tilde{y}^1_v + \sum_{(u,v) \in E_1} c_{uv} \tilde{x}^1_{uv} + \sum_{(u,v) \in E_{12}} (c_{uv} + d^{\star}_{uv}) \tilde{x}^1_{uv} - \sum_{(u,v) \in E_{21}} d^{\star}_{uv} \bar{x}^2_{uv} \big] \end{aligned}$$

Let $(\hat{y}^1, \hat{x}^1)$ be the optimal solution of SC-FLR for Player 1. We can write the following inequality between linear relaxation optimal solution and the optimal integer solution of Player 1's problem.

$$\begin{aligned} & \alpha \big[ \sum_{v \in F_1} f_v \tilde{y}^1_v + \sum_{(u,v) \in E_1} c_{uv} \tilde{x}^1_{uv} + \sum_{(u,v) \in E_{12}} (c_{uv} + d^{\star}_{uv}) \tilde{x}^1_{uv} - \sum_{(u,v) \in E_{21}} d^{\star}_{uv} \bar{x}^2_{uv} \big] \\ \leq & \alpha \big[ \sum_{v \in F_1} f_v \hat{y}^1_v + \sum_{(u,v) \in E_1} c_{uv} \hat{x}^1_{uv} + \sum_{(u,v) \in E_{12}} (c_{uv} + d^{\star}_{uv}) \hat{x}^1_{uv} - \sum_{(u,v) \in E_{21}} d^{\star}_{uv} \bar{x}^2_{uv} \big] \end{aligned}$$

$$\leq \alpha u_1(\tilde{z}_1, \bar{z}_2)$$

We conclude that $(\bar{y}^1, \bar{x}^1)$ is an $\alpha$-approximate pure Nash equilibrium for Player 1 with the fees $d^\star_{uv}$ obtained for $(u, v) \in E_{12} \cap E_{21}$ from the $\alpha$-approximation optimal solution. Similarly, we can prove that $(\bar{y}^2, \bar{x}^2)$ is $\alpha$-pure Nash equilibrium for Player 2 with the fees $d^\star$. □

Note that for some $\alpha \geq 1$ values, the algorithm might be infeasible. One way to find an $\alpha$ value is first to set it to one and increase it with a pre-specified step size until finding a feasible solution to the approximation algorithm. In section 4.7, we provide the trade off between the total perturbation in the inter-edge fees and $\alpha$ value, which can be used to make better decision for choosing $\alpha$ by setting a limit in the total perturbation.

## 4.7 Computational Results

After disasters, the performance of the telecommunication systems become integral to save lives and to help the recovery of other infrastructure systems more effectively by providing communication. Destruction of the communications companies' facilities and so the communication services, which disaster victims rely on creates vulnerabilities to response disaster casualties (Miller (2006)). Ice storms, hurricanes affect telecommunications systems by damaging the parts of the systems. Telecommunication companies are driven by the goal to improve performance of their systems, particularly the receipt and the transmission of signals generated by the system (Lee and Chang (2007)). During disaster the goal of the telecommunication companies is to repair cell towers and signal transmissions to provide services for their customers.

We present a stylized example to illustrate the potential applicability of the proposed games and mechanism design algorithms using real-world data from two telecommu-

nication companies in Chicago, each company represents a player and has a network, which consists of cell tower and demand nodes. We create a two-layer network and model opening and sharing cell towers, recovering edges, and assigning demand to cell towers in the network. Opening a facility can be considered as repairing a disrupted cell tower by providing power or locating mobile cell tower (O'Reilly et al. (2006)). Sharing facilities involves a mutual sharing of active elements of the network such that cell towers, mobile network equipment, access node switches, and fiber optic networks (Meddour et al. (2011)). Recovering an edge represents setting signal transmission between cell tower and demand nodes. We consider the first day recovery efforts after disasters.

We use exact locations of the cell towers by obtaining the latitude and longitude of them from the Antenna Structure Registration website (Ant (2019)) advance search. We use census tracts of Chicago, 76 in total, to generate demand nodes for players. We assume each demand is located in the middle of each census tract and owned by only one of the players. Each demand represents a cluster of subscribers (Lee and Chang (2007)). Each player has 16 cell tower locations and 38 demand points in their network. We calculate the Euclidean distances between the total 32 cell tower locations and 76 demand nodes. We use a random number generator to select installable and initially available edges from the set of edges whose distances are smaller than or equal to five kilometers (Sarkar et al. (2018)). As a result, Player 1 has 148 initially available intra-edges and 24 installable intra-edges. Player 2 has 139 initially available intra-edges and 27 installable inter-edges. There are 292 initially available intra-edges and 50 installable inter-edges, half of which are connected to the demand of Player 1 and the other half are connected to the demand of Player 2.

In the computational experiments, we consider the cost to open a facility as a fixed value for each cell tower. Note that, if a facility is initially open, the opening cost for that facility is zero. We set the cost of assigning a demand to a facility as proportional to the distance between them (Lee and Chang (2007)). Edges represent existing signal transmitting between demand and cell towers. Thus, installing an edge is considered as

setting signal transmission between demand and a facility location. We consider the cost for installing an edge as proportional to the distance. In the telecommunication systems, a service measure is the distance from demand to cell towers (Lee and Chang (2007)). When we minimize the total cost, we implicitly improve the service quality, since we set the cost of using an edge proportional to the distance between demand and facility locations.

Computations for the models and algorithms were performed on a computer with a 1.4 GHz Intel Core 5 Duo Processor with 4GB of RAM. We used Gurobi 6.5.2. to solve the models that were coded in Python. Note that our case study experiments are solved fairly quickly (less than 600 seconds).

Next, we present and compare pure Nash equilibria for SC-FLRs by using two different techniques. The first pure Nash equilibrium is found by minimizing the potential function. The second pure Nash equilibrium is found by using the best response dynamics method. We use three different ways to set inter-edge usage fees and use them while constructing the Nash equilibria. The three different ways are as follows; using the $\alpha$-approximation algorithm, using the inverse optimization algorithm, and generating the fees proportional to the costs of using edges. Table 4.4 compares the total cost associated to each player in the optimal solution of the centralized model and the payoff for each player in the pure Nash equilibria found with the three sets of inter-edge fees. In Table 4.4, "Optimal solution of the centralized model" rows represent the total cost for opening facilities and satisfying demand of each player in the optimal solution of the centralized model with the given total budget. Note that the social welfare solution does not include the inter-edge usage fees. To analyze the results further, we also vary the total budget to install edges in the centralized model. The pure Nash equilibrium payoffs with the fees proportional to costs in the potential function and best response dynamics pure Nash equilibrium are obtained by setting the fees proportional to the costs of using associated edges. We observe that when we construct the inter-edge usage fees proportional to the costs of using the inter-edges, the payoffs of the players are close to each other in both of the Nash equilibria.

Table 4.4: Optimal solutions of the centralized model and payoffs at the pure Nash equilibria in SC-FLR for players obtained by minimizing the potential function and using the best response dynamics with different budget. The fees used by players in the Nash equilibria are obtained from the $\alpha$-approximation algorithm, the inverse optimization algorithm, and the fees are generated proportional to the cost of edges.

| Budget | | Fees | Player 1 payoff | Player 2 payoff |
|---|---|---|---|---|
| 0 | Optimal solution of the centralized model | No fees | 1053.85 | 960.81 |
| | Potential function | $\alpha$-approximation | 1075.65 | 960.46 |
| | | Inverse optimization | 1098.28 | 1039.46 |
| | | Proportional to cost | 1026.94 | 1159.92 |
| | Best response dynamics | $\alpha$-approximation | 1100.58 | 1003.95 |
| | | Inverse optimization | 1076.08 | 971.98 |
| | | Proportional to cost | 1018.13 | 1171.59 |
| 40 | Optimal solution of the centralized model | No fees | 992.75 | 973.27 |
| | Potential function | $\alpha$-approximation | 1087.35 | 915.45 |
| | | Inverse optimization | 844.88 | 1211.48 |
| | | Proportional to cost | 970.00 | 1159.60 |
| | Best response dynamics | $\alpha$-approximation | 1107.91 | 1003.95 |
| | | Inverse optimization | 944.26 | 1228.42 |
| | | Proportional to cost | 1009.82 | 1185.39 |
| 80 | Optimal solution of the centralized model | No fees | 941.78 | 1007.40 |
| | Potential function | $\alpha$-approximation | 1052.25 | 919.30 |
| | | Inverse optimization | 1153.28 | 956.48 |
| | | Proportional to cost | 956.21 | 1132.00 |
| | Best response dynamics | $\alpha$-approximation | 637.22 | 1396.80 |
| | | Inverse optimization | 926.08 | 1191.86 |
| | | Proportional to cost | 1008.21 | 1147.98 |
| 120 | Optimal solution of the centralized model | No fees | 986.49 | 952.56 |
| | Potential function | $\alpha$-approximation | 1056.32 | 909.67 |
| | | Inverse optimization | 1004.50 | 996.08 |
| | | Proportional to cost | 956.21 | 1132.00 |
| | Best response dynamics | $\alpha$-approximation | 1112.94 | 940.93 |
| | | Inverse optimization | 924.37 | 1217.77 |
| | | Proportional to cost | 1008.21 | 1147.08 |

Further, we present the total of payoffs of both players in the Nash equilibria in Figure 4.3, and compare them with the optimal solution of the centralized model using different total recovery budget. Note that even though the pure Nash equilibrium payoff for each player includes the fees to use inter-edges, the total of both players payoffs does not include the fees, since the received and payed fees for using inter-edges cancel each other when we sum the payoffs of both players. The social welfare solution does not include the inter-edge fees, since the optimal solution of the centralized model does not consider the fees. Therefore, the total payoffs of both players and the social welfare solutions are comparable and provide us the trade-off between the centralized model and the non-cooperative environment when

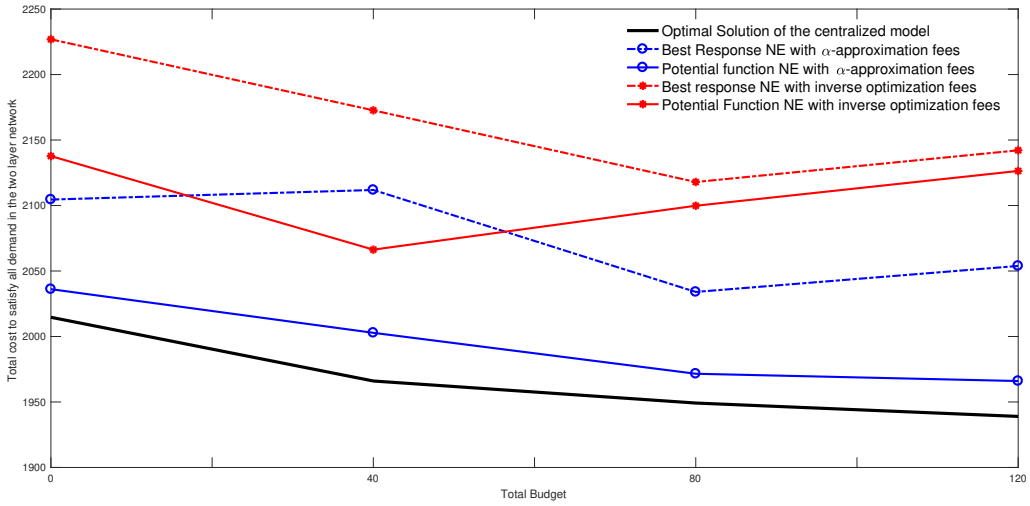


Figure 4.3: Total payoffs of both players in the pure Nash equilibria (NE) in which fees are calculated in three different ways for SC-FLR. Nash equilibria are constructed by minimizing the potential function and using the best response dynamics in the two-layer network with different budget.

we consider the different ways to construct inter-edge usage fees and Nash equilibria. Figure 4.3 shows us that the potential function pure Nash equilibrium is closer to the social welfare solution compared to the best response dynamics pure Nash equilibrium regardless of the way to construct inter-edge usage fees. The closest pure Nash equilibrium to the social welfare solution is achieved by minimizing the potential function and using the inter-edge fees obtained from the $\alpha$-approximation algorithm.

In Figure 4.4, we compare the social welfare solutions and the total payoffs of the players in the Nash equilibria for LC-FLR and SC-FLR. We observe that the total payoffs in the pure Nash equilibrium found by minimizing the potential function is closer to the social welfare solution in both versions of the game compare to the pure Nash equilibrium found by the best response dynamics. In addition, we notice that SC-FLR provides more effective disaster recovery when we compare the total payoffs of the Nash equilibria and the social welfare solution with LC-FLR. As a result, by considering strict control of the central decision maker, the players install-inter edges and achieve better overall payoffs by collaborating in

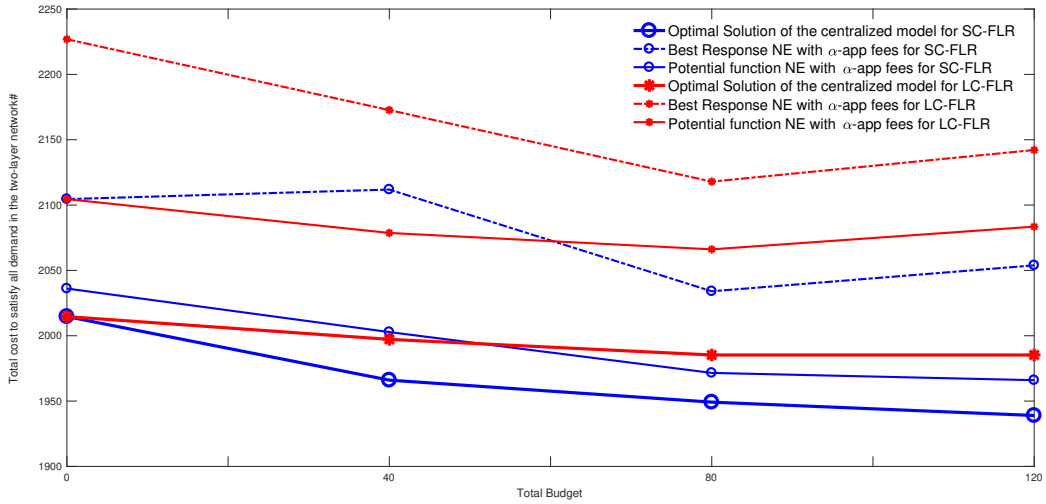


Figure 4.4: The total cost of the optimal solution of the centralized model (the social welfare solution) and the total payoffs of both players in the pure Nash equilibria (NE) for LC-FLR and SC-FLR. Nash equilibria are constructed by minimizing the potential function and using the best response dynamics in the two-layer network with different total budget, where fees are obtained from $\alpha$- approximation algorithm ($\alpha$-app).

the non-cooperative environment.

Figure 4.5 compares the total cost of the Nash equilibria obtained by minimizing the potential function with the fees proportional to the fees we obtain from $\alpha$-approximation algorithm and the social welfare solution. We set the ratio between fees and the $\alpha$-approximation algorithm fees as 0.1, 0.5, 1, 2, and 3, respectively. We observe that when we increase or decrease the ratio between the fees and $\alpha$-approximation fees, the total payoffs of the pure Nash equilibrium is moving away from the optimal solution value of the centralized model. Figure 4.5 highlights that when we use the fees from the $\alpha$-approximation algorithm, the total payoffs of both players is closest to the social welfare solution. That highlights the importance of setting the right inter-edge fees to achieve a Nash equilibrium, which is close to the social welfare solution.

Even though we are unable to provide an efficient way to decide the best $\alpha$ value, one can use the similar results as in Figure 4.6, and set a limit in the total perturbation

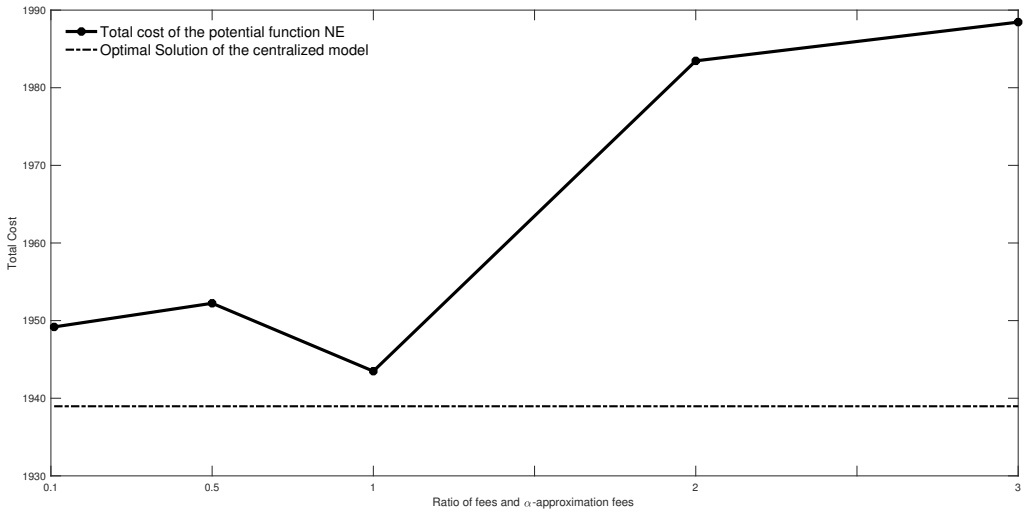


Figure 4.5: The dashed line represents the cost of the optimal solution of the centralized model (the social welfare solution) and the solid line represents the total cost of both players' payoffs in the potential function pure Nash equilibrium for SC-FLR with the budget 120. Nash equilibria are constructed by minimizing the potential function and fees are set to different ratio (0.1, 0.5, 1,2,3) of the fees obtained from $\alpha$-approximation algorithm.

to decide a value for $\alpha$. Figure 4.6 presents the trade-off between the total perturbation (without any weight) in the inter-edge usage fees and $\alpha$ in the $\alpha$-approximation algorithm. We observe that when we increase the $\alpha$, the approximation solution moves far away from the social welfare solution, which we are approximating. When we set $\alpha = 1$, our approximation solution provides us a solution with a perturbation in the initial inter-edge fees, that means for this instance the strong duality conditions hold. When we set $\alpha = 1.6$, the total perturbation in the inter-edge usage fees becomes $0$. Note that we set the initial inter-edge fees as same as the cost for using inter-edges.

Figure 4.7a shows the open facility locations and demand-facility assignments in the optimal solution of the centralized model. Eight facility locations belonging to Player 1 and three facility locations belonging to Player 2 satisfy the demand. Figures 4.7b and 4.7c visualize the open facility locations and demand-facility assignments in the pure Nash equilibrium obtained by minimizing the potential function in which the fees are obtained from $\alpha$-approximation algorithm in SC-FLR and LC-FLR, respectively in Figure 4.7b and

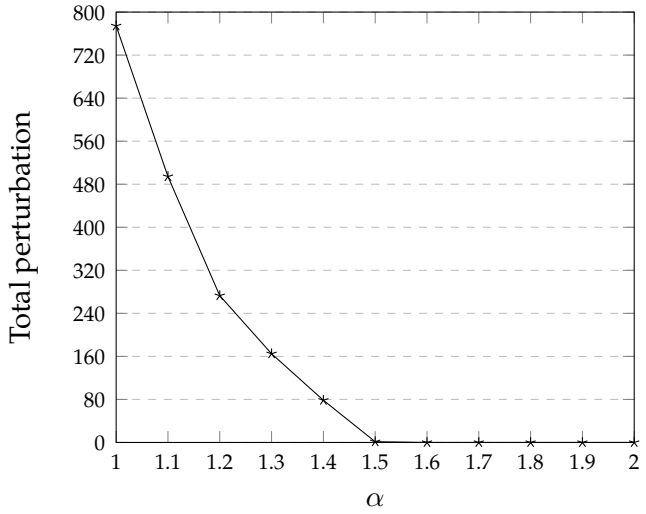


Figure 4.6: The trade-off between the total perturbation ($||d^0_{uv} - d_{uv}||_1$) in the inter-edge fees and the $\alpha$ in the $\alpha$-approximation algorithm for SC-FLR with total budget 120. The total perturbation becomes zero when we set $\alpha = 1.6$ or higher.

4.7c. Eight of the open facility locations belong to Player 1 and four belong to Player 2. Even though LC-FLR does not allow players to install inter-edges, we observe that players share facilities using initially available inter-edges in Figure 4.7c. While most of open facilities and the demand-facility assignments are similar in all of the figures, we observe a few selfish assignments of Player 1 and Player 2 in Figure 4.7b such that players do not satisfy any demand of the other player with their open facilities.

## 4.8 Conclusion

In this chapter, we establish a game-theoretic framework to provide a fundamental understanding for a class of facility location and restoration problems in a non-cooperative setting.

We present two different versions of non-cooperative facility location and restoration games. The first version is *the strict control facility location and restoration game* (SC-FLR). In this version of the game, the central decision maker controls players in a way that players use their budget for installing inter-edges according to the optimal solution of the

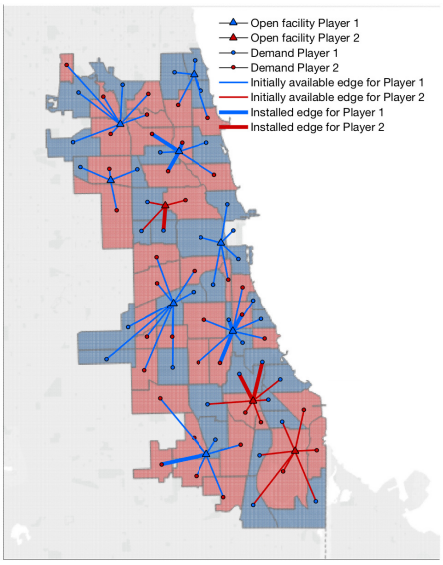


(a) Centralized model

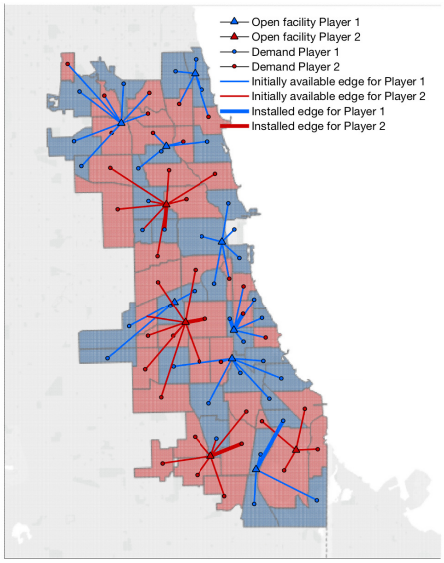


(b) SC-FLR

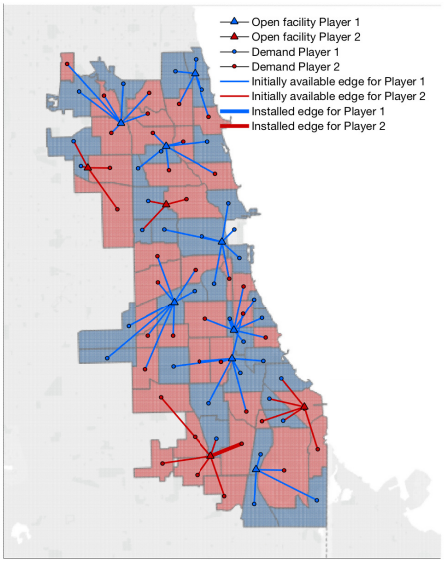


(c) LC-FLR

Figure 4.7: Optimal solution of the centralized model with the total budget 120 for the centralized model, the pure Nash equilibrium solution, which is obtained by minimizing the potential function with the fees obtained from $\alpha$-approximation algorithm for SC-FLR and LC-FLR, respectively.

centralized model. If there is no strict control, it is not guaranteed that players use the installed inter-edges and pay the associated fees for the inter-edges. Further, we prove that there is always a pure Nash equilibrium, in which none of the players uses installed inter-edges. As a result, we present the second version, *the limited control facility location and restoration game* (LC-FLR). In this version, we consider that players do not install inter-edges. We show that both versions of the game are potential games and we prove the existence of a pure Nash equilibrium for each version by constructing a potential function for the games. We also use best response dynamics to construct another Nash equilibrium for the games. We compare the optimal solution value of the centralized model with the total payoffs of both players in the pure Nash equilibria of the games and provide a bound for the price of stability using the potential function method.

We propose mechanisms using an inverse optimization method and $\alpha$-approximation algorithm to decide the fees for using inter-edges. The goal of the mechanisms is to set fees so that the pure Nash equilibrium aligns with the centralized model optimal solution. We prove that when players use the inverse optimization fees, the optimal solution of the centralized model aligns with the total cost of a pure Nash equilibrium and when players use $\alpha$-approximation algorithm fees, the optimal solution of the centralized model becomes an $\alpha$-approximate pure Nash equilibrium. We provide computational results for two telecommunication companies in Chicago to show the effectiveness of the mechanism designs by comparing the Nash equilibria payoffs with the optimal solution value of the centralized model. In the computational results, we observe that the total payoffs of the players in the pure Nash equilibrium obtained by minimizing the potential function is the closest one to the total cost of the optimal solution of the centralized model (the social welfare solution) compare to the others. A future research direction can be extending the games to more than two players and including different types of interdependencies as identified in details by Sharkey et al. (2015a). Another research direction can be considering a cooperative game setting and studying the core of the games in the possible sub-coalitions.

# Chapter 5

# Conclusion

We propose three research models that apply integer programming formulations to improve the disaster recovery efforts of interdependent infrastructure systems.

In Chapter 2, we introduce an integrated restoration and location problem (IRLP) and model the interdependencies between road infrastructure system and emergency service providers. We study a P-median model variation with the goal of minimizing the cumulative weighted distance between emergency responders and demand nodes over a time horizon. We also introduce the c-IRLP, an extension to this model to approximately model components of disrupted arcs between demand and facility locations. The models can be used to model the delivery of a variety of time-sensitive critical services after a disaster event occurs. The models provide insight into how the activities of the two types of service providers should be coordinated and which network components should be restored sooner during recovery.

In the Chapter 3, we introduce a maximal multiple coverage and network restoration problem (MMCaNR) for recovery and restoration of infrastructure systems after disasters. The MMCaNR problem is a maximal expected coverage problem variation with the goal of maximizing cumulative multiple coverage of emergency service demand over the time

horizon. The MMCaNR problem solution provides insights into how to prioritize disrupted component installations into the network and relocate emergency responders to cover demand more effectively using available arcs following the installations.

In the Chapter 4, we establish a game-theoretic framework to provide a fundamental understanding for a class of facility location and restoration problems in a non-cooperative setting. We present two different versions of non-cooperative facility location and restoration games. The first version is *the strict control facility location and restoration game* (SC-FLR). We show that both versions of the game are potential games and we prove the existence of a pure Nash equilibrium for each version by constructing a potential function for the games. We also use best response dynamics to construct another Nash equilibrium for the games. We propose mechanisms using an inverse optimization method and $\alpha$-approximation algorithm to decide the fees for using inter-edges. We prove that when players use the inverse optimization fees, the optimal solution of the centralized model aligns with the total cost of a pure Nash equilibrium and when players use $\alpha$-approximation algorithm fees, the optimal solution of the centralized model becomes an $\alpha$-approximate pure Nash equilibrium. We provide computational results for two telecommunication companies in Chicago to show the effectiveness of the mechanism designs by comparing the Nash equilibria payoffs with the optimal solution value of the centralized model. In the computational results, we observe that the total payoffs of the players in the pure Nash equilibrium obtained by minimizing the potential function is the closest one to the total cost of the optimal solution of the centralized model (the social welfare solution) compare to the others.

# Appendix A

# Appendix

## A.1 A Special Case for c-IRLP Problem

In the original c-IRLP problem, we consider each component in the set $C'$ to have an associated processing time. One particular case of interest is when each component in $C'$ has identical processing times. Without loss of generality, we assume that all processing times are one. In this case, we can simplify the formulation, and we present the simplified formulation here.

In the recovery unit, we no longer need to assign component installations to individual network recovery crews. Instead, we select the $K$ components that are installed by any of the network recovery crews in each time period. As a result, the design decision variables $\tilde{x}_{cijt}$, $c \in C', (i,j) \in A',\ t = 1,\ldots,T$ and $y_{jt}$, $j \in J,\ t = 1,\ldots,T$ remain the same. The recovery decisions variables are simplified to:

- $\xi_{ct} = 1$ if one of the recovery crews complete the repairing of component $c \in C'$ and $0$ otherwise, for $t = 1,\ldots,T$.

The integer programming model is formulated as follows.

$$Z = \min \sum_{t=1}^{T} \sum_{c \in C'} \sum_{(i,j) \in AC(c)} w_{it} d_{cij} \tilde{x}_{cijt} + \sum_{t=1}^{T} \sum_{(i,j) \in A} w_{it} d_{0ij} \tilde{x}_{0ijt} \tag{A.1.1}$$

$$\text{s. t.} \sum_{c \in C'} \sum_{j:(i,j) \in AC(c)} \tilde{x}_{cijt} + \sum_{j:(i,j) \in A} \tilde{x}_{0ijt} = 1 \quad \text{for} \quad i \in I,\ t = 1, \ldots, T \tag{A.1.2}$$

$$\sum_{j \in J} y_{jt} \leq P \quad \text{for} \quad t = 1, \ldots, T \tag{A.1.3}$$

$$\tilde{x}_{cijt} - y_{jt} \leq 0 \quad \text{for} \quad c \in C',\ (i,j) \in AC(c),\ t = 1, \ldots, T \tag{A.1.4}$$

$$\tilde{x}_{0ijt} - y_{jt} \leq 0 \quad \text{for} \quad (i,j) \in A,\ t = 1, \ldots, T \tag{A.1.5}$$

$$\tilde{x}_{cijt} \in \{0,1\} \quad \text{for} \quad c \in C',\ (i,j) \in AC(c),\ t = 1, \ldots, T \tag{A.1.6}$$

$$\tilde{x}_{0ijt} \in \{0,1\} \quad \text{for} \quad (i,j) \in A,\ t = 1, \ldots, T \tag{A.1.7}$$

$$y_{jt} \in \{0,1\} \quad \text{for} \quad j \in J,\ t = 1, \ldots, T \tag{A.1.8}$$

$$x_{cijt} \leq \sum_{s=1}^{t} \xi_{cs} \quad \text{for} \quad c \in C',\ (i,j) \in AC(c),\ t = 1, \ldots, T \tag{A.1.9}$$

$$\sum_{c \in C'} \xi_{ct} \leq K \quad \text{for} \quad t = 1, \ldots, T \tag{A.1.10}$$

$$\xi_{ct} \in \{0,1\} \quad \text{for} \quad c \in C',\ t = 1, \ldots, T \tag{A.1.11}$$

The objective and constraint sets $(A.1.1) - (A.1.8)$ are the same as in the c-IRLP. Constraint set $(A.1.9)$ ensures that a component can be used to assign demand only if its installation was completed at any time prior to time $t$. Constraint set $(A.1.10)$ ensures that the number of component installed cannot exceed the total number of recovery crews. Constraint set $(A.1.11)$ requires the recovery decision variables to be binary.

Computational experiments suggest that this formulation drastically improves computational time when solving the models using off-the-shelf MILP solvers such as Gurobi as compared to the original component based IRLP formulation, particularly in cases when there are a large number of recovery crews.

# References

2019. Antenna Structure Registration. `https://wireless2.fcc.gov/UlsApp/AsrSearch/asrAdvancedSearch.jsp`. Accessed: 03.24.2019.

Abeliuk, Andres, Haris Aziz, Gerardo Berbeglia, Serge Gaspers, Petr Kalina, Nicholas Mattei, Dominik Peters, Paul Stursberg, Pascal Van Hentenryck, and Toby Walsh. 2016. Interdependent scheduling games. *arXiv preprint arXiv:1605.09497*.

Agarwal, Richa, and Özlem Ergun. 2008. Mechanism design for a multicommodity flow game in service network alliances. *Operations Research Letters* 36(5):520–524.

Ahuja, Ravindra K, and James B Orlin. 1998. Inverse optimization, part i: linear programming and general problem. *Sloan School of Management, Cambridge, MA*.

Almoghathawi, Yasser, Kash Barker, and Laura A Albert. 2019. Resilience-driven restoration model for interdependent infrastructure networks. *Reliability Engineering & System Safety* 185:12–23.

Anshelevich, Elliot, Anirban Dasgupta, Jon Kleinberg, Eva Tardos, Tom Wexler, and Tim Roughgarden. 2008. The price of stability for network design with fair cost allocation. *SIAM Journal on Computing* 38(4):1602–1623.

Averbakh, Igor, and Jordi Pereira. 2012. The flowtime network construction problem. *Iie Transactions* 44(8):681–694.

Barron, Emmanual N. 2013. *Game theory: an introduction*, vol. 2. John Wiley & Sons.

Baxter, Matthew, Tarek Elgindy, Andreas T Ernst, Thomas Kalinowski, and Martin WP Savelsbergh. 2014. Incremental network design with shortest paths. *European Journal of Operational Research* 238(3):675–684.

Baycik, N Orkun, and Thomas C Sharkey. 2019. Interdiction-based approaches to identify damage in disrupted critical infrastructures with dependencies. *Journal of Infrastructure Systems* 25(2):04019013.

Beasley, John E. 2015. The operational research library. `http://people.brunel.ac.uk/~mastjjb/jeb/orlib/pmedinfo.html`.

Berthold, Timo. 2014. RENS: The optimal rounding. *Mathematical Programming Computation* 6(1):33–54.

Blake, Eric S., and David A. Zelinsky. 2018. National hurricane center tropical cyclone report hurricane harvey. Tech. Rep., National Hurricane Center.

Bloch, Francis, and Matthew O Jackson. 2006. Definitions of equilibrium in network formation games. *International Journal of Game Theory* 34(3):305–318.

Brotcorne, Luce, Gilbert Laporte, and Frederic Semet. 2003. Ambulance location and relocation models. *European Journal of Operational Research* 147(3):451–463.

Buchbinder, Niv, and Joseph Naor. 2009. Online primal-dual algorithms for covering and packing. *Mathematics of Operations Research* 34(2):270–286.

Cardinal, Jean, and Martin Hoefer. 2010. Non-cooperative facility location and covering games. *Theoretical Computer Science* 411(16-18):1855–1876.

Carvalho Rodrigues, Félix, and Eduardo Candido Xavier. 2017. Non-cooperative capacitated facility location games. *Information Processing Letters* 117:45–53.

Cavdaroglu, Burak, Erik Hammel, John E Mitchell, Thomas C Sharkey, and William A Wallace. 2013. Integrating restoration and scheduling decisions for disrupted interdependent infrastructure systems. *Annals of Operations Research* 203(1):279–294.

Çelik, Melih, Özlem Ergun, and Pınar Keskinocak. 2015. The post-disaster debris clearance problem under incomplete information. *Operations Research* 63(1):65–85.

Chen, Juntao, and Quanyan Zhu. 2016. Interdependent network formation games with an application to critical infrastructures. In *American control conference (acc), 2016*, 2870–2875. IEEE.

Church, Richard, and Charles ReVelle. 1974. The maximal covering location problem. *Papers of the Regional Science Association* 32(1):101–118.

Church, Richard L, Maria P Scaparra, and Richard S Middleton. 2004. Identifying critical infrastructure: the median and covering facility interdiction problems. *Annals of the Association of American Geographers* 94(3):491–502.

Church, Richard L, and Maria Paola Scaparra. 2007. Protecting critical assets: the r-interdiction median problem with fortification. *Geographical Analysis* 39(2):129–146.

Cordeau, JF, F Furini, and I Ljubic. 2019. Benders decomposition for very large scale partial set covering and maximal covering problems. *European Journal of Operational Research* 275: 882–896.

Cui, Tingting, Yanfeng Ouyang, and Zuo-Jun Max Shen. 2010. Reliable facility location design under the risk of disruptions. *Operations Research* 58(4-part-1):998–1011.

Curiel, Imma. 2013. *Cooperative game theory and applications: cooperative games arising from combinatorial optimization problems*, vol. 16. Springer Science & Business Media.

Danna, Emilie, Edward Rothberg, and Claude Le Pape. 2005. Exploring relaxation induced neighborhoods to improve MIP solutions. *Mathematical Programming* 102(1):71–90.

Daskin, Mark S. 1983. A maximum expected covering location model: formulation, properties and heuristic solution. *Transportation Science* 17(1):48–70.

———. 2011. *Network and discrete location: models, algorithms, and applications*. John Wiley & Sons.

Degel, Dirk, Lara Wiesche, Sebastian Rachuba, and Brigitte Werners. 2015. Time-dependent ambulance allocation considering data-driven empirically required coverage. *Health Care Management Science* 18(4):444–458.

Dhamal, Swapnil, Walid Ben-Ameur, Tijani Chahed, and Eitan Altman. 2018. Resource allocation polytope games: Uniqueness of equilibrium, price of stability, and price of anarchy. In *Aaai 2018-32nd conference on artificial intelligence*, 1–10.

Duan, Zhaoyang, and Lizhi Wang. 2011. Heuristic algorithms for the inverse mixed integer linear programming problem. *Journal of Global Optimization* 51(3):463–471.

Ehsani, Shayan, Saber Shokat Fadaee, MohammadAmin Fazli, Abbas Mehrabian, Sina Sadeghian Sadeghabad, Mohammadali Safari, and Morteza Saghafian. 2015. A bounded budget network creation game. *ACM Transactions on Algorithms (TALG)* 11(4):34.

Engel, Konrad, Thomas Kalinowski, and Martin WP Savelsbergh. 2013. Incremental network design with minimum spanning trees. Tech. Rep., arXiv preprint arXiv:1306.1926.

Feder, Tomas, Hamid Nazerzadeh, and Amin Saberi. 2007. Approximating nash equilibria using small-support strategies. *EC* 7:352–354.

FEMA. 2007. Public Assistance – Debris management guide.

FEMA. 2013a. Emergency management considerations. Tech. Rep., Federal Emergency Management Agency.

———. 2013b. Hurricane sandy recovery efforts one year later. Tech. Rep., Federal Emergency Management Agency.

———. 2019. National response framework.

Fisher, Marshall L. 2004. The Lagrangian relaxation method for solving integer programming problems. *Management Science* 50(12_supplement):1861–1871.

Force, Hurricane Sandy Rebuilding Task. 2013. Hurricane Sandy rebuilding strategy. *US Department of Housing and Urban Development, Washington DC*.

Furgate, W. C. 2012. Testimony before the Committee on Transportation and Infrastructure, U.S. House of Representatives. Tech. Rep., Federal Emergency Management Agency.

Galvão, Roberto Diéguez, and Charles ReVelle. 1996. A Lagrangean heuristic for the maximal covering location problem. *European Journal of Operational Research* 88(1):114–123.

Gendreau, Michel, Gilbert Laporte, and Frédéric Semet. 1997. Solving an ambulance location model by tabu search. *Location Science* 5(2):75–88.

———. 2001. A dynamic model and parallel tabu search heuristic for real-time ambulance relocation. *Parallel Computing* 27(12):1641–1653.

———. 2006. The maximal expected coverage relocation problem for emergency vehicles. *Journal of the Operational Research Society* 57(1):22–28.

Goemans, Michel X, and Martin Skutella. 2004. Cooperative facility location games. *Journal of Algorithms* 50(2):194–214.

Goemans, Michel X, and David P Williamson. 1997. The primal-dual method for approximation algorithms and its application to network design problems. *Approximation algorithms for NP-hard problems* 144–191.

Gutfraind, Alexander, Milan Bradonjić, and Tim Novikoff. 2012. Optimal recovery of damaged infrastructure network. Tech. Rep., University of Texas at Austin, Austin.

Held, Michael, and Richard M Karp. 1971. The traveling-salesman problem and minimum spanning trees: Part ii. *Mathematical programming* 1(1):6–25.

Henry, Devanandham, and Jose Emmanuel Ramirez-Marquez. 2016. On the impacts of power outages during hurricane sandy—a resilience-based analysis. *Systems Engineering* 19(1):59–75.

Heuberger, Clemens. 2004. Inverse combinatorial optimization: A survey on problems, methods, and results. *Journal of combinatorial optimization* 8(3):329–361.

Hogan, Kathleen, and Charles ReVelle. 1986. Concepts and applications of backup coverage. *Management Science* 32(11):1434–1444.

Houghtalen, Lori, Özlem Ergun, and Joel Sokol. 2011. Designing mechanisms for the management of carrier alliances. *Transportation Science* 45(4):465–482.

Iloglu, Suzan, and Laura A Albert. 2018. An integrated network design and scheduling problem for network recovery and emergency response. *Operations Research Perspectives* 5: 218–231.

Jain, Kamal, and Vijay V Vazirani. 1999. Primal-dual approximation algorithms for metric facility location and k-median problems. In *40th annual symposium on foundations of computer science (cat. no. 99cb37039)*, 2–13. IEEE.

Jennings, Charles R. 2013. Fires during the 2012 Hurricane Sandy in queens, new york: A first report. Tech. Rep., John Jay College of Criminal Justice The City University of New York, USA.

Kaufman, Sarah, Carson Qing, Nolan Levenson, and Melinda Hanson. 2012. Transportation during and after Hurricane Sandy. Tech. Rep., Rudin Center for Transportation, NYU Wagner Graduate School of Public Service.

Keogh, Miles, and Thomas Sharon. 2015. Regional mutual assistance groups: A primer. Tech. Rep., The National Association of Regulatory Utility Commissioners.

Lã, Quang Duy, Yong Huat Chew, and Boon-Hee Soong. 2016. *Potential game theory: applications in radio resource allocation*. Switzerland.

Lee, Earl E, John E Mitchell, and William A Wallace. 2007. Restoration of services in interdependent infrastructure systems: A network flows approach. *IEEE Transactions on Systems, Man, and Cybernetics, Part C (Applications and Reviews)* 37(6):1303–1317.

———. 2009. Network flow approaches for analyzing and managing disruptions to interdependent infrastructure systems. *Wiley handbook of science and technology for Homeland Security*.

Lee, Shine-Der, and Wen-Tin Chang. 2007. On solving the discrete location problems when the facilities are prone to failure. *Applied mathematical modelling* 31(5):817–831.

Liu, Lindong, Xiangtong Qi, and Zhou Xu. 2016. Computing near-optimal stable cost allocations for cooperative games by lagrangian relaxation. *INFORMS Journal on Computing* 28(4):687–702.

Losada, Chaya, M Paola Scaparra, and Jesse R O'Hanley. 2012. Optimizing system resilience: a facility protection model with recovery time. *European Journal of Operational Research* 217(3):519–530.

Marianov, Vladimir, and Charles Revelle. 1994. The queuing probabilistic location set covering problem and some extensions. *Socio-Economic Planning Sciences* 28(3):167–178.

Martin, Richard Kipp. 2012. *Large scale linear and integer optimization: a unified approach*. Springer Science & Business Media.

Maya Duque, Pablo A, Irina S Dolinskaya, and Kenneth Sörensen. 2016. Network repair crew scheduling and routing for emergency relief distribution problem. *European Journal of Operational Research* 248(1):272–285.

Meddour, Djamal-Eddine, Tinku Rasheed, and Yvon Gourhant. 2011. On the role of infrastructure sharing for mobile network operators in emerging markets. *Computer Networks* 55(7):1576–1591.

Miller, Robert. 2006. Hurricane katrina: Communications & infrastructure impacts. Tech. Rep., National Defense Univ Fort McNair DC.

Morshedlou, Nazanin, Andrés D González, and Kash Barker. 2018. Work crew routing problem for infrastructure network restoration. *Transportation Research Part B: Methodological* 118:66–89.

Murray, Alan T. 2016. Maximal coverage location problem: impacts, significance, and evolution. *International Regional Science Review* 39(1):5–27.

Nisan, N., T. Roughgarden, E. Tardos, and V. Vazirani. 2007. *Algorithmic game theory*. Cambridge University Press. New York, NY, USA.

Nurre, Sarah G, Burak Cavdaroglu, John E Mitchell, Thomas C Sharkey, and William A Wallace. 2012. Restoring infrastructure systems: An integrated network design and scheduling (INDS) problem. *European Journal of Operational Research* 223(3):794–806.

Nurre, Sarah G, and Thomas C Sharkey. 2014. Integrated network design and scheduling problems with parallel identical machines: Complexity results and dispatching rules. *Networks* 63(4):306–326.

NYC OpenData. 2012. FDYN firehouse listing. `https://data.cityofnewyork.us/Public-Safety/FDNY-Firehouse-Listing/hc8x-tcnd`. [Online; accessed November, 2017].

———. 2013. Hurricane evacuation centers. https://data.cityofnewyork.us/Public-Safety/Hurricane-Evacuation-Centers/ayer-cga7. [Online; accessed October 11, 2017].

Office of Emergency Management. 2014. New york city hazard mitigation plan 2014. Tech. Rep., Office of Emergency Management.

O'Hanley, Jesse R, M Paola Scaparra, and Sergio García. 2013. Probability chains: A general linearization technique for modeling reliability in facility location and related problems. *European Journal of Operational Research* 230(1):63–75.

O'Reilly, Gerard, Ahmad Jrad, Ramesh Nagarajan, Theresa Brown, and Stephen Conrad. 2006. Critical infrastructure analysis of telecom for natural disasters. In *Networks 2006. 12th international telecommunications network strategy and planning symposium*, 1–6. IEEE.

Pinedo, Michael, and Khosrow Hadavi. 1992. Scheduling: theory, algorithms and systems development. In *Operations research proceedings 1991*, 35–42. Springer.

Polyak, Boris T. 1987. Introduction to optimization. translations series in mathematics and engineering. *Optimization Software*.

Qi, Zhiqiang, Tao Peng, and Wenbo Wang. 2018. Distributed resource scheduling based on potential game in dense cellular network. *IEEE Access* 6:9875–9886.

Rajagopalan, Hari K, Cem Saydam, and Jing Xiao. 2008. A multiperiod set covering location model for dynamic redeployment of ambulances. *Computers & Operations Research* 35(3):814–826.

Rinaldi, Steven M, James P Peerenboom, and Terrence K Kelly. 2001. Identifying, understanding, and analyzing critical infrastructure interdependencies. *IEEE control systems magazine* 21(6):11–25.

Rosenthal, Robert W. 1973. A class of games possessing pure-strategy nash equilibria. *International Journal of Game Theory* 2(1):65–67.

Roughgarden, Tim. 2009. Intrinsic robustness of the price of anarchy. In *Proceedings of the forty-first annual acm symposium on theory of computing*, 513–522. ACM.

Sarkar, Tapan K, Magdalena Salazar-Palma, and Mohammad Najib Abdallah. 2018. *The physics and mathematics of electromagnetic wave propagation in cellular wireless communication*. Wiley Online Library.

Scaparra, Maria P, and Richard L Church. 2008. A bilevel mixed-integer program for critical infrastructure protection planning. *Computers & Operations Research* 35(6):1905–1923.

Sharkey, Thomas C, Burak Cavdaroglu, Huy Nguyen, Jonathan Holman, John E Mitchell, and William A Wallace. 2015a. Interdependent network restoration: On the value of information-sharing. *European Journal of Operational Research* 244(1):309–321.

Sharkey, Thomas C, Sarah G Nurre, Huy Nguyen, Joe H Chow, John E Mitchell, and William A Wallace. 2015b. Identification and classification of restoration interdependencies in the wake of hurricane sandy. *Journal of Infrastructure Systems* 22(1):04015007.

Slikker, Marco. 2001. Coalition formation and potential games. *Games and Economic Behavior* 37(2):436–448.

Smith, Andrew M, Andrés D González, Leonardo Dueñas-Osorio, and Raissa M D'Souza. 2017. Interdependent network recovery games. *Risk Analysis*.

Snyder, Lawrence V, and Mark S Daskin. 2005. Reliability models for facility location: the expected failure cost case. *Transportation Science* 39(3):400–416.

Swersey, Arthur J. 1994. The deployment of police, fire, and emergency medical units. *Handbooks in Operations Research and Management Science* 6:151–200.

Tardos, Eva, and Tom Wexler. 2007. Network formation games and the potential function method. *Algorithmic Game Theory* 487–516.

Texas Department of Transportation. 2017. Txdot removes more than 10 million cubic feet of debris. Tech. Rep., Texas Department of Transportation.

Toregas, Constantine, Ralph Swain, Charles ReVelle, and Lawrence Bergman. 1971. The location of emergency service facilities. *Operations Research* 19(6):1363–1373.

Van Buuren, Martin, Rob van der Mei, Karen Aardal, and Henk Post. 2012. Evaluating dynamic dispatch strategies for emergency medical services: Tifar simulation tool 1–12.

Vatsa, Amit Kumar, and Sachin Jayaswal. 2016. A new formulation and benders decomposition for the multi-period maximal covering facility location problem with server uncertainty. *European Journal of Operational Research* 251(2):404–418.

Verdonck, Lotte, Patrick Beullens, An Caris, Katrien Ramaekers, and Gerrit K Janssens. 2016. Analysis of collaborative savings and cost allocation techniques for the cooperative carrier facility location problem. *Journal of the Operational Research Society* 67(6):853–871.

Wang, Lizhi. 2009. Cutting plane algorithms for the inverse mixed integer linear programming problem. *Operations Research Letters* 37(2):114–116.

Wang, Qian, Rajan Batta, Joyendu Bhadury, and Christopher M Rump. 2003. Budget constrained location problem with opening and closing of facilities. *Computers & Operations Research* 30(13):2047–2069.

Wolsey, Laurence, Gérard Cornuéjols, and Georges-L Nemhauser. 1990. The uncapacitated facility location problem.